2017

An Experimental Approach to Explore Abdominal Aortic Aneurysms in Rabbit Model

Altamimi, Manal Nasser

UNIVERSITY OF CALGARY

An Experimental Approach to Explore Abdominal Aortic Aneurysms in Rabbit Model

by

Manal Altamimi

A THESIS

SUBMITTED TO THE FACULTY OF GRADUATE STUDIES

IN PARTIAL FULFILMENT OF THE REQUIREMENTS FOR THE

DEGREE OF MASTER OF SCIENCE

GRADUATE PROGRAM IN BIOMEDICAL ENGINEERING

CALGARY, ALBERTA

JANUARY, 2017

Abstract

The diagnosis of an Abdominal Aortic Aneurysm (AAA) is currently made based on maximum diameter, which fails to accurately predict risks of rupture. The purpose of this study was to advance our understanding of AAA evolution using a rabbit model. AAAs were developed in rabbits using a periaortic incubation of $CaCl_2$ and elastase. Rabbits were imaged using 3D angiography at 0 (healthy), 2, 4, and 6 weeks. Material properties and histological analyses were obtained for each stage. Results showed an increase in maximum diameter and wall thickness with aneurysmal tissue. The healthy aorta was stronger than all aneurysmal tissue. Tissue at 6 weeks had the stiffest and strongest properties compared to aneurysmal tissue. Elastin degradation and separation between wall layers was observed in all aneurysmal tissue with the highest collagen remodeling at 6 weeks. Because human aneurysms are diagnosed at an unknown time after initial formation, control animal experiments are necessary to understand the evolution of the mechanical and histological properties of the aortic tissue.

Acknowledgements

Foremost, I would like to express my sincere gratitude to Elena Di Martino and Alim Mitha for the continuous support of my study and research, for their patience, motivation, enthusiasm, and immense knowledge. Their guidance helped me in all the time of research and writing of this thesis. Besides my supervisors, I would like to thank my mentor Giampaolo Martufi for his great advice and support.

Dedication

This thesis is dedicated to my father Nasser Hamad Altamimi with love and admiration for believing in me, rest in peace father.

Table of Contents

List of Tables

List of Figures and Illustrations

List of Symbols, Abbreviations and Nomenclature

Symbol	Definition
2W	Two weeks
4W	Four weeks
6W	Six weeks
AAA	Abdominal aortic aneurysm
PBS	Phosphate buffered saline
$CaCl_2$	Calcium chloride
FEA	Finite element analysis
VVG	Verhoeff van gieson
PSR	Picro sirius red
VSMC	Vascular smooth muscle cell

CHAPTER 1 BACKGROUND

In this chapter we will discuss the cardiovascular system specifically aortic anatomy, physiology, and histology. Also, we will introduce abdominal aortic aneurysms, a disease that alters the physiology and histology of the aorta, and poses serious health risks for the patient. We will provide current medical practices to minimize the risk of aortic aneurysm rupture and explain the limitation of these practices.

Cardiovascular System

The cardiovascular system consists of heart, vessels and approximately five liters of blood. Blood transports oxygen, hormones, nutrients, and cellular waste throughout the body. The organ that powers the cardiovascular system is the heart, a hollow muscular organ that pumps blood throughout the vascular system. The human heart has four chambers: two receiving chambers (atria) and two discharging chambers (ventricles). The cardiac cycle refers to a complete heartbeat and is composed of systolic and diastolic phases, which allow the contraction and relaxation of the heart and its pumping function. The contraction of the heart forces blood into the ventricles (atrial systole) and then out of the heart (ventricular systole) through the aorta and pulmonary artery. During diastole (both atrial and ventricular) the heart is relaxed and the blood can fill the chambers. The cycle of average human heart occurs (beats) at 70 / 75 beats per minute (Boron and Boulpaep, 2016, Iaizzo, 2009).

In the cardiovascular system there are two main circulatory loops: the pulmonary circulation loop and the systemic circulation loop. The right side of the heart supports the pulmonary

circulation that transports deoxygenated blood to the lungs, where the blood picks up oxygen and returns it to the left side of the heart. From the left side of the heart starts the systemic circulation that carries highly oxygenated blood to all of the organs and tissues of the body (except for the lungs and the heart), removes the cells' waste and returns deoxygenated blood to the right side of the heart completing the loop (Boron and Boulpaep, 2016, Iaizzo, 2009).

The blood vessels are the part of the system that transports blood throughout the body. There are three types of vessels: the arteries, which carry the high pressured blood away from the heart, the capillaries, which allow exchange of substances between blood and tissues, and finally the veins, which carry the blood from the capillaries back to the heart (Boron and Boulpaep, 2016).

The Aorta

The aorta is the largest artery in the human body (figure 1). Originating from the left ventricle of the heart and extending down to the abdomen, the aorta allows the distribution of the oxygenated blood to all the organs of the body through the systemic circulation. The aortic valve lets the one-way flow of blood from the heart into the systemic circulation at each beat. The aorta is commonly divided into four sections: the ascending thoracic aorta, the aortic arch, the descending thoracic aorta and the abdominal aorta. The aorta sections are generally similar but vary in function and histology (Boron and Boulpaep, 2016, Iaizzo, 2009).

The ascending aorta starts at the upper base of the left ventricle and is about 5 cm in length and 3 cm in diameter; the coronary arteries branch off the ascending aorta to supply the heart with blood. The aortic arch is the part of the aorta that curves over the heart giving rise to branches

that carry blood to the head, neck and arms: the common carotid artery, the innominate artery and the left subclavian artery. The upper curvature presents a region of higher pressure that forces the blood to the upper regions of the body. The aortic arch contains baroreceptors and chemoreceptors that relay information concerning blood pressure, blood pH and carbon dioxide levels. The descending aorta is the part of the aorta starting from the end of the aortic arch to the diaphragm. The thoracic aorta travels down through the chest and presents a smaller diameter (1.5 - 2 cm) and several branches that supply blood to the chest organs and structures; in descending order: bronchial arteries, mediastinal arteries, esophageal arteries, pericardial arteries, superior phrenic artery. Most of the major organs of the body receive blood from the last part of the aorta, the abdominal aorta that begins from the diaphragm and presents branches, including: celiac artery, superior and inferior mesenteric arteries, renal artery and common iliac arteries (Boron and Boulpaep, 2016, Iaizzo, 2009).

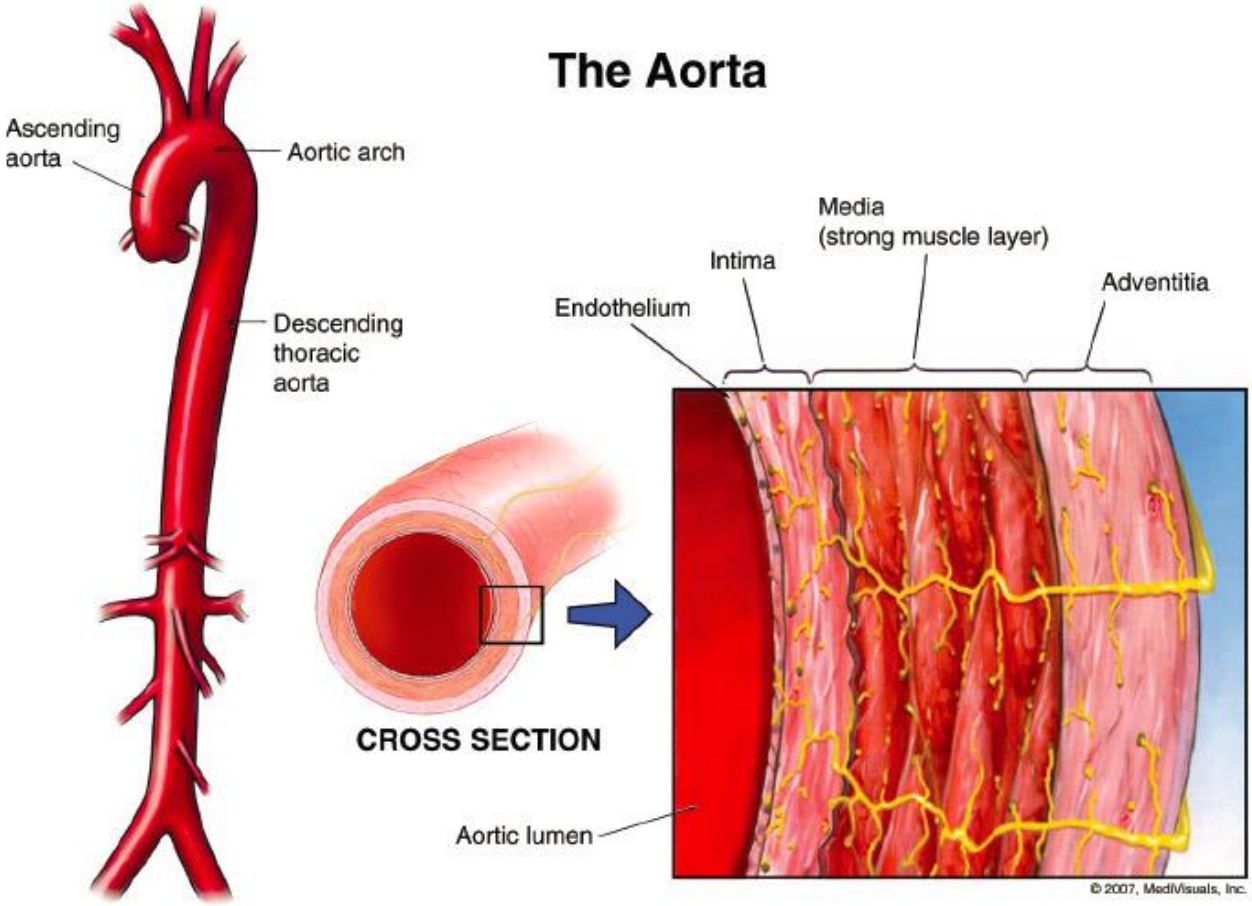

Figure 1: Aorta wall anatomy and histology (Northwell, 2016). The three main sections of the aorta are explained on left side (Ascending, arch, descending, and abdominal). On the right side, we demonstrate the three layers of aortic wall (intima, media, and adventitia).

Connective tissue has two main components: extracellular matrix and cells. The main cells seen in connective tissue are: fibroblast, mesenchymal cells, adipocytes, mast cells, macrophages, and white blood cells (neutrophils, eosinophils) (figure 2). The most common type of cell found in the connective tissue is the fibroblast. Fibroblasts produce the two major classes of extracellular material found in connective tissue: fibers and ground substance. Ground substance is a complex viscous material that makes up the matrix in which the fibers and cells are embedded. Fibers are

long bundles of proteinaceous macromolecules that make connective tissues strong, resilient, and elastic. The main types of fibers in the connective tissue are collagen fibers and elastic fibers. Elastic fibers are made of elastin proteinaceous and confer high distensibility to the tissue and elastic properties (the ability to resume its normal shape after deformation). Collagen fibers are the strongest component and limit excessive deformation of the vessel by being very stiff at high deformations. The aorta is one example of connective tissue and its properties; it must stretch at each cardiac beat to withstand large hydrostatic forces and then instantly recover its original shape when those forces are removed (Barbara Young, 2000).

Mesenchymal cells are embryonic cells capable of developing into any type of connective tissue cell required. They can differentiate into fibroblasts, cartilage cells, bone cells, and, on occasion, smooth muscle cells. In addition to mesenchymal cells, adipocytes (fat cells) are responsible for the storage and metabolism of fat. Also, macrophages, mast cells, and white blood cells are widely distributed throughout connective tissue. Macrophages are large cells filled with enzyme-packed lysosomes that can digest unwanted foreign particles and cellular debris. On the other hand, mast cells are filled with large granules containing heparin and histamine. Mast cells can slow blood clotting, and increase capillary permeability in response to injury. Mast cells participate in the inflammatory response by promoting blood flow out of the bloodstream and into tissue spaces where white blood cells and antibodies can fight infection (Barbara Young, 2000).

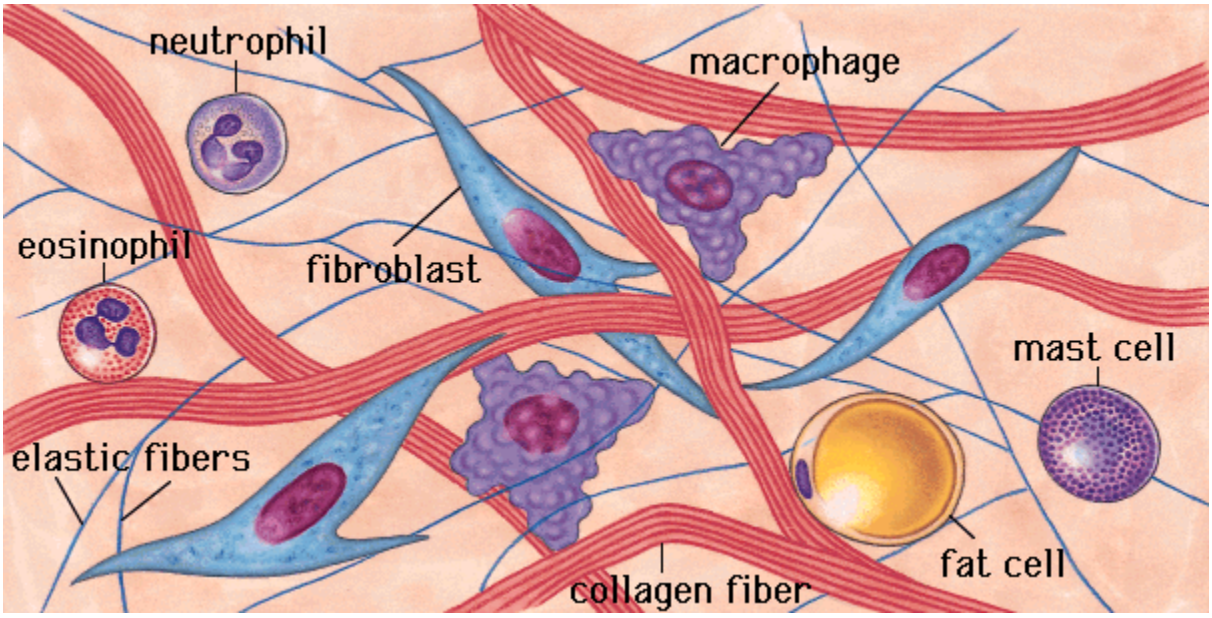

Figure 2: Schematic representation of connective tissue (Collin, 2016). This schematic shows different parts of connective tissue including fibers and cells.

The structure of arteries and veins consists of three main layers, tunica intima, tunica media and tunica adventitia (figure 1). These layers have unique roles in the mechanical response of the vessels. The tunica intima is the most internal layer. It consists mainly of a layer of endothelial cells that forms an interface between the blood in the lumen and the rest of the vessel wall. The tunica intima is supported by the internal elastic lamina, which is composed by a regular layer of elastin protein (figure 3) (Barbara Young, 2000).

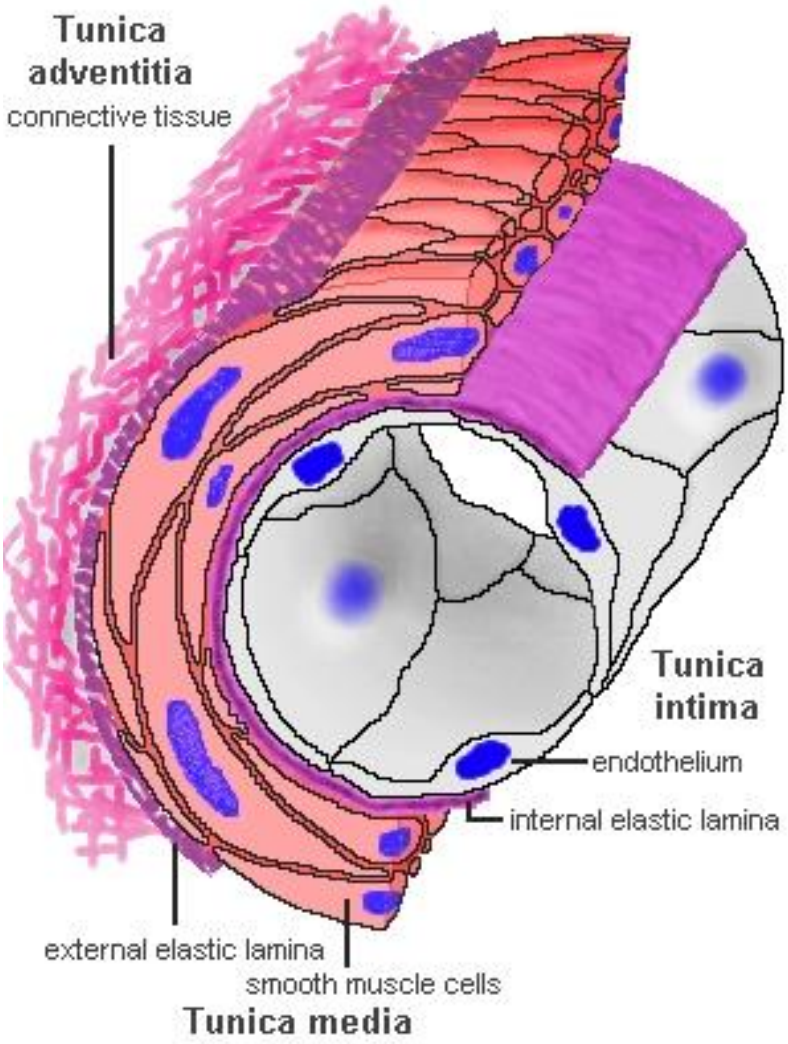

Figure 3: Aorta wall layers showing both internal and external elastic lamina (Hill, 2016).

The tunica media, which is the middle layer, is made of circumferentially arranged elastic fibers and smooth muscle that control the vasodilatation or vasoconstriction of the vessel. The external elastic lamina separates the tunica media from the last layer. The tunica adventitia is the outermost layer and consists of connective tissue containing fibroblasts and elastic/collagen fibers. It also contains nerves and capillaries (vasa vasorum) in the larger vessels (Barbara Young, 2000, Boron and Boulpaep, 2016).

The aorta's ability to handle large volume of blood at each systolic pulse resides in the great strength and resilience of its tunica media. The strength of the tunica media comes from large sheets of elastic fibers that appear black wavy lines when viewed in cross section using a **Verhoeff–Van Gieson stain** (VVG), under a microscope (figure 4) (Barbara Young, 2000). Any change or loss of these fibers alters the function of the aorta and has catastrophic consequences.

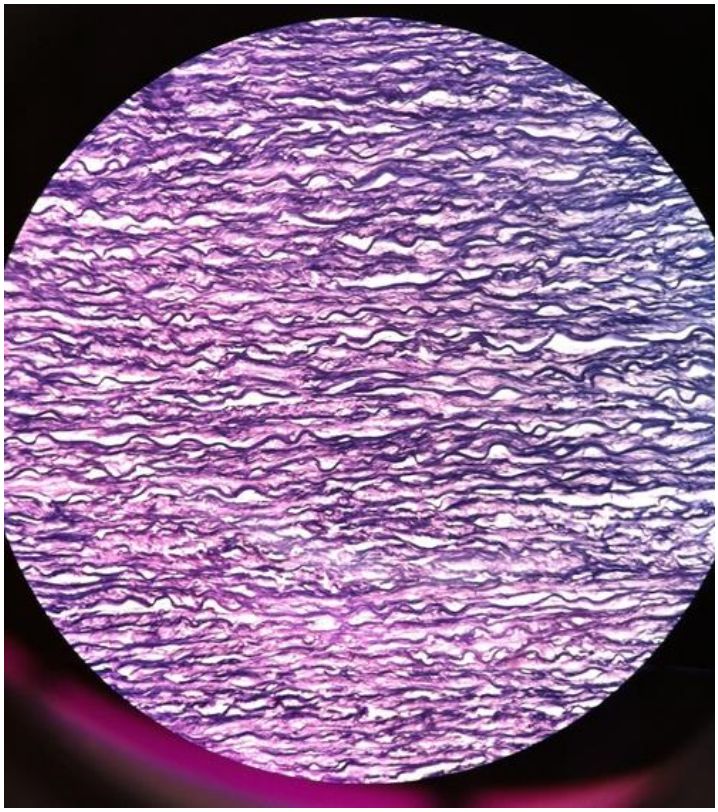

Figure 4: Elastin fibers in the aortic wall looking wavy black lines at 400X magnification (VVG stain) (John Varellas, 2016).

Abdominal Aortic Aneurysm

The abdominal aortic aneurysm (AAA) is a local dilation in the aorta of at least 50% of its original diameter size (figure 5). The normal size of the abdominal aorta can range from 1 cm to 2.4 cm depending on sex, age, and health conditions (Smolock and Lyden, 2014).

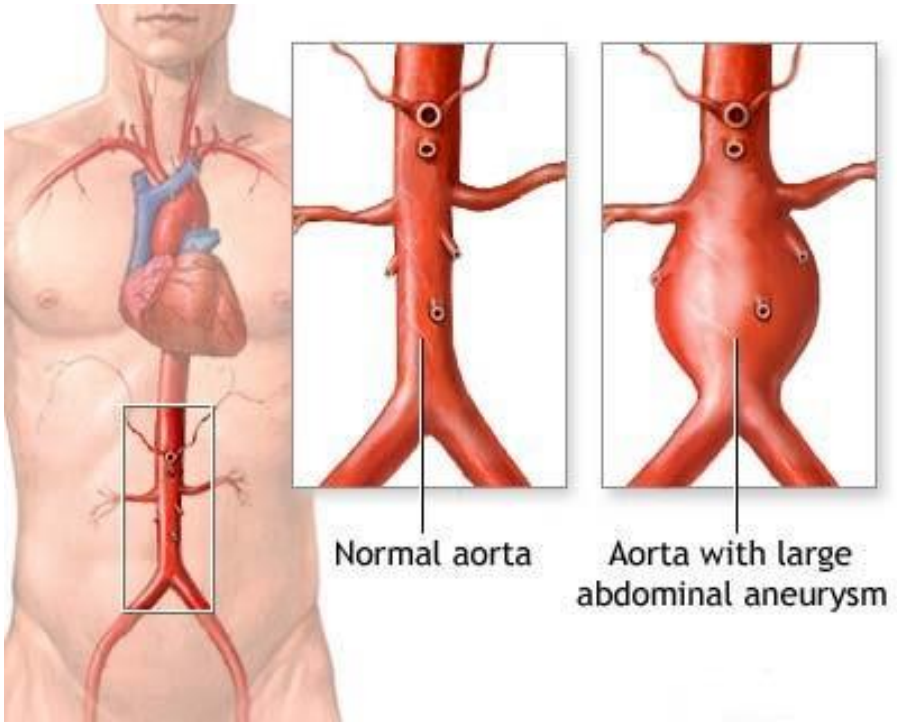

Figure 5: Abdominal aortic aneurysm specifically in infrarenal location (Medlineplus, 2016).

The aneurysmal aorta expands and eventually ruptures with a mortality rate of 75-90% (LeFevre, 2014). AAA rupture is the 13th leading cause of death in United States (Smolock and Lyden, 2014). Many risk factors contribute to the development of AAA such as ageing, male gender, smoking, family history, associated atherosclerotic disease, and genetic disease, like Marfan's syndrome. AAA is usually asymptomatic and consequently its detection prior to rupture is very

challenging. In general, AAA is diagnosed accidentally when a patient is scanned for a different purpose (Smolock and Lyden, 2014, Shimazaki and Ueda, 2014). When detected, the clinical approach to avoid AAA rupture is endovascular or open surgery repair (Shimazaki and Ueda, 2014). The cost of AAA treatment is a great burden to the healthcare system with an approximate cost of USD 37,000 and USD 42,000 for endovascular and open repair respectively (Epstein et al., 2014). The clinical decision to recommend surgery is based on assessing the risk of rupture of the aneurysm versus the risks introduced by the surgery itself. It is important to mention that due to health conditions not all patients are suitable candidate for surgery (Epstein et al., 2014). Specific conditions of the aorta, in particular the absence of a long enough "neck" above the aneurysm itself, poses limitations regarding the use of endovascular approaches. Due to the high risks of the pathology and of the associated surgical repairs, it is important to understand which patients are truly at risk for aortic rupture so that risks can be weighed against benefits. Further research is essential to better understand AAA and reduce its mortality rate and health cost.

AAA is more common in the male population with an overall incidence of 498/100,000 (Jahangir et al., 2015, Choke et al., 2005, Norman and Powell, 2007). The reason behind it is still not understood but estrogen appears to protect against cardiovascular disease in premenopausal women (Norman and Powell, 2007, Jahangir et al., 2015). Therefore, estrogens could be playing a role in reducing or delaying the prevalence of AAA in women even after menopausal. In an animal model of AAA, the incidence of AAA was 100% in male but only 29% in female mice (Lysgaard Poulsen et al., 2016). Estrogens have been shown to lower the aortic collagen elastin ratio, whereas testosterone increases the proportion of collagen (Norman

and Powell, 2007). No research has been conducted in humans to understand the effect of gender, and all available data are based on animal models. Smoking is the most important modifiable risk factor for AAA, both the duration of smoking and daily cigarette number (Norman and Powell, 2007, Jahangir et al., 2015, LeFevre and on behalf of the, 2014). Studies evaluating smoking and aortic aneurysm demonstrated a significant prevalence of 75% of 4 cm AAA dilatations (Jahangir et al., 2015). Jahangir et al, (Jahangir et al., 2015) showed that former smokers have a lower risk of AAA compared to current smokers but that the risk is higher than in people who never smoked.

Abdominal Aortic Aneurysm Pathology

Aneurysmal disease is a focal lesion in the vessel wall that typically affects the tunica media and the adventitia layer of the aortic wall. The development of an aneurysm has not been completely understood but researchers have evaluated the onset and progression of an AAA and divided it into two related processes: extracellular matrix (EM) degeneration and inflammation (figure 6). The extracellular degradation can be due to genetic factors such as Marfan syndrome (Choke et al., 2005). Marfan syndrome is a disorder of the connective tissue that could lead to aortic dilatation and dissection due to different genetic mutations, specifically fibrillin-1 (Robinson and Booms, 2001). Lindeman et al, (Lindeman et al., 2010) suggested that aneurysms associated with Marfan syndrome are associated more with distinct defects in the collagen orientation than with a collagen defect at the biochemical level. They demonstrated that the collagen structures in the adventitia of a healthy abdominal aorta are a loosely knitted network of interwoven collagen ribbons encasing the medial layer. Conversely, in aneurysms associated with Marfan syndrome

the collagen fibrils are almost parallel, thereby limiting their ability to stretch which can contribute to failure of the aortic wall (Lindeman et al., 2010).

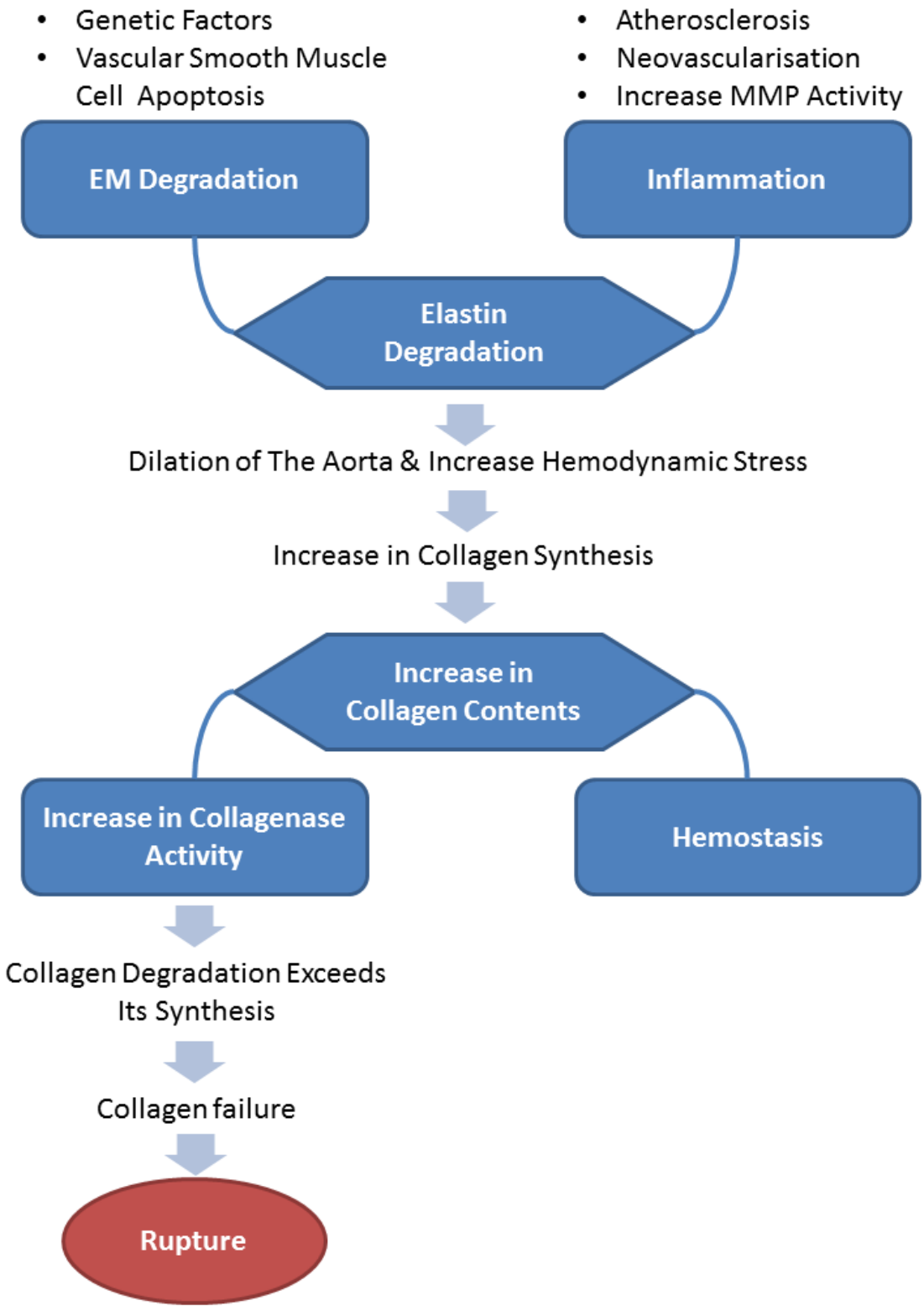

Figure 6: Chain of biological events that lead to abdominal aortic aneurysm rupture.

The degradation of extracellular matrix is often accompanied by apoptosis of vascular smooth muscle cells (VSMCs) (Choke et al., 2005). VSMCs are essential for maintaining blood pressure through contraction and relaxation, which alter the luminal diameter. However, they also perform a repair-remodeling function by synthesizing extracellular matrix components and increase proliferation and migration (Thompson et al., 1997, Rensen et al., 2007, Lopez-Candales et al., 1997, Henderson et al., 1999, Rowe et al., 2000). This function is very important during vessel remodeling in physiological or injury conditions (Rensen et al., 2007). Apoptosis is a naturally occurring mechanism of cell death in the healthy wall vessel but alteration in this mechanism could lead to excessive cell death. VSMCs death is associated with biochemical, morphological, and molecular changes (Thompson et al., 1997). Thompson et al, (Thompson et al., 1997) suggested that elevated cellular production of p53, which is an apoptosis initiator in cancer cells, and p21 could participate in VSMCs death (Rowe et al., 2000). Lopez-Candales et al, (Lopez-Candales et al., 1997) found higher levels of p53 protein within aneurysmal aortic tissue when compared with normal human aortas. Fukui et al, (Fukui et al., 2003) suggested that over expression of transforming growth factor β1 is associated with VSMCs apoptosis and reduction in proliferation. Contrary to the generally held opinion that apoptosis is non-inflammatory, Henderson et al, (Henderson et al., 1999) suggested that cytokines, perforin, and Fas/FasL protein produced by macrophages and T lymphocytes infiltration promote VSMCs death. The apoptosis of VSMCs is still unclear due to the lack of human AAA specimens collected at initial stages. However, there is clear correlation between VSMCs death and elastin degradation that lead to AAA formation.

Numerous extracellular proteinases contribute to the degeneration process which leads to AAA formation. The protease enzymes, mostly represented by matrix metalloproteinases (MMPs), are secreted by inflammatory cells including macrophages, neutrophils, lymphocytes, mast cells, and resident VSMCs (Di Martino et al., 1998, Choke et al., 2005). MMPs are a family of endopeptidases with proteolytic activity that affect elastin-collagen contents in the aortic wall. There are two main types of MMPs: elastase based, namely MMP-2, MMP-9, MMP-7, and MMP-12, and collagenase based, namely MMP-1, MMP-8 and -MMP13 (Choke et al., 2005). The MMPs are locally activated either by other MMPs, mast cell-derived chymase, or plasmin generated by plasminogen activators (Di Martino et al., 1998). The exact mechanisms of proteinase activation is still unknown, but it is commonly believed that increased activity in MMPs contributes to vessel expansion by degrading elastin (S Raut et al., 2013, Choke et al., 2005, Wilson et al., 2006, Kadoglou and Liapis, 2004). MMP-2, 9 and 12 have been assumed to have a significant role in aneurysm formation (Wilson et al., 2006, Kadoglou and Liapis, 2004, S Raut et al., 2013, Ailawadi et al., 2003). Freestone et al, (Freestone et al., 1995) reported high activation of MMP-9 in AAAs with diameter larger than 5.5 cm in contrast to AAAs of smaller diameter. Sakalihasan et al, (Sakalihasan et al., 1996) revealed that activated MMP-9 was present in AAAs with a mean diameter of 7.5 cm but was absent in AAAs with mean diameter of 5.8 cm. Similarly, McMillan et al, (McMillan et al., 1997) demonstrated higher transcription levels of MMP-9 in medium sized aneurysms (5 - 6.9 cm) compared with both smaller and larger aneurysms. Wilson et al, (Wilson et al., 2003) reported significantly higher concentrations of MMP-8 and MMP-9 at the site of rupture compared to those on the anterior side. Many investigators have also examined the role of MMP-2 in the development of aneurysms. Freestone et al, (Freestone et al., 1995) reported similar activation level of MMP-2 with small and large

aneurysm. However, high concentrations of MMP-2 are found in small aneurysmal aortas (Ailawadi et al., 2003, McMillan and Pearce, 1999). On the other hand, other studies demonstrated that MMP-12 is highly expressed along the superior and inferior edge of AAAs in humans, which suggests that MMP-12 is important in aneurysm initiation. Moreover, Higashikata et al, (Higashikata et al., 2004) showed elevated levels of MMP-1 and MMP-8, that are associated with the degradation of collagen, in aneurysmal tissue when compared to normal aortic tissue. In general, it is believed that MMP-2 plays a role during early aneurysm formation whereas MMP-9 is related to continuous expansion of aneurysms. However, the lower levels of MMP-9 expression in aneurysms with diameter of 7 cm implied that the high rupture rates in larger aneurysms were related to other factors (S Raut et al., 2013, Ailawadi et al., 2003, Wilson et al., 2006). This relationship between MMPs and AAA is derived from patients with established AAAs, but not from individuals who are prone to develop AAA. A clear understating of MMPs role in AAA formation will only be demonstrated by using studies in patients at early stages of AAA or in healthy individuals with great tendency to AAA development (Kadoglou and Liapis, 2004).

Atherosclerosis is a chronic condition described by the formation of lipid-rich plaques within the large arteries walls, which is believed to contribute to elastin degradation that leads to AAA (Palazzuoli et al., 2008, Golledge and Norman, 2010). It is commonly believed that atherosclerosis leads to increase in the intima thickness by formation of a smooth muscle cell layer between the endothelium and internal elastic lamina. The thickening of intima layer with lipid-rich plaques degrades the internal elastic lamina (Jones, 2011, Ailawadi et al., 2003, Golledge and Norman, 2010). This reduces the arterial compliance leading to increased pulse

pressure and pressure wave velocities in aging individuals with advanced atherosclerosis. On the other hand, the neovascularization process disrupts the structure of the media layer by introducing inflammatory cells which leads to medial atrophy (Choke et al., 2005, Jones, 2011, Choke et al., 2006, Holmes et al., 1995). The media of the human infrarenal aorta is vastly avascular and its supply of nutrients is mainly through luminal diffusion. If the diffusion is insufficient due to intima thickening, the vasa vasorum becomes an important alternative nutrient supply. The adventitial vasa vasorum network begins to penetrate the media which allow direct recruitment of inflammatory cells, such as macrophages, plasma cells and T-lymphocytes. These cells secrete cytotoxic mediators, such as perforin, which induce smooth muscle apoptosis resulting in continues matrix degradation (Holmes et al., 1995, Choke et al., 2006, Jones, 2011)

It is generally accepted that elastic fibers are responsible for load-bearing at physiologic pressures whereas adventitial collagen acquires load-bearing function at higher pressure. Aneurysm walls have a significant reduction in the elastin-collagen ratio compared to healthy aortic wall (Smolock and Lyden, 2014, Vorp and Geest, 2005, Martufi and Gasser, 2013, J. Thubrikar, 2001, Schlatmann and Becker, 1977). 75–80 % reductions of adventitial elastin content are seen in small as well as large aneurysms suggesting that adventitial elastin destruction is an initial step in aneurysm formation and promotes the enlargement of the vessel (White and Mazzacco, 1996). In addition to degradation of elastic lamellae in the wall, urinary elastin-derived peptides are significantly higher in patients with AAA. The urinary elastin peptides are the product of elastin degradation. Since elastin is synthesized in early life and has an extremely long half-life, about 50 years, loss of elastin in aneurysm wall as a result of elastolysis and cannot be promptly reversed (Shimazaki and Ueda, 2014). The dilatation of the

aorta wall changes the geometry of the aorta and generates increasing wall tension over a period of years and haemodynamic stress (J. Thubrikar, 2001, Canchi et al., 2015). Therefore, it transfers the load bearing in the aortic wall to collagen fibers (Martufi and Gasser, 2013, Vorp and Geest, 2005). The body repairs the aneurysm by increasing collagen synthesis during the early stages of aneurysm formation. This network contains predominantly type I and III collagen with collagen type III responsible for most of its tensile characteristics (Choke et al., 2005, Tsamis et al., 2013). Rodella et al, (Rodella et al., 2016) demonstrated that fibroblasts and VSMCs in aneurysmal tissue increase local production of type I collagen which is more resistant and less elastic compared to type III collagen. Bode et al, (Bode et al., 2000) demonstrated that Collagen type III was highly present in the media layer of AAA tissue. Menashi et al, (Menashi et al., 1987) suggested that only limited collagen turnover occurs in the media of abdominal aortic aneurysms before rupture. Other studies have suggested that the rupture occurs when collagen degradation exceeds its synthesis (Wadgaonkar et al., 2015, Martufi and Gasser, 2013).

The shape of an abdominal aortic aneurysm results in alteration of the haemodynamic milieu, disordered flow, blood recirculation, and stagnation that contribute to the formation and progression of an intraluminal thrombus (Martufi et al., 2015, Golledge et al., 2014, Martinez-Pinna et al., 2013, Jones, 2011, Ailawadi et al., 2003, Di Martino et al., 1998). Intraluminal thrombus is found in about 75% of all AAAs and it is a mutli-layered structure of fresh red blood clot (platelets), fibrin clot (fibrin is non-globular protein involved in the clotting of blood by changing normally-fluid blood into a jelly-like solid) (Michel et al., 2010) , and an actively fibrinolysed ablumenal layer (Choke et al., 2005, Jones, 2011, O'Leary et al., 2014). The thrombus has variable integration location with the aortic intima including regions of intramural

haemorrhage. The thrombus affects the aneurysm by introducing further hypoxia by blocking the path of oxygen and nutrients to reach the aortic wall (Vorp et al., 2001, Choke et al., 2005, Jones, 2011). This may lead to increase neovascularization in the aortic wall which eventually introduce inflammation (Vorp et al., 2001). Also, thrombus is a rich source of proteases and their activators, and the increase in their activity may introduce additional inflammatory response that promotes further wall weakening (Choke et al., 2005, Jones, 2011). From a mechanical point of view, some studies reported that thrombus significantly lowers aneurysm wall stress whereas others suggested that thrombus fails to reduce transmission of pressure to the aneurysm wall (Choke et al., 2005, O'Leary et al., 2014). Studies have suggested that rupture is associated with growth of thrombus in the aneurysm but the association between thrombus and risk of AAA rupture remains controversial (Martinez-Pinna et al., 2013, Golledge et al., 2014). Further research is required to better understand AAA formation and progression. However, the development of this type of research is very challenging because when an AAA is found in a patient there is no information on its "age" or its likely progression.

There are three types of aneurysm according to its morphology: fusiform, saccular, and pseudoaneurysm (figure 7) (Khan et al., 2015). Fusiform abdominal aneurysms are the most common accounting for 80% of cases (Shang et al., 2013). Fusiform refers to a spindle-shaped aneurysm that enlarges symmetrically and equally on all sides of the aorta for the given length of the aneurysm. However, there are non-symmetric fusiform aneurysms where the enlargement of the wall is not equal on all side (Khan et al., 2015). It is commonly believed that fusiform aneurysms of the abdominal aorta often arise in the setting of wall degeneration which is caused by atherosclerotic disease. Fusiform aneurysms may be at higher risk of rupture starting at a

threshold of 5.5 cm (Shang et al., 2013). On the other hand, saccular aneurysms are spherical with a narrow neck where the aneurysm sac has expanded. This dilation shape is called eccentric aortic dilatation (Khan et al., 2015, Shang et al., 2013, Wadgaonkar et al., 2015). Saccular aneurysms develop from aortic infection, degeneration of a penetrating atherosclerotic ulcer, trauma, or previous aortic surgery. Saccular aneurysms are less common and are normally perceived by vascular surgeons as having higher risk of rupture. As a result, saccular aneurysms are surgically repaired regardless of their diameters (Shang et al., 2013, Wadgaonkar et al., 2015).

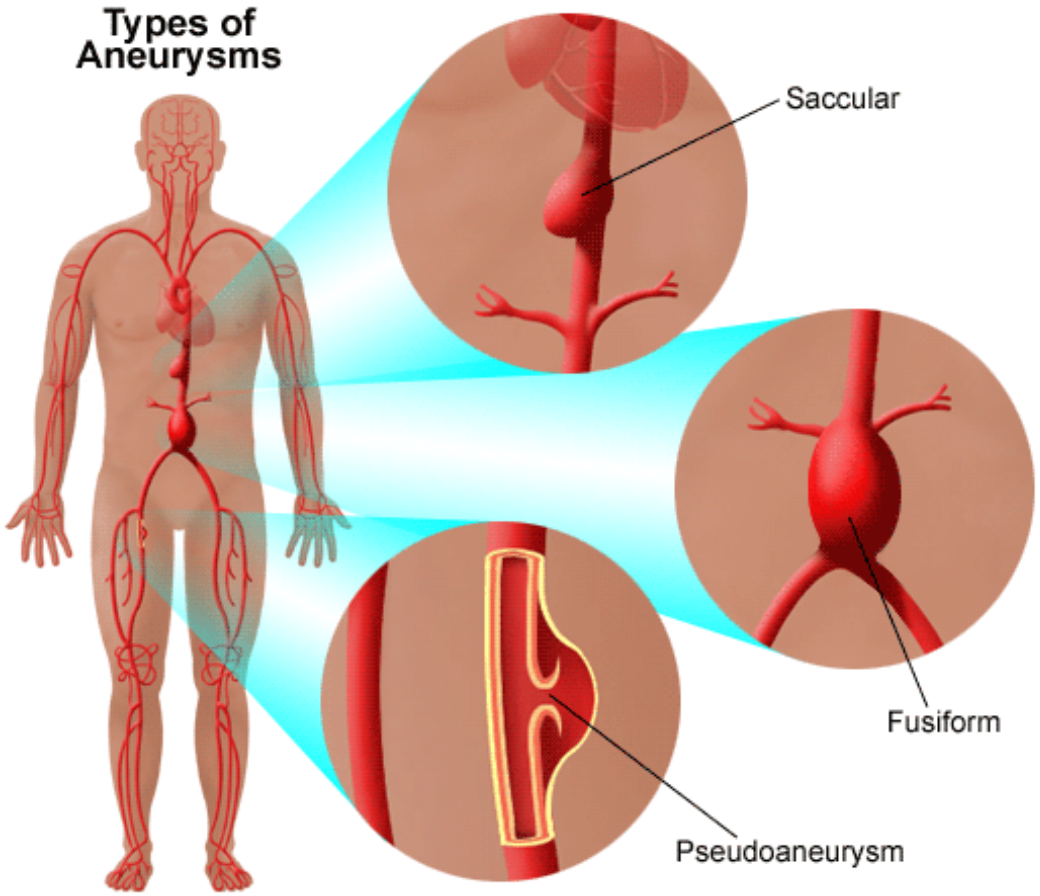

Figure 7: Aneurysm types depending on its morphology (Stanford, 2016).

Pseudoaneurysm or false aneurysm is not an enlargement of the aortic wall but a leakage to the outer layer of the blood vessel wall. The leakage is due to a tear inside the vessel wall that develops an enlargement due to blood filling. The main causes of false aneurysms are prior surgery or trauma (Hopkins, 2016).

Current Risk Assessment Practices

Current risk assessment practice for AAA uses the maximum diameter and the rate of growth of the aorta as surrogate for risk of aortic rupture.

Maximum aortic diameter.

The current medical practice suggests repairing AAA when the maximum diameter reaches 5.5cm to 6 cm. Many reports have challenged this practice (Smolock and Lyden, 2014, Volokh and Vorp, 2008). There are reported cases of patients that experienced rupture with a smaller diameter, while others with larger diameter never rupture. The Laplace law represents the theoretical basis to define the maximum diameter as the gold-standard criterion for rupture risk assessment (Choke et al., 2005). According to this law the circumferential wall stress σ is defined as:

$$\sigma = \frac{p \times D}{2 \times t}$$

Where p is the intraluminal pressure, D is the maximum diameter, and t is the vessel wall thickness. The Laplace law estimates the average wall stress in a thin wall cylinder and is not appropriate for structures with complex shape, such as aneurysms. In addition this simple mechanical approach to explain AAA rupture does not take into account the complex

multifactorial biological processes that are at the basis of aneurysm formation and rupture (Choke et al., 2005).

Rate of expansion.

Failure to accurately predict AAA rupture by using only diameter size led researchers to seek alternative indicators. There is evidence in the literature suggesting that the rate of aneurysm expansion can be an influential factor in rupture. The faster the expansion rate, the higher is the chance of rupture even for diameters smaller than 5 cm (Choke et al., 2005). Fast expansion could explain rupture in AAA with small diameters. However, computing the growth rate requires frequent monitoring every three-six months and would require assessment of growth at all locations not only the maximum diameter location. The use of AAA expansion rate as an independent rupture risk predictor is not widely accepted because there are correlations between the rate of aneurysm expansion and the initial diameter. It is difficult to separate the influence of expansion rate on rupture risk from the effect of expansion rate on absolute diameter, which suggests that expansion rate is dependent on diameter. Nevitt et al, (Nevitt et al., 1989) demonstrated that the absolute diameter size was associated with increased rupture rate, while the expansion rate was not. In order to determine whether expansion rate is an independent predictor of rupture, a large series of patients with similar sized aneurysms but different expansion rates may need to be followed and monitored at least every three months. Such a study would be time consuming, expensive, and potentially dangerous when done using CT due to the high dose of radiation (Choke et al., 2005).

Abdominal aortic aneurysm wall weakening.

The inaccuracy of current methods to predict AAA rupture led researchers to investigate aneurysms in terms of tissue mechanical behavior. From a mechanical point of view, AAA rupture occurs locally when the stress exceeds the tensile strength of the aortic wall. Histology and mechanical tests were both conducted on healthy and aneurysmal aorta (Choke et al., 2005). It has been shown that AAA samples presented with degradation of elastin, increased collagen synthesis, apoptosis of vascular smooth muscle cells, and marked inflammation (Monteiro et al., 2014, J. Thubrikar, 2001). Changes in elastin and collagen content alter the structural integrity of the tissue leading to local wall weakening, a key factor involved in AAA rupture. It is widely accepted that elastin in the aortic tissue is responsible for load bearing at physiologic pressures whereas collagen is engaged in load-bearing function at higher pressures (Choke et al., 2005, Di Martino et al., 2006). During the formation of an AAA, the elastin concentration decreases with consequent decrease of elasticity of the aorta. The tissue reacts to this change by increasing collagen concentration, which makes the tissue stiffer in order to carry higher stresses. It is speculated that the degradation of elastin in aneurysmal tissue is responsible for arterial dilatation, whereas collagen degradation is responsible for AAA rupture (Choke et al., 2005). However, no indicator or parameter that measures wall weakening has been developed or implemented in medical practice.

Abdominal aortic aneurysm wall thickness and stiffness.

Biomechanical properties of AAA wall tissue encouraged further research about AAA rupture. Di Martino et al, (Di Martino et al., 2006) suggested that for large aneurysms, wall thickness or stiffness might be a better indicator of rupture rather than diameter. The study compared the

biomechanical properties of AAA tissue harvested from patients who experienced rupture with that of patients who received elective repair. Results showed that ruptured AAA tissue had lower tensile strength and a thicker wall when compared to repaired AAA tissue (Di Martino et al., 2006). It is theoretically known that stretching a cylindrical sample will cause the wall to get thinner, which is not the case here. This suggests that the body may react to aortic enlargement by synthesizing collagen and other tissue constituents as previously described. However, the study illustrated that wall tissue from ruptured AAA had lower stiffness than tissue harvested from elective repaired patients, indicating that the increase in wall thickness is not due to collagen synthesis. Di Martino et al, (Di Martino et al., 2006) suggested that the increase in size is due to inflammation. Martufi et al, (Martufi et al., 2015) recently supported this idea by suggesting that a thicker AAA wall presents severe inflammation and accumulation of non-loadbearing tissue components that may locally reduce the wall strength predisposing the wall to higher risk of rupture. Choke et al, (Choke et al., 2005) suggested that there is an accelerated apoptosis of smooth muscle cell in large aneurysm. To date, the relationship between wall thickness and AAA rupture has not been completely clarified.

Finite element models.

The progression and rupture of an AAA are not simple biomechanical problems that can be predicted from simple geometric parameter, such as maximum diameter, rate of expansion, or wall thickness. FEA is a numerical technique that finds an approximate solution by dividing a large complex structure into a finite number of smaller elements with their own geometric shape and material properties (Choke et al., 2005, Martufi and Gasser, 2011). Engineering analysis techniques are then used to determine the behavior and calculate the stress for each element. The

development of imaging techniques, such as computed tomography (CT), represent a tool that provides clinicians with meaningful information, such as maximum aortic diameter and aneurysm shape (Reeps et al., 2010). At the same time, medical imaging enables researchers to construct a 3D model of AAA for each patient that can be used to compute patient-specific stress distributions (figure 8). The region with the highest stress is believed to be the alarming area where rupture is more likely to occur.

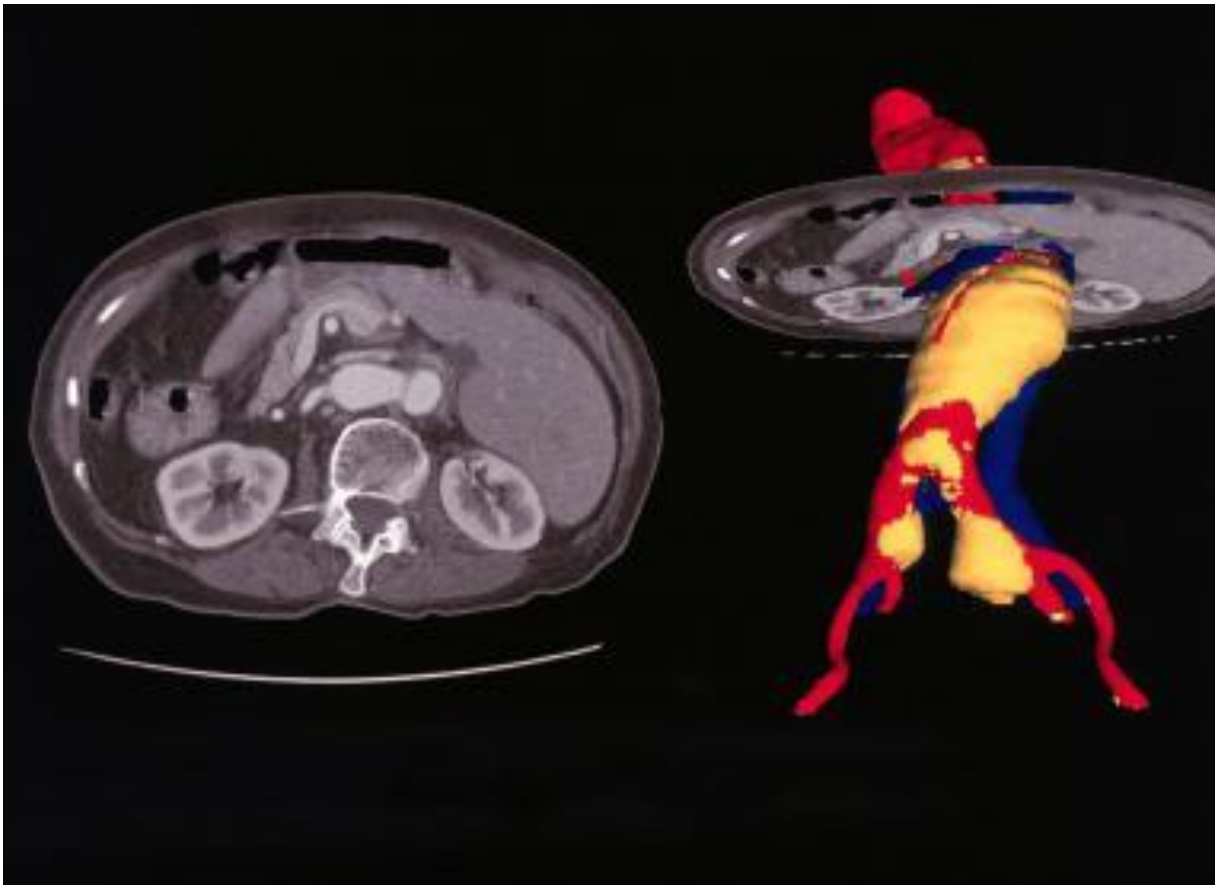

Figure 8: 3D reconstruction of abdominal aorta using imaging techniques. FEA can be used on patient specific geometry (Emedicine, 2016).

However, FEA requires critical assumptions that can alter the final results. The quality of FEA results depend on the patient-specific AAA geometry, the mechanical model used to describe the

material properties of AAA wall, the applied blood pressure, and the boundary conditions. Also, the computed strains and stresses are highly affected by the quality and complexity of the 3D reconstruction (the meshing, the number and type of finite elements) (Reeps et al., 2010). The arterial wall can be modeled as thick solid wall or as thin shell wall, and each assumption can result in a different stress distribution. Shell theory assumes the wall thickness to be small when compared to the diameter and many researchers have agreed to consider this theory a valid assumption. Zendehbudi et al, (Zendehbudi and Kazemi, 2007) reported that wall thickness is 6% of the aneurysmal diameter providing a justification for using shell theory. It is known that thick-wall theory allows the calculation of stress distribution along both the aneurysm length and wall thickness, while the thin-shell theory calculates the stress distribution only along the aneurysm length. Zendehbudi et al, (Zendehbudi and Kazemi, 2007) compared the maximum stress in circumferential and longitudinal direction for both thick wall and thin shell theory. The study assumed that thick wall theory is the most accurate method because it resolves stress in circumferential and longitudinal direction. The error in thin shell theory was calculated according to results obtained from thick wall theory. Results showed that thin shell theory had an error of 23% in axial stress and 0.1% in circumferential stress. Since circumferential stress is the main focus for AAA, it justifies the assumption that thin shell theory is accurate as well as faster. However, Zendehbudi et al, (Zendehbudi and Kazemi, 2007) proved that the percentage error for circumferential stress varies as blood pressure changes, providing evidence that the errors depend on physical and geometrical characteristics such as aneurysm radius, wall thickness, blood pressure, and axial tension.

Material property assumptions in FEA also greatly affect the final stress distribution. The AAA wall is a highly non-linear incompressible material that undergoes large strains (20-40%) prior to failure (Raghavan and Vorp, 2000). Stress prediction is critically affected by the material properties assumptions used to model the arterial wall. Generally, the aneurysmal wall is assumed to be isotropic, i.e. the material properties are identical in all the directions. The isotropy assumption is invalid since aortic tissue shows an anisotropic behavior, i.e. material properties differ between longitudinal and circumferential directions, with the circumferential direction presenting higher stiffness than the longitudinal (Volokh and Vorp, 2008). Finally, it is important to consider that the wall of an aneurysm has varying local material properties that can have a 20-fold difference in the space of a few centimeters (unpublished data, Di Martino's lab, (J. Thubrikar, 2001)). Therefore, an accurate prediction of the stress distribution can only be achieved accounting for the local variability in material properties and material strength.

Abdominal aortic aneurysm tissue models.

Many efforts were conducted to generate a mathematical model useful for describing the relationship between stress and strain in aortic tissue. Raghavan et al, (Raghavan and Vorp, 2000) proposed a two material parameter, hyperelastic, isotropic, and incompressible material model to describe the material behavior of AAA tissue. This model is not patient-specific nor does it take in to account the stage of AAA formation. The model has been a great step in theoretical simulation of AAA but it has rarely been used in clinical practice because of its lack of patient specific qualities. Martufi et al, (Martufi and Gasser, 2011) suggested a novel constitutive model for the vascular wall, which integrates the collagen's fibril and fiber levels with the tissue's continuum level. The model uses a probability distribution function that defines

the load-carrying mechanism at the fibril level to define material properties. However, this model requires initial material properties, which make the model not patient-specific. An important step in the improvement of material constitutive models for aneurysm tissue would be understanding how the tissue properties change at the different stages of the pathology.

CHAPTER 2 MOTIVATIONS

Advancement in AAA risk assessment and treatment are very limited because factors contributing to the development of AAA in human are still unknown. The evolution of human aneurysms can be described by four phases: formation, remodeling, pre-rupture, and rupture (figure 9). The general accepted characteristics of human AAA in literature are continuous increase in diameter, degradation of elastin as formation stage, increase in collagen synthesis during the repair stage (collagen I, III), degradation of collagen during the pre-rupture stage, and finally local failure of collagen that leads to rupture (Henderson et al., 1999, Martinez-Pinna et al., 2013, Rensen et al., 2007, Thompson et al., 1997, Raghavan et al., 1996, Wilson et al., 2003, Di Martino et al., 2006, Kadoglou and Liapis, 2004, Vorp and Geest, 2005, Martufi and Gasser, 2013). Since AAA is usually asymptomatic, collecting any data from the initial stages (formation and remodelling) is almost impossible because even when detected, most aneurysms are not surgically removed before they reach a threshold diameter of 5 - 5.5 cm (Smolock and Lyden, 2014, Shimazaki and Ueda, 2014). At this size an aneurysm is normally well-developed and cannot offer information on AAA formation and on the factors contributing to its development. In addition, there is no information collected at the time of surgical repair on the exact time frame and stage of aneurysm development. For example, we cannot speculate whether a patient with an aneurysm with maximum diameter of 5.5 cm had an aneurysm for 1, 5, or 10 years.

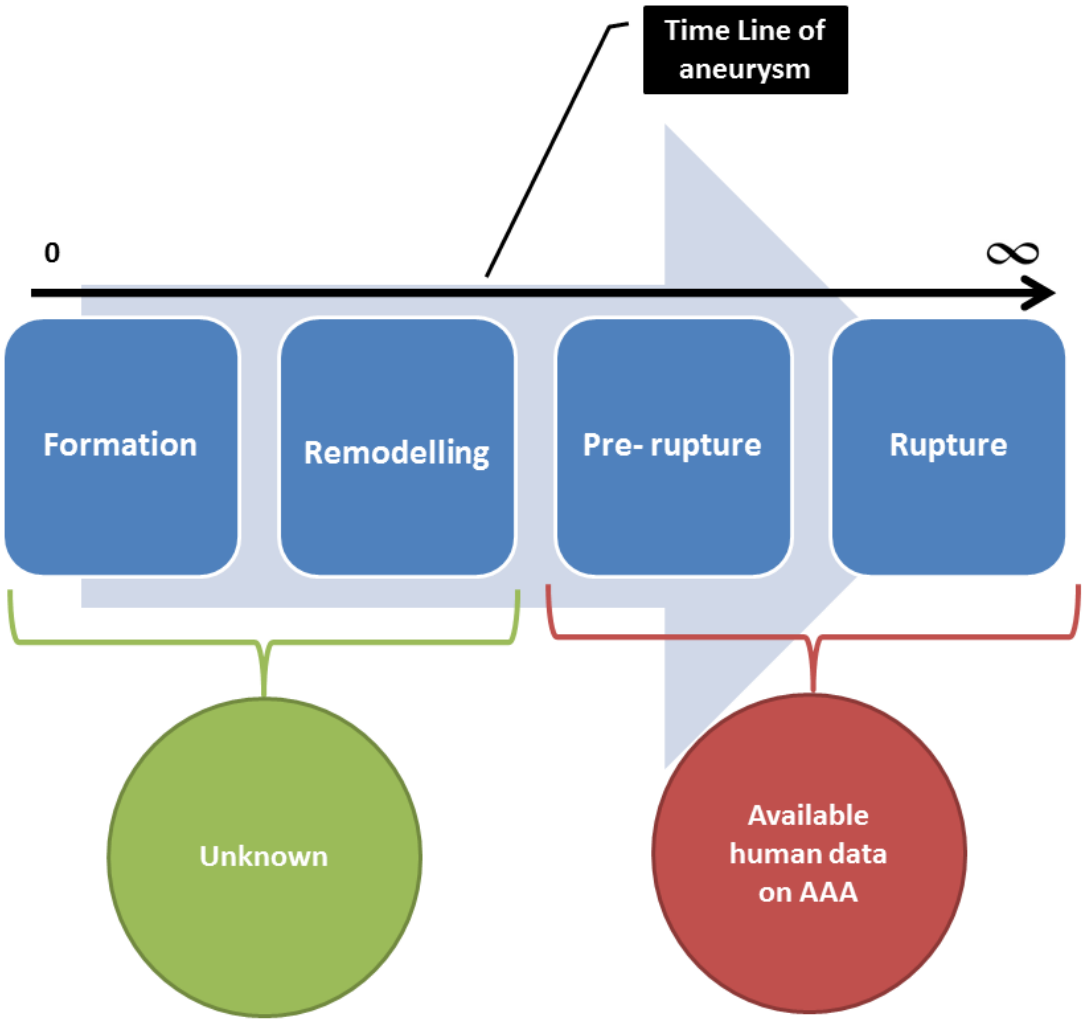

Figure 9: Lifespan of AAA in human. Most collected data from human are at advanced stages and there is a clear lack of data evaluating the remodeling of the aortic wall in the initial stages.

Problem Definition

One of the main issues facing the advancement of risk assessment of AAA is the lack of information on the AAA progression and detailed information on the remodeling of the aortic wall due to the alteration of extracellular matrix microstructure. In particular, loss of elastin has been consistently reported to accompany the development of aneurysms in humans.

Aims and Tasks

The main aim of this work was to understand the evolution of the mechanical and histological properties of the aortic tissue when elastin and extracellular matrix are disrupted, which have been proposed as one of the key aspects of aneurysm development. To achieve our aim, we developed a controlled model of AAA in rabbit and investigated the link between local wall material properties and structural damage. Finally, we observed similarities and differences between this model and human aneurysms. This study is a pilot study that was completed on a very limited number of animals to confirm the viability of the animal model and of the results before any further studies are conducted.

The tasks of this study are:

1. To create controlled AAA in rabbits.
2. To image rabbits using 3D angiography at different time points.
3. To characterize the local mechanical properties and strength using uniaxial and biaxial testing.
4. To characterize the microstructure and its changes during aneurysm formation and remodeling in a rabbit model.
5. To observe similarities and differences between this model and human AAA.

CHAPTER 3 ANEURYSM GENERATION AND IMAGING

Animals have been a crucial player in advancing medicine throughout history. They have been used to improve pharmaceutical drugs, medical devices, while also enhancing general understanding of many diseases (Tsui, 2010, Gertz et al., 2013). For example, they have been used to develop many new medical devices for the treatment of AAA. Since AAA is asymptomatic, most histopathological and mechanical testing studies of human AAA have been performed on advanced aneurysms that were collected at the time of autopsy or resected during surgery after exceeding maximum threshold diameter (Gertz et al., 2013, Lysgaard Poulsen et al., 2016). Therefore, animal models provide the researcher with in vivo understanding of the pathophysiology of AAAs and continue to play essential role in the development of pharmacotherapy and new technologies for aneurysm repair. Different animals are used for AAA models, such as rats, rabbits, dogs, sheep, and pigs, each with their own limitations and advantages. The method employed for the aneurysm generation has significant impact because it is commonly believed that animals do not naturally develop AAA. This could potentially be due to the possibility that it is challenging to discover them. In any case, this justifies the need to surgically induce AAA in animals for research purposes.

In this chapter, we present the most common animal models that have been used for AAA, including some recent findings from the rabbit model. These models provide researchers with important insights related to the early stages of AAA progression and assist in the development of biomechanical technology to better evaluate and treat it (Tsui, 2010, Gertz et al., 2013).

Techniques to Develop Aneurysm in Animals

Calcium chloride model.

Chemical substances such as calcium chloride ($CaCl_2$) have been used to generate aneurysms in animals since 1980s. This was first reported by Gertz et al, (Gertz et al., 1988) when he applied $CaCl_2$ to the right carotid artery in male New Zealand rabbits to study myocardial infraction in normal coronary arteries. He applied 0.5M $CaCl_2$ solution to the adventitial surface of the carotid artery and kept the entire vessel segment submerged in the solution for 15 minutes. Three weeks later the aneurysm was generated and endothelial cells were fragmented at the segment exposed to $CaCl_2$ solution. Histological examination demonstrated elastin calcification, loss of SMCs, and infiltration of inflammatory cells in the site of the arterial dilation (Gertz et al., 1988).

This approach to form aneurysm in New Zealand rabbits was first applied to the abdominal aorta by Freestone et al, (Freestone et al., 1997) using painting techniques. The isolated abdominal aorta was painted with $CaCl_2$ for 15 min. However, applying 0.25M $CaCl_2$ alone to the abdominal aorta resulted in no AAA formation up to 12 weeks after surgery. On the other hand, applying 0.25M $CaCl_2$ and 0.05 M thioglycollate, along with exposing the rabbits to a high cholesterol diet, developed AAA after three weeks (Freestone et al., 1997). This observation was confirmed by Bi et al, (Bi et al., 2013b) using bathing techniques. The isolated abdominal aorta is wrapped with sterile gauze and a syringe was used to wet the gauze with 0.5M $CaCl_2$ for 20 mins. However, there was no significant generation of AAA after one month of follow up (Bi et al., 2013b).

Many studies applied $CaCl_2$ technique not only in rabbits but also in other animals. Chiou et al, (Chiou et al., 2001) generated AAA in C57BL/6 mice by applying 0.68M $CaCl_2$ to the abdominal aorta for 10 min. Histological examination on AAA generated three weeks after surgery demonstrated SMC depletion, elastin degradation and infiltration of lymphocytes and macrophages. $CaCl_2$ solution was successful in creating AAA in genetically modified mice, and pigs. Gertz et al, (Gertz et al., 2013) investigated how the $CaCl_2$ affects aorta wall using Von Kossa-stained with correlative transmission electron microscopy. Their group demonstrated that the peri-adventitially applied $CaCl_2$ diffused into the aortic wall and bounded to the internal elastic lamina and the elastic lamellae in the media layer. This calcium– elastic complex altered the antigenicity of the elastic tissue and attracted inflammatory cells (monocytes and macrophages) that appeared to degrade the calcium– elastic tissue complex and disrupt the normal lamellar unit of the arterial media, resulting in progressive luminal dilatation (Gertz et al., 2013).

Elastase model.

The elastase-induced model was first described by Anidjar et al, (Anidjar et al., 1990). He infused pancreatic elastase into an isolated segment of rat abdominal aorta, resulting in the degradation of the medial elastic lamellae, an increase of inflammatory cells, and aneurysmal dilatation (Anidjar et al., 1990). Other studies have shown similar results in mice, rats, and rabbits, using different techniques to deliver elastase whether intraluminally or perivascularly to the adventitial surface (Lysgaard Poulsen et al., 2016).

In the studies of Bi et al, (Bi et al., 2013a), elastase infusion into the abdominal aorta of the male New Zealand White rabbit was delivered with different solution concentrations. He wrapped the isolated segment of abdominal aorta with sterile gauze and soaked it with elastase solution at 0.1, 5, and 10 units ml^{-1} for 30 mins. The aneurysm was generated in higher concentration, specifically 10 units ml^{-1}, and the size maintained after 5 months follow up. Another study of Bi et al, (Bi et al., 2013b) reported that the combination of elastase and 0.5M $CaCl_2$ was successful in developing aneurysm in New Zealand rabbits with no specification of gender. A 2 cm segment of abdominal aorta was wrapped with sterilized gauze and wetted with the mix solution of elastase (1 units/ µl) and 0.5M $CaCl_2$ for 20 min. Dilatation of the aorta was observed after 5 days and the aneurysm enlarged significantly after a month follow up. This combination stimulates an elastolytic cascade and inflammatory response in the aortic wall which results in continued enlargement of the aneurysm.

Physical model.

Chemicals have been mainly used to generate aneurysm but physical techniques have also been proven to be successful in large animals. These physical techniques generate aneurysms by damaging the aortic wall through cryogenic probes, carbon dioxide lasers or simply surgically resecting the media and adventitia of the aorta. Parodi et al, (Parodi et al., 1991) replaced a segment of infrarenal aorta in dogs with a fusiform synthetic aneurysm made of woven Dacron (Graft Model); whereas Whitbread et al, (Whitbread et al., 1996) replaced large white pig infrarenal aorta with fusiform segment of glutaraldehyde-tanned bovine internal jugular vein (Patch model). Another patch model was created by Criado et al, (Criado et al., 1995) where he sutured full thickness jejunal patches to longitudinal anterior aortotomies in dogs creating

infrarenal aortic aneurysms. Since the physical models do not replicate the pathology of aneurysms in humans, their use is mainly limited to the assessment of new intervention techniques for AAA repair.

Diagnostic Imaging

Medical imaging is a rapidly evolving technology for non-invasive vascular assessment and diagnosis. The increased use of advanced imaging technology, including computed tomography (CT), magnetic resonance (MR), ultrasound, and arteriography has led to the increased incidental detection of asymptomatic aneurysms (Edelman, 1993). Medical images can provide the clinicians with unique information about aneurysm progression and growth allowing for an improved planning of the clinical/surgical intervention (Golestani et al., 2015). MRI was used to detect motion properties of the blood but there were remarkable drawbacks. The use of contrast-enhanced MRI improved the noninvasive investigation of the vascular system and also tumor detection (Miraux et al., 2004). However, MRI lacks an important feature of direct three-dimensional (3D) volumetric reconstruction of the aneurysm which is important for precise planning of further endovascular interventions (Sherif et al., 2009). As an alternative to MRI, there is 3D angiography which is a technical revolution in imaging technology. It is mainly used in neurosurgery; when used in vascular applications, it allows improvement in the quality and safety of diagnostic and endovascular treatment procedures. 3D angiography images are obtained by reconstruction of a rotational angiography acquisition done on a C-arm spinning at 40 degree per second (Anxionnat et al., 1998). The 3D reconstruction of vessel provides a clear view of lesions, dissection, and adjacent structures (Abe et al., 2002).

Material and Methods

Surgical techniques.

Surgical techniques as described by Bi et al (Bi et al., 2013b), were used to generate aneurysms in three male New Zealand White rabbits (3 -3.5 kg, 13- 16 weeks, Charles River Laboratories, Quebec, Canada). The three rabbits were randomly assigned as follows: two weeks AAA, four weeks AAA, and six weeks AAA. One control rabbit was healthy and did not undergo surgery. The experimental models of AAA in the three rabbits were created via a 20 min periaortic incubation using 0.5 mol/L $CaCl_2$ (Zymetrix Lab, Calgary) and elastase (25.3 – 25.9 mgP/ml (0.5 ml), and 4.83 – 5.31 units/mgP, Cedarlane, Burlington, Canada). Animal care followed the conjoint health research ethics board standard for care and use of laboratory animals, and the protocols for animal experimentation were approved by the ethics committee. All surgeries were performed by a professional veterinarian technician, and all efforts were made to minimize suffering. The rabbits were housed in individual cages at room temperature in the animal care facilities. Rabbits were checked daily for any sign of pain or discomfort. No specific diet was followed as food and water were available all time.

The abdominal cavity was accessed by a midline abdominal incision where a 2 cm aortic segment between caudal mesenteric artery and median caudal artery was isolated (figure 10).

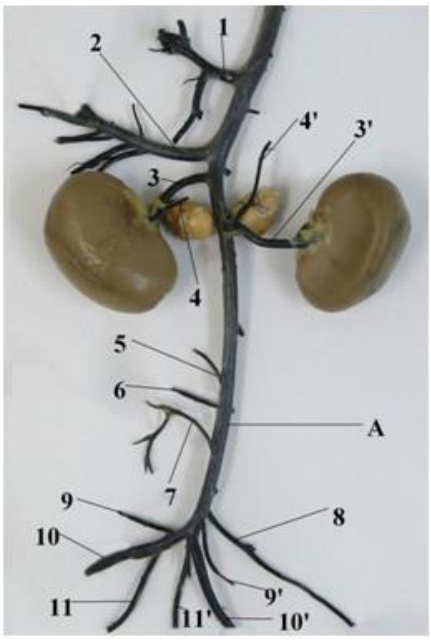

Figure 10: Pattern of abdominal aorta in rabbits.1 – celiac trunk, 2 – cranial mesenteric artery, 3 – dextral renal artery, 3' – sinister renal artery , 4 – dextral cranial abdominal artery , 4' – sinistral cranial artery, 5 and 6 – testicular/ ovarian arteries , 7 – caudal mesenteric artery, 8 – median caudal artery, 9 – dextral profound iliac circumflex artery , 9' – sinistral profound iliac circumflex artery, 10 – dextral external iliac artery, 10' – sinistral external iliac artery, 11 – dextral internal iliac artery, 11' – sinistral internal iliac artery (Nowicki et al., 2010).

The isolated region of the aorta was then circumferentially wrapped with a piece of sterile gauze and half-cradle (figure 11). The gauze was wetted with the mixture of $CaCl_2$ and elastase solution using a syringe needle where the solution was distributed to the gauze in all directions. The veterinarian technician and the principle researcher had to agree that the solution was distributed homogenously by visualizing different parts of the gauze. The cradle was used to protect other surrounding tissues from coming in contact with the solution.

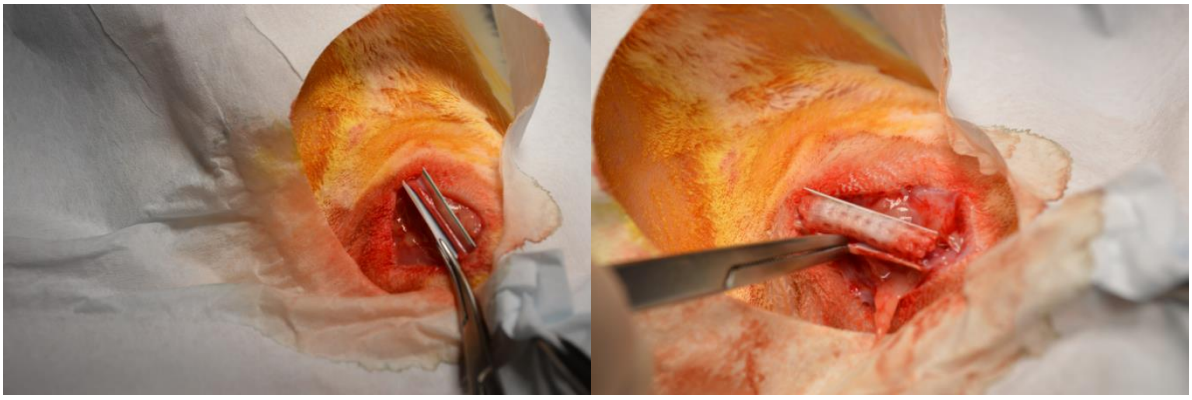

Figure 11: Generating aneurysm in rabbits using bathing techniques by wrapping gauze around the vessel.

After 20 min, the gauze was removed and the arterial segment was washed with a physiological saline solution. The abdominal incision was sutured and the rabbits were placed in a warm cage to recover.

Intra-arterial digital imaging.

On week 0 (healthy), 2, 4, and 6, the rabbits underwent serial intra-arterial digital imaging. We used 3D rotational angiography (Siemens, USA) (figure 12). The 3D rotational angiogram 5-second protocol resulted in a rotation angle of 200° with 1.5° increment and 133 projections (figure 11). Rotation speed was 40°/s and frame rate was 26.6 frame/s. Five ml of iodinated contrast agent (Optiray 300) was manually injected into the femoral artery through an angiocatheter at a rate of 1 ml/sec for a total volume of 7 mL per injection. The matrix of the FPD system was 1.024×1.024 (useful matrix was 960×960) and the pixel size was 0.184.

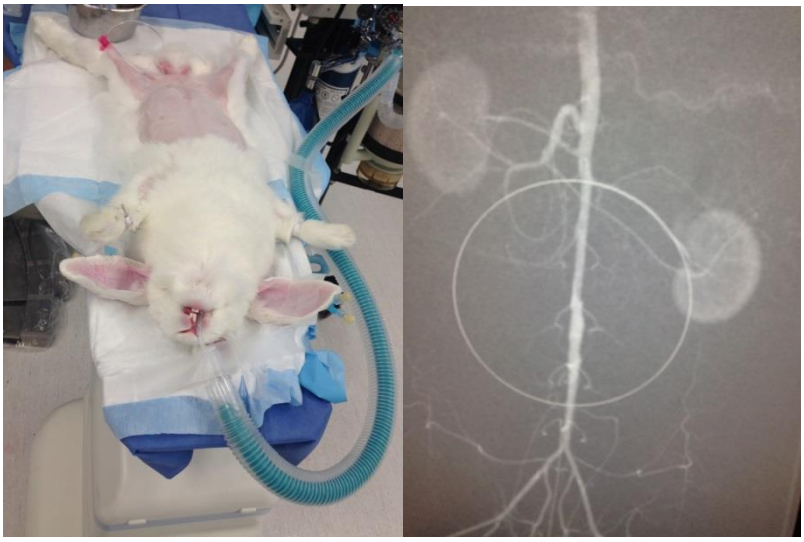

Figure 12: 3D Angiographic imaging of rabbits at six weeks AAA. A contrast agent was used to highlight the aorta.

Tissue collection.

After imaging, the rabbits were anesthetized with an ear vein injection of sodium pentobarbital at a dose of 30 mg/kg. The rabbits were anesthetized at week 0, 2, 4, and 6. All rabbit aortic tissue specimens were obtained according to the guidelines of the ethics board. Segments of aorta were obtained fresh, were placed in phosphate buffered saline (PBS) immediately, frozen at -80°C, and tested within 4-6 weeks after careful and slow thawing to preserve tissue quality.

3D model reconstruction.

The ScanIP software environment (Simpleware, Exeter, UK) was used for segmentation and 3D reconstruction of the AAA wall by thresholding, region growing algorithms, and manual corrections. Maximum diameter was measured from 3D reconstruction and 3D Angio Dicom using measuring tools in Simpleware (figure 13).

Statistical analysis.

No sample size justification or statistical analysis was performed because of the pilot nature of the study that included only one subject per treatment.

Results

All rabbits survived the surgical procedure and the imaging procedure. All three rabbits developed AAA. The maximum aneurysm diameter was observed in the four weeks AAA stage which was 6.92 mm, an increase of two times the original size (table 1). The smallest aneurysm diameter was observed in the six weeks AAA stage which was 4.45 mm.

Table 1: Maximum diameter of the aorta at healthy, two, four, and six weeks AAA in mm. The maximum diameter is measured using Simpleware tool.

	Maximum diameter mm
Healthy	3.25
2 weeks AAA	5.11
4 weeks AAA	6.92
6 weeks AAA	4.45

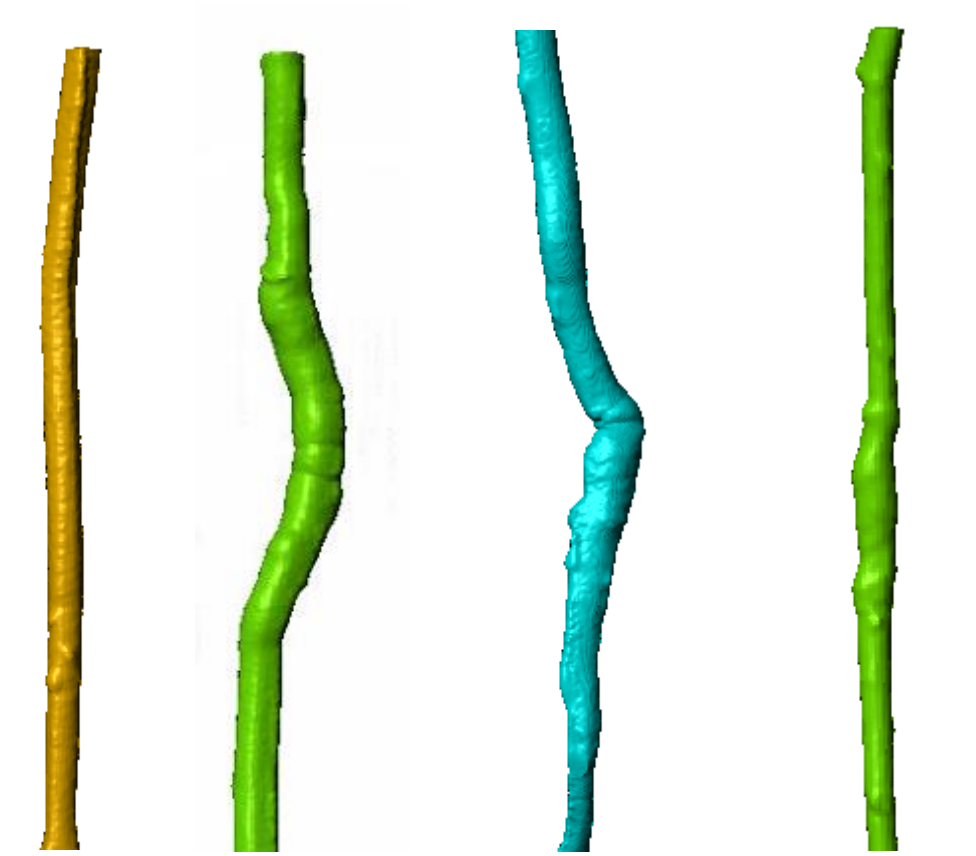

Figure 13: 3D reconstruction of AAA progress in rabbits. Dilation in the aorta is observed over time until it reduces at six weeks AAA.

Challenges

Acquiring 3D imaging of rabbits AAA was a big challenge for this study due to time management. Originally, the scanning of the rabbits was planned to be conducted by magnetic resonance imaging (MRI), which delayed the surgical procedures. Since we are using imaging techniques that are usually used for patients, we are limited with specific time mainly after 6 PM. Also, the MRI technician, principle investigator, surgeons, and veterinarian need to attend this

scanning, which caused more delays due to time conflicts. Finally, the MRI technician was not available to continue the study; therefore, we replaced MRI with 3D Angiography.

CHAPTER 4 MECHANICAL AND HISTOLOGY PROPERTIES

Understanding the biomechanical behaviour of the arterial wall is important to study AAA progression. This chapter reports the methods employed to assess the local biomechanical response of aneurysmal tissue obtained after AAA induction in a rabbit aorta. The study of mechanical properties of aneurysmal tissue at different time points is crucial to advance our understanding of aortic dilation, progression, and rupture of AAA. We performed uniaxial and biaxial mechanical testing following established protocols. Uniaxial tests are conducted by subjecting a sample to controlled deformation until failure, whereas in biaxial testing, the sample is stretched in two directions at different strain ratios (Monteiro et al., 2014, Teng et al., 2015). Uniaxial tests provide important parameters such as yield strength, ultimate strength, maximum elongation, and maximum tangential modulus while biaxial testing allows for anisotropy characterization of the tissue and provides complete experimental data that can be used to fit non-linear material models.

Mechanical properties of human healthy abdominal aorta and AAA have been quantified using uniaxial tests. Raghavan et al, (Raghavan et al., 1996) reported that the aneurysm failure stress in the circumferential direction was lower than healthy aorta. This was supported by Thubrikar et al, (J. Thubrikar, 2001) by comparing stress-strain curves for healthy aorta and AAA. The evidence suggests an overall stiffening of the AAA tissue. This phenomenon of material stiffening was also described in other publications. Di Martino et al, (Di Martino et al., 2006) performed uniaxial tests on ruptured and electively repaired AAA, and demonstrated that ruptured AAA had lower uniaxial strength and significantly thicker wall compared to electively

repaired AAA. Vorp et al, (Vorp et al., 2001) investigated the effects of thrombus on AAA, specifically hypoxia effects. He suggested that localized hypoxia occurs in regions of thicker thrombus in AAA which leads regional wall weakening. Raghavan et al, (Raghavan et al., 2006) demonstrated that the mechanical behavior of AAA tissue varied regionally and the failure tension of the specimen strip closer to the rupture site was low compared to its neighborhood in the same aneurysm. Vande Geest et al, (Vande Geest et al., 2006a) demonstrated that there were no statistical differences in strength between specimens taken from male and female patients, only a trend toward a decrease in strength in females as compared to males. Xiong et al, (Xiong et al., 2008) confirmed that AAA is stiffer and less distensible than healthy aorta under the same maximal stress. However, Raghavan et al, (Raghavan et al., 2011) demonstrated from his findings that ruptured AAAs are not weaker than unruptured ones on an average. This is not consistent with previous studies that supported the hypothesis that ruptured aortic aneurysms are globally weaker than unruptured ones. Monteiro et al, (Monteiro et al., 2014) performed uniaxial testing on 90 AAA patients and showed that failure properties are higher with patients who have maximum diameter more than or equal to 5.5 cm. Teng et al, (Teng et al., 2015) tested the different layers of aortic wall (Media, Adventitia) of AAA and healthy tissue. He suggested that the adventitia and media from AAA were less extensible compared with those of healthy, but the ultimate strength remained similar. Studies using destructive uniaxial biomechanical tests with fragments of human AAA are few; they tested different regions of aneurysms, ruptured or elective repair and each reported different values of failure stress (Table 2). There are clearly inconsistent results and further research is needed.

Biaxial tensile tests were also used to study the biomechanical behavior of human AAAs. The biaxial testing provides the multi-axial mechanical response of the aortic tissue, which can demonstrate important characteristics (Geest et al., 2004). Specifically, the nonlinearity of the AAA wall was more noticeable under biaxial than under uniaxial testing (Polzer et al., 2013a). Also, the biaxial mechanical testing allows for the investigation of the nature of mechanical anisotropy (Geest et al., 2004). An isotropic structure is one which exhibits the same properties or structure in all direction whereas an anisotropic shape exhibits different characteristic with different directions (figure 14) (Mitchell and Tojeira, 2013). Ideally the biaxial test produces the same behavior in axial or circumferential directions for isotopic materials. The orientation of fibers in the tissue is responsible for anisotropy where a high organized structural arrangement of fibers causes the arterial wall to be anisotropic (Gasser et al., 2006). Vande Geest et al, (Geest et al., 2006) tested 26 human AAA specimens and healthy aorta using biaxial testing. He demonstrated that AAA tissues are stiffer than healthy and concluded that aneurysmal tissue had an increase in mechanical anisotropy, with preferential stiffening in the circumferential direction (Geest et al., 2006). This was confirmed by O'Leary et al, (O'Leary et al., 2014) by testing AAA tissue form 28 patients as well as Pancheri et al, (Pancheri et al., 2016) by testing AAA tissue from 13 patients. Finally, the biomechanical response of biaxial testing is essential to understand AAA mechanical properties and specifically anisotropy.

Table 2: Summary of previous studies that used uniaxial testing on human AAA used. The number of patients, gender, ages is listed when applicable. The failure stress was measured according to specific criteria for each study.

Papers	Number of patients	Gender	Age years M ± SD	Failure stress MPa M ± SD or IQR
(Raghavan et al., 1996)	45 (Axial) 19 (Circumferential) 7 (Cadaveric donors)	-	69 ± 2 76 ± 2 47 ± 4	Elective repair axial, 0.86 ± 0.1 Elective repair circumferential, 1.02 ± 0.16 healthy aorta axial, 2.01 ± 0.39
(J. Thubrikar, 2001)	5		71 ± 10	Elective repair anterior circumferential with diameter >5 cm, 0.52 ± 0.2 Elective repair lateral circumferential with diameter > 5 cm, 0.73 ± 0.22 Elective repair posterior circumferential with diameter > 5 cm, 0.45 ± 0.14 Elective repair anterior axial with diameter >5 cm, 0.38 ± 0.18 Elective repair lateral axial with diameter > 5 cm, 0.51 ± 0.14 Elective repair posterior axial with diameter > 5 cm, 0.47 ± 0.3
(Vorp et al., 2001)	7	-	67 ± 6	Anterior wall with thrombus, 1.38 ± 0.19 Anterior wall without thrombus, 2.16 ± 0.34
(Raghavan et al., 2006)	4	1F 3M	68 ± 17	Ruptured anterior, 1.26 ± NA Ruptured posterior, 1.47 ± NA
(Di Martino et al., 2006)	16 (Elective repair) 9 (Ruptured AAA)	4F,12M 1F,8M	73 ± 3 72 ± 3	Ruptured, 0.54 ± 0.09 Elective repair, 0.82 ± 0.06
(Vande Geest et al., 2006a)	34	10F 24M	-	Elective repair anterior female, 0.67 ± 0.08 Elective repair anterior Male, 0.87 ± 0.07
(Vande Geest et al., 2006b)	29	11F 18M	73 ± 13	Elective repair, 0.80 ± NA
(Xiong et al., 2008)	14 (Elective repair) 6 (Cadaveric donors)	3F,11M 3F, 3M	68 ± 6.22	Elective repair anterior axial, 0.93 ± 0.25 Healthy aorta axial, 1.15 ± 0.28 Healthy aorta circumferential, 1.03 ± 0.33
(Raghavan et al., 2011)	13	4 F 9 M	74 ± 11	Ruptured, 0.95 ± 0.28 Anterior elective repair, 1.02 ± 0.28 Posterior elective repair, 1 ± 0.46 Axial elective repair, 1.03 ± 0.21 Circumferential elective repair, 0.65 ± 0.09
(Reeps et al., 2013)	50	3 F 47 M	68 ± 8	Elective repair, 1.06 ± 0.49
(Monteiro et al., 2014)	90	24 F 66 M	69 ± NA	Elective repair asymptomatic Max Diameter < 5.5 cm, 0.77 (0.34 – 1.02) Elective repair asymptomatic Max Diameter > 5.5 cm, 0.90 (0.70 – 1.30) Elective repair symptomatic (Ruptured) Max Diameter < 5.5 cm, 0.86 (0.57 – 1.29) Elective repair symptomatic (Ruptured) Max Diameter > 5.5 cm, 1.05 (0.82 – 1.51)
(Teng et al., 2015, Monteiro et al., 2014)	11	3 F 8 M	61 ± 7	Healthy adventitia, 0.65 (5.33, 8.42) Healthy Media, 0.33 (2.33, 4.41) Elective repair adventitia, 0.45 (2.32 – 5.93) Elective repair media, 0.34 (1.81 – 7.18)

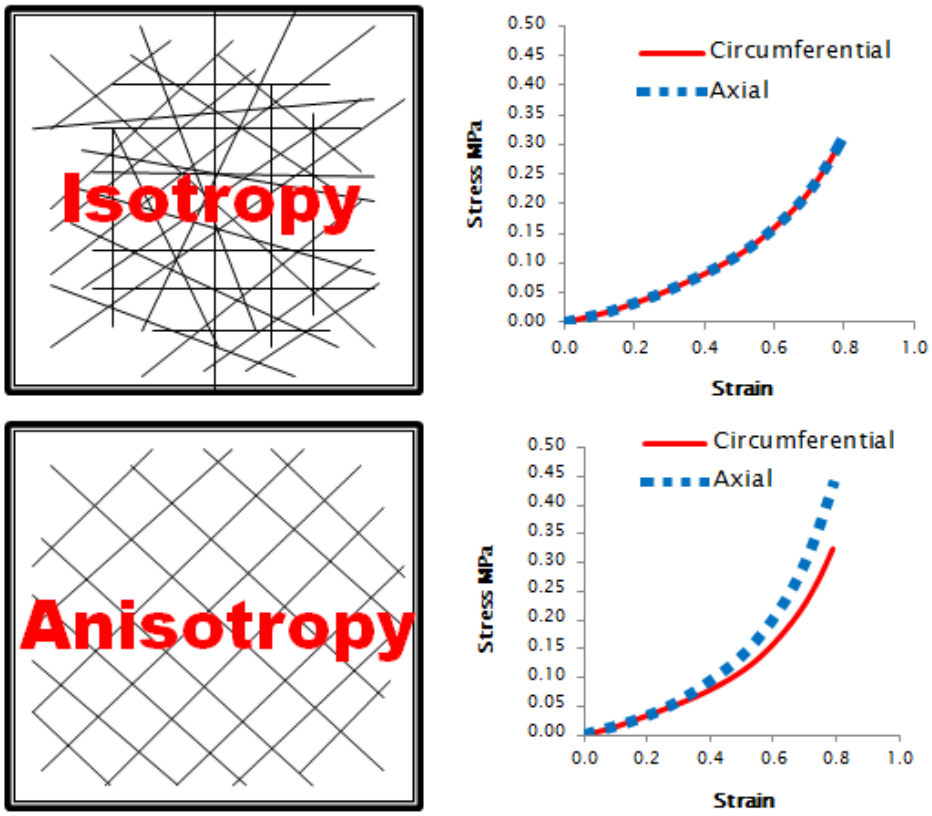

Figure 14: Left: schematic representation of fiber orientation in a tissue; Right: example of isotropic (top right) and anisotropic (bottom right) mechanical behaviour obtained from a biaxial test. A biaxial test produces ideally a similar behavior in all directions for isotropy material whereas anisotropy result in a different behavior depending on the direction.

Histological examination of AAA demonstrates the pathophysiological processes in aortic aneurysm wall which is important to understand the wall weakening phenomena. The studies that investigated histopathology of AAA revealed degradation of elastin with increased disorganized collagen fibers, disruption in the wall layers, increased wall thickness, proliferation of fibroblasts, and media and adventitia inflammation. The elastin fibers were disrupted in the media of AAA compared with the media of healthy aorta (figure 15). Also, increased turnover of collagen was observed in AAA compared with control, which is related positively to increase

stiffness in the wall of AAA (Amalinei and Căruntu, 2013, Vorp et al., 2001, Tsamis et al., 2013, Rodella et al., 2016, Lindeman et al., 2010, Michel et al., 2010, Schlatmann and Becker, 1977).

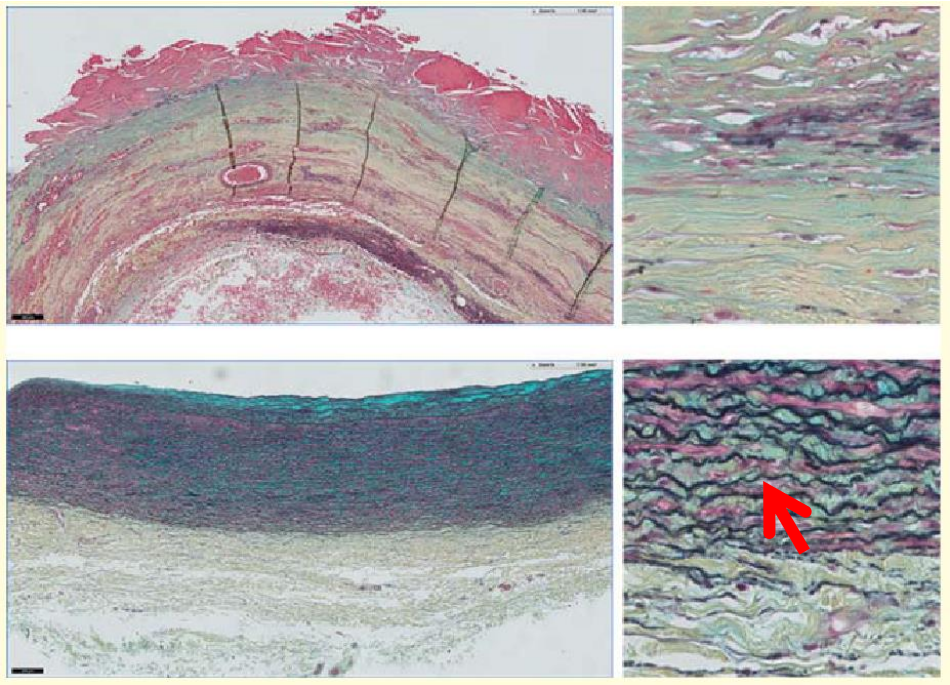

Figure 15: Movat staining of a large abdominal aortic aneurysm (top) and a normal infra-renal aorta (bottom) (overview (5x, left) and detail (40x, right). The red arrow indicates the elastin (black) (Lindeman, 2015).

In addition to mechanical testing, we performed detailed histological analysis to provide additional information on the microstructure of the aortic tissue and the changes after acute induction of AAA in a rabbit aorta. We performed Verhoeff-Van Gieson (VVG), Movat's, and Picro Sirius Red (PSR) staining. VVG stain highlights elastin fibers in connective tissue whereas PSR stain highlights collagen fibers with fluorescence microscopy (Vogel et al., 2015). Movat pentachrome stain highlights different components of the connective tissue including elastin fibers, collagen fibers, ground substance, and muscle cells (Doello, 2014).

Methodology

Specimen preparation.

Samples were collected after surgery from the abdominal aorta; refer to chapter 3 for a description of the surgeries. Seventy-four uniaxial and seven biaxial samples were collected from the three rabbit aortas (table 3).

Table 3: Number of specimens tested for uniaxial and biaxial.

	Circumferential Specimen Tested	Axial specimen Tested	Biaxial Specimen Tested
Healthy	25	4	2
2 week AAA	8	10	1
4 week AAA	8	6	3
6 week AAA	6	5	1

All the samples were gently defrosted by placing the tissue in a cold PBS bath and left at a temperature of 4C. The aortic tissues were first cleaned from surrounding adipose and connective tissue, and anatomical landmarks (the branching of common iliac arteries) were used to ensure consistent sample locations. Uniaxial and biaxial samples were cut into small pieces in longitudinal and circumferential directions. The typical uniaxial sample size was 8×1.8 mm for aneurysmal tissue and 4×1 mm for healthy tissue, whereas, the biaxial sample size was 5×5 mm for both tissues. Another eighteen samples were immediately submerged in 10% buffered formalin for the histologic study. Finally, the specimens were frozen at -80C until testing. Prior to testing, the thickness was measured using digital caliper at three locations for all tissue samples.

Uniaxial testing.

A Bose electroforce 3200, 10 N load cell, Benchtop Tester (TA instrument, New Castle, United State) device with custom fabricated specimen bath and custom soft tissue grips were used to conduct uniaxial testing (figure 16). Each specimen strip was clamped and glued to the grips attached to the crossheads of the test device. The gage length (L_o) of the specimen strip between the clamps was recorded using caliper after preloading the specimen with a 0.01N force. All specimen tests were performed with the tissue submerged in a 37C PBS solution bath to maintain moisture. The testing protocol consists of an extension at 20% of specimen length/min until failure, while recording the force and extension at an acquisition rate of 5 Hz. Since the specimens were very small, the location of specimen failure with respect to the clamps was recorded to identify and discard specimens that failed too close to the clamp (within 1 mm). The resulting uniaxial force-displacement data were converted to first Piola–Kirchhoff and strain measure, by using the following equations:

$$P = \frac{F}{A}$$

Where P is the first Piola-Kirchoff stress, F is the applied force and A is the initial surface area.

$$\varepsilon = \frac{\Delta L}{L_0}$$

Where ε is the engineering strain, ΔL is the deformation, and L_o is the gage length.

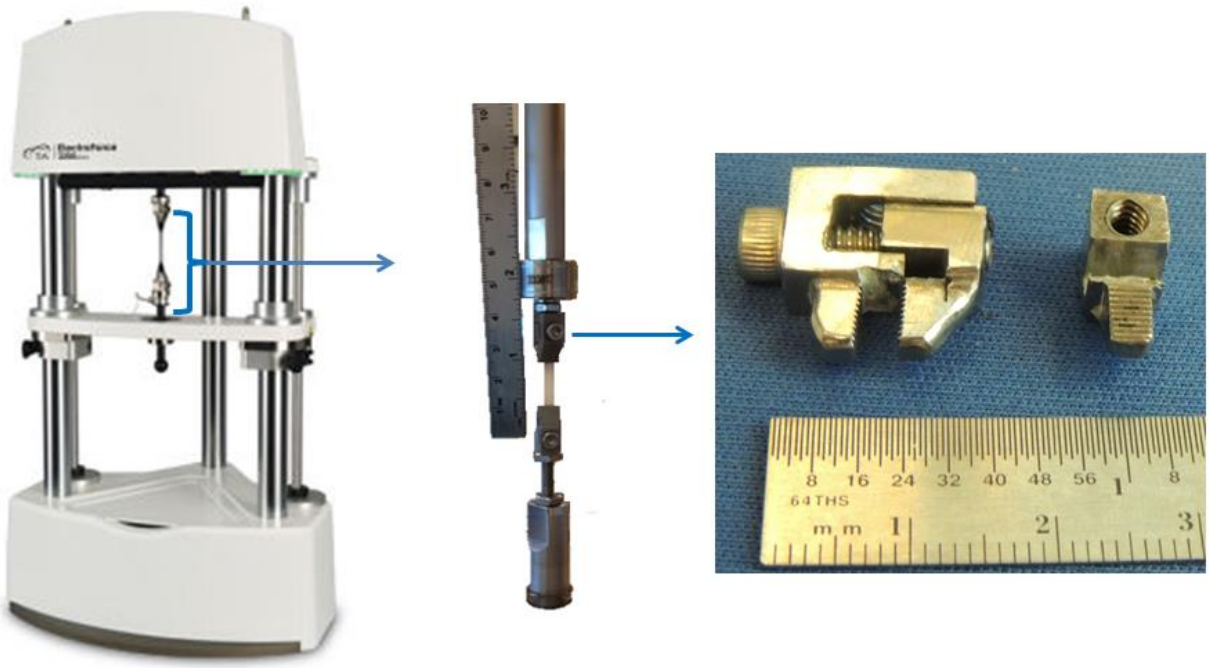

Figure 16: Uniaxial test setup (Zymetrix lab, 2016).

Biaxial testing.

Specific details of the biaxial test methods have been recently reported (Rosin et al., 2016). AAA wall samples were tested using a four-motor biaxial testing system (ElectroForce Systems, TA Instruments, Springfield, MO), designed to allow independent control of each motor. 5×5 mm samples were mounted to the four linear motors with four hooks per each side, attached with surgical sutures and small hooks (Figure 17), and submerged in PBS 37C. Five markers (dots) were drawn in the middle of the specimen allowing contactless tracking of tissue strain with a camera tracking system. These dots were made using a surgical skin marker. Prior to testing, all specimens were pre-stressed in circumferential and axial directions by 0.05N to avoid any bending effect during biaxial testing and force values were recorded using two 22 N load cells.

The testing protocol was controlled displacement under cyclic sinusoidal loading. The stress and stretch data were recorded for the following protocols:

- u_x: u_y =1 : 1, equal biaxial loading where an equal maximum stretch of 40% , 60%, and 80% of the original sample length was reached in both deformed directions.
- u_x: u_y =1 : 0.75, one direction was pulled to the maximum and the other to 75% of the original sample length .
- u_x: u_y =1 : 0.5, one direction was pulled to the maximum and the other to 50% of the original sample length.
- u_x: u_y =0.5 : 1, one direction was pulled to 50% and the other is to the maximum of the original sample length.
- u_x: u_y =0.75 : 1, one direction was pulled to 75% and the other to maximum of the original sample length.

Each sample was tested by running each testing protocol for 10 cycles at a rate of 0.3 mm/s. Data were then collected on the 10th cycle at a frequency rate of 200 Hz after achieving pre-conditioning. Due to the low strain rate, the test can be regarded as quasi-static equilibrium state, where the strain relaxation is assumed to be negligible. Global and local stretches were tracked using the motor control and the digital video extensometer (with a resolution of 1,024×1,024 pixels), respectively.

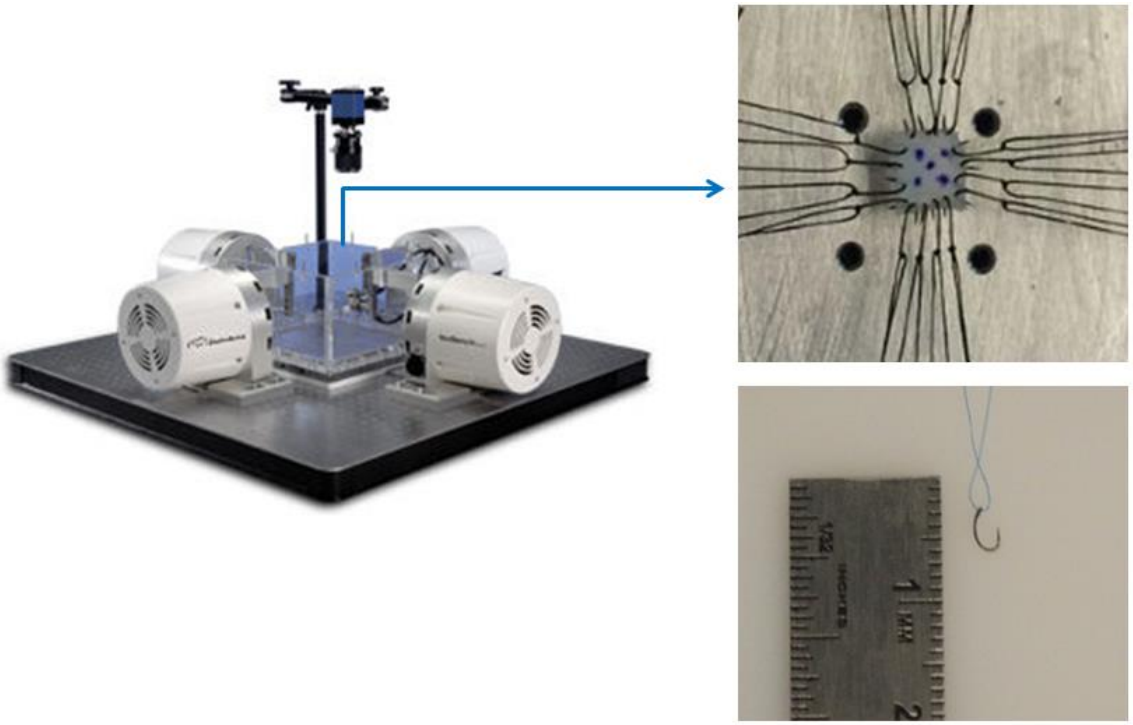

Figure 17: Biaxial testing setup (Zymetrix, 2016).

For homogeneous planar biaxial deformation under low shear assumption, the deformation gradient F has a diagonal form:

$$F = \begin{bmatrix} \lambda_1 & 0 & 0 \\ 0 & \lambda_2 & 0 \\ 0 & 0 & \lambda_3 \end{bmatrix}$$

Where λ_1, λ_2, λ_3 are the principal stretches.

From F we obtained the right Cauchy–Green deformation tensor as:

$$C = F^T F$$

And then the Green–Lagrange strain tensor according to the equation:

$$E=1/2\ (C- I)$$

where I is the second order identity tensor. Due to the homogeneity assumption, the stress field in the specimen can be estimated in terms of the first Piola– Kirchhoff tensor P, expressed as force per unit of undeformed area:

$$P = \begin{bmatrix} f_1/L_2h & 0 & 0 \\ 0 & f_2L_2/L_1h & 0 \\ 0 & 0 & 0 \end{bmatrix}$$

where f_1 and f_2 are the forces measured by the load cells, L_1 and L_2 are the in-plane undeformed tissue lengths and h is the undeformed tissue thickness.

The second Piola–Kirchhoff stress tensor S can be computed from P:

$$S = \begin{bmatrix} P_{11}\lambda_2\lambda_3 & -P_{11}\kappa_2\lambda_3 & 0 \\ -P_{22}\kappa_1\lambda_3 & P_{22}\lambda_1\lambda_3 & 0 \\ 0 & 0 & 0 \end{bmatrix}$$

where the in-plane shear components (off-diagonal) of the S tensor approach zero due to negligible shear ($\kappa_1 = \kappa_2 = 0$). The stress- strain curves were plotted in both directions.

In order to evaluate the difference in behavior between the two loading directions an anisotropic constitutive model was used to fit the data. The nonlinear behavior of the stress–strain curves suggests a hyperelastic behavior such as a 4-parameter Fung-elastic material model for soft tissues. According to the constitutive equation of the Fung model, the strain energy function has the form:

$$W(Q) = \tfrac{1}{2} c_f (e^Q - 1)$$

with

$$Q = a_1E_{11}^2 + a_2E_{22}^2 + 2a_3E_{11}E_{22}$$

where c_f, a_1, a_2, and a_3 are material parameters. For an incompressible material, the second Piola–Kirchhoff stress tensor can be represented as

$$S = pC^{-1} + \frac{\partial W(E)}{\partial E}$$

where p is the Lagrange multiplier introduced to enforce incompressibility. In our case, the only nonzero components of S are as follows;

$$S_{11} = C_F(a_1 E_{11} + a_3 E_{22})$$

$$S_{22} = C_F(a_2 E_{22} + a_3 E_{11})$$

The stress–strain curves for each of the five protocols obtained experimentally for each specimen were fitted to the above relationships (Levenberg–Marquardt nonlinear regression algorithm; SigmaPlot, Systat Software, Inc., San Jose, CA). To provide a representative index of the tissue mechanical response, the parameter ϕ was computed

$$\phi = \min\left(\frac{a_1 + a_3}{a_2 + a_3}, \frac{a_2 + a_3}{a_1 + a_3}\right)$$

This parameter evaluates how the mechanical properties along the two in-plane directions of loading contribute to the stiffness, with 1 indicating a perfectly isotropic material and smaller values indicating increasing anisotropic behavior.

The biaxial curves were averaged for the same rabbit when applicable using Matlab (The MathWorks Inc, 2016). Strain values for each rabbit were averaged and the stress for each curve was identified at fixed strain points. The stress values were then averaged for the same fixed strain value to obtain average curves, for representative purposes.

Histological analysis.

The samples fixed in 10% buffered formalin solution were processed at The Core Histopathology of Libin Cardiovascular Institute of Alberta, University of Calgary. Aortic

specimens were cut in 5 μm thick slices and prepared by the same laboratory technician. The slices were stained with Movat's pentachrome stain, VVG for elastin, and PSR for collagen under conventional light or polarized microscopy (table 4). The image of the stained sections obtained by microscopy was captured by a DP73 Olympus video camera (Olympus, Massachusetts, USA), coupled to the microscope, and transmitted to the computer with the software Image Analysis System from Leica (Quantimet-500; Leica Microsystems, Wetzlar, Germany). The magnification used for all histology images is 10X. The color code for all stains is provided in table 4. Neither scoring system nor blind viewing was conducted in this study.

Movat pentachrome stain highlights vascular smooth muscle cells, elastin, collagen, fibrin, and ground substance in the tunica media that can be observed as red, black, yellow, bright red, and blue respectively. In order to quantify the different constituents, all slides were scanned and turned into digital images. The computer software (Aperio) uses a color algorithm that measures hue and saturation that has been pre-assigned by a pathologist experienced in colorimetric analysis. The regions of interest were analysed and a percentage intensity of each of the pixels were identified and recorded.

Because the mechanical properties of the arterial wall depend largely on orientation and density of collagen fiber bundles, we used the semi-automated method developed by Novak et al, (Novak et al., 2015) to evaluate the direction of the fibers from two-dimensional polarized light microscopy images of PSR stained sections. On average, four areas were analyzed per slide, two for media and two for adventitia. The proposed algorithm took between 15 and 35 min to analyze points in the aortic tissue. The result of the algorithm is a map of local orientations and

histograms of the distribution of the orientation of the fibers in the tissue. The parameter b (dispersion) of the Von Mises distribution of the fibers orientation was calculated for each individual slice and for the two layers (media and adventitia) when possible (Novak et al., 2015, Polzer et al., 2013b). We analyzed 72 areas and capture 1440 pictures. The analysis of the PSR slices was conducted by Kamil Novak and Stanislav Polzer from Brno University of Technology.

Table 4: Color code for different histology stains.

	Movat	VVG	PSR (polarized)
Black	Elastic fibres	Elastic fibers	
Yellow	Collagen fibers	Tissue elements	
Blue	Ground substance		
Red	Muscle	Collagen fibers	
Bright red	Fibrin		
Yellow-orange			Thick collagen fibers
Green			Thin reticular fibers

Statistical analysis.

No sample size justification or statistical analysis was performed because of the pilot nature of the study that included only one subject per treatment.

Results

The results from the uniaxial tests of healthy and AAAs samples were compared in term of sample width, wall thickness, failure stress, and failure strain (Table 5 and 6). All results are reported based on observation not statistical significance due to the pilot nature of this study. Only samples that had failure in the middle of the gauge length were considered for analysis, which is at least 1 mm away from grips. The mean values of failure stress were higher in the

healthy aorta compared to the two, four, and six weeks AAA. The wall thickness mean value was smaller in the healthy aorta compared to all the aneurysmal tissues. The mean values of Failure strain of the healthy and the two weeks AAA were higher than four and six weeks AAA, with four weeks AAA being the smallest. The curves of healthy, two, four, and six weeks AAA were plotted in axial and circumferential direction (figure20, figure 21). In general, all aneurysmal walls exhibited a trend where thicker walls were showing lower failures stress especially in the four weeks AAA (figure 23). The uniaxial properties of aneurysmal walls differ with location in the same rabbit (figure 24, 25, 26, 30, 31, 36, 37).

The stress-strain curves suggest stiffer behavior of circumferential samples compared to longitudinal samples for both the healthy and the six weeks aneurysmal aorta. This observation was the opposite for two and four weeks AAA which presented stiffer properties in the longitudinal direction (figure 22, 27, 32, and 38). The degree of anisotropy, which indicates the relative amount of parallel fibers, was calculated based on the Fung constitutive model. The healthy tissue had more anisotropic behavior than aneurysmal tissue. In aneurysmal tissues, more isotropic behavior was detected with the most isotropic behavior observed in four weeks sample 1 (table 7, figure 18).

Histological examination of the healthy segments revealed that the aortic wall was regular, and the tunica media as well as the elastic internal and external lamina were intact (figure 24). On the other hand, histological examination of aneurysmal aortic wall revealed that the aortic wall was disorganized and the elastin fibers had almost entirely disappeared (figure 28, 29, 33, 34, 35, 36, and 39). Based on visual observation, the two week aneurysm had more elastin component when

compared with four and six week aneurysmal tissue. The aneurysm is not homogenous and shows a variation in histological analysis for the same rabbit. For example, we observed variation in elastin component throughout the same slice for the four weeks AAA, pointing out that elastin degradation is not uniform in adjacent areas (figure 35). The same histological variability is observed in two and six weeks aneurysms. Based on visual observation, we noticed an increase in fibrin in all stages of aneurysm formation, especially in the four weeks aneurysm. Also, the collagen content increased as the aneurysm progressed and increases in size. The six week AAA presented particularly high collagen content in the media layer but also a reduction in fibrin content opposite to the trend observed for the other phases of the AAA formation.

The maps of local fibers orientation and corresponding histograms of samples processed using PSR stain under polarized microscopy were analyzed (figures 40). The histogram of healthy aorta, in adventitia layer, clearly exhibits multiple peaks corresponding to different orientation angles, and points to a larger variability in fibers orientation, without a predominant direction. On the contrary for the two and four week aortas, the histograms show almost homogeneous fiber orientations with one distinct peak corresponding to the predominant direction. For the last aneurysm stage, the six week AAA, the histogram presents again multiple peaks showing a higher dispersion in fibers orientation, similar to the healthy tissue. The overall results indicate that the mean b-value for the media layer increases sharply from two week AAA to four week AAA and then decreases back for the six week AAA (table 8, figure 19), with a dispersion value very similar to the healthy reference tissue. On the other hand the adventitia layer exhibits an increase in orientation variability until the four week aneurysm and a decrease at six weeks induction stage, which is again similar to the healthy aorta.

Table 5: Uniaxial mechanical properties in the circumferential direction for all the aortas.

	Mean width mm	Mean Thickness mm	Mean Failure Stress MPa	Mean Failure Strain
Healthy	1.29±0.18	0.1	3.11±1.96	0.35±0.15
2 week AAA	1.15±0.24	0.56±0.24	0.68±0.79	0.35±0.32
4 week AAA	1.30±0.34	0.65±0.30	0.59±0.41	0.15±0.07
6 week AAA	1.25±0.23	0.55±0.20	1.84±1.54	0.25±0.09

Table 6: Uniaxial mechanical properties in the longitudinal direction for all the aortas.

	Mean width mm	Mean Thickness mm	Mean Failure Stress MPa	Mean Failure Strain
Healthy	1.27±0.44	0.1	3.28±2.71	0.34±0.19
2 week AAA	1.67±0.36	0.74±0.25	0.69±0.39	0.28±0.19
4 week AAA	1.30±0.30	0.61±0.16	0.62±0.43	0.15±0.08
6 week AAA	1.10±0.27	0.39±0.21	1.64±1.42	0.26±0.11

Table 7: Biaxial anisotropy properties of aorta walls.

	Anisotropy parameter	Maximum displacement %
Healthy Sample 1	0.45	80
Healthy Sample 2	0.76	60
2 week AAA Sample 1	0.87	40
4 week AAA Sample 1	0.97	60
4 week AAA Sample 2	0.84	80
4 week AAA Sample 3	0.73	60
6 week AAA Sample 1	0.86	60

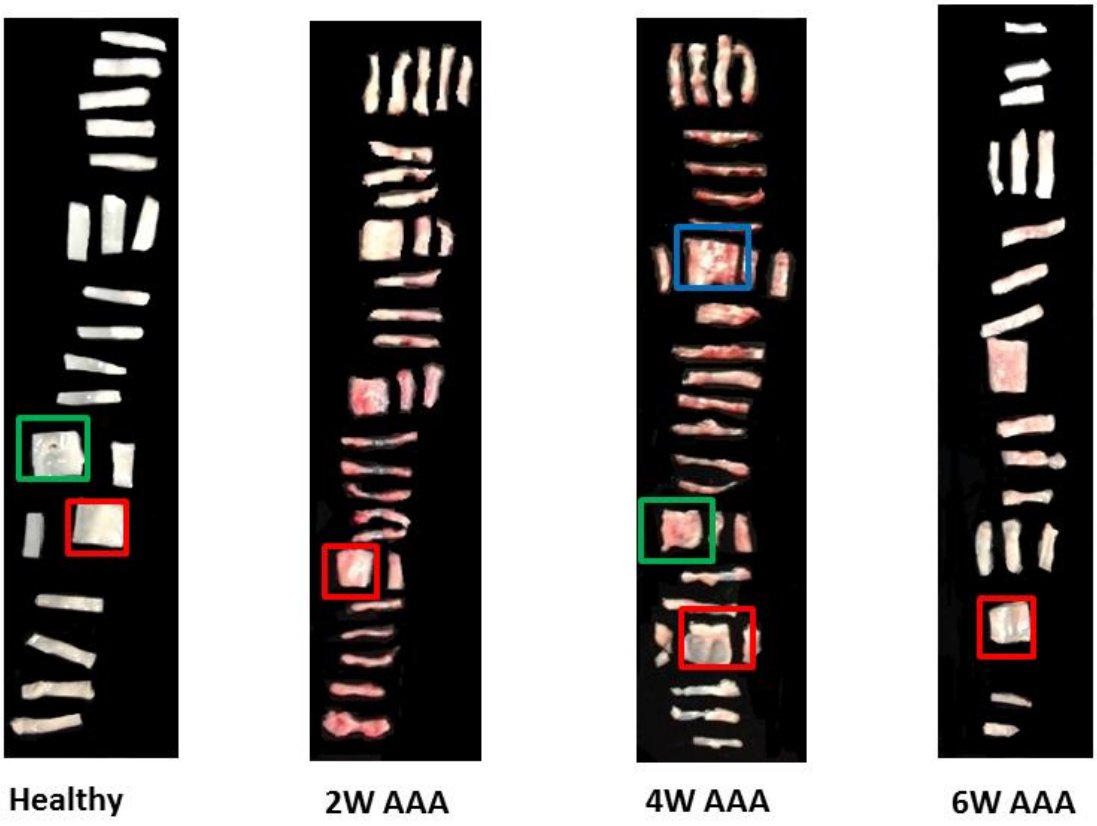

Figure 18: Biaxial sample location in healthy, two, four, and six weeks AAA.

Table 8: Dispersion parameter (b) for the media and adventitia layers in all the aortas.

b-parameter of Von Mises Distribution (Polzer et al., 2013b)

	Media Layer			Adventitia Layer		
	Mean	Median	S.D.	Mean	Median	S.D.
Healthy	4.47	3.49	3.24	1.48	1.23	0.80
2 week AAA	6.40	6.60	3.10	2.60	1.69	2.04
4 week AAA	9.45	7.30	7.58	2.01	1.43	1.80
6 week AAA	4.48	4.41	1.50	1.20	0.64	0.82

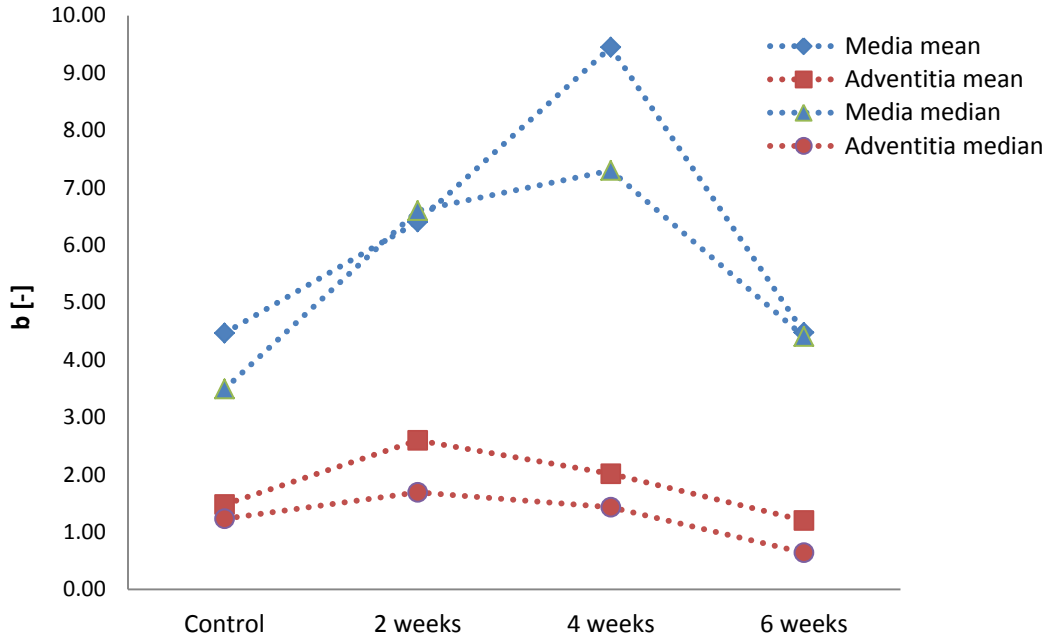

Figure 19: Von Mises dispersion parameter b obtained from the analysis of the PSR stained sections for the different experimental times (two weeks, four weeks, six weeks, and control).

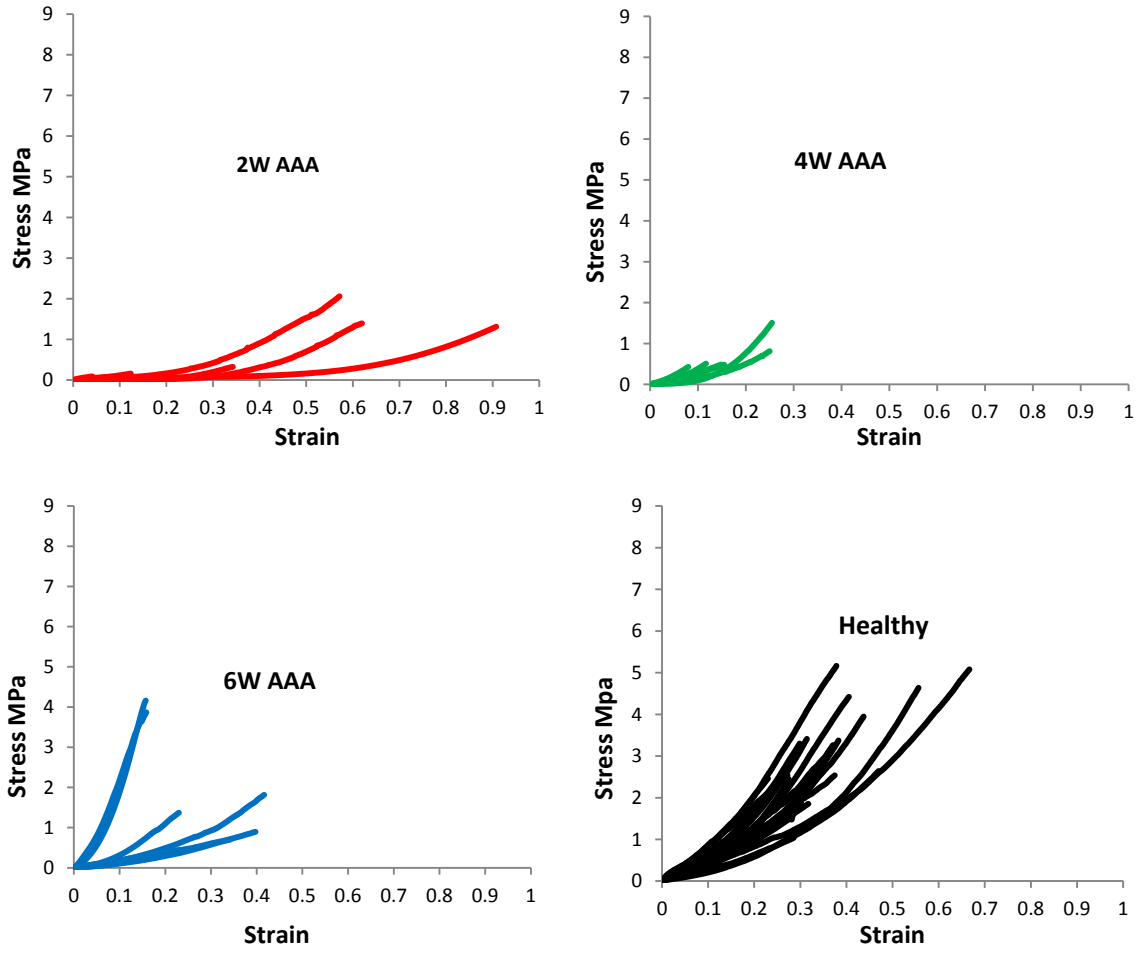

Figure 20: Uniaxial test data in the circumferential directions for healthy, two week AAA, four week AAA, and six week AAA.

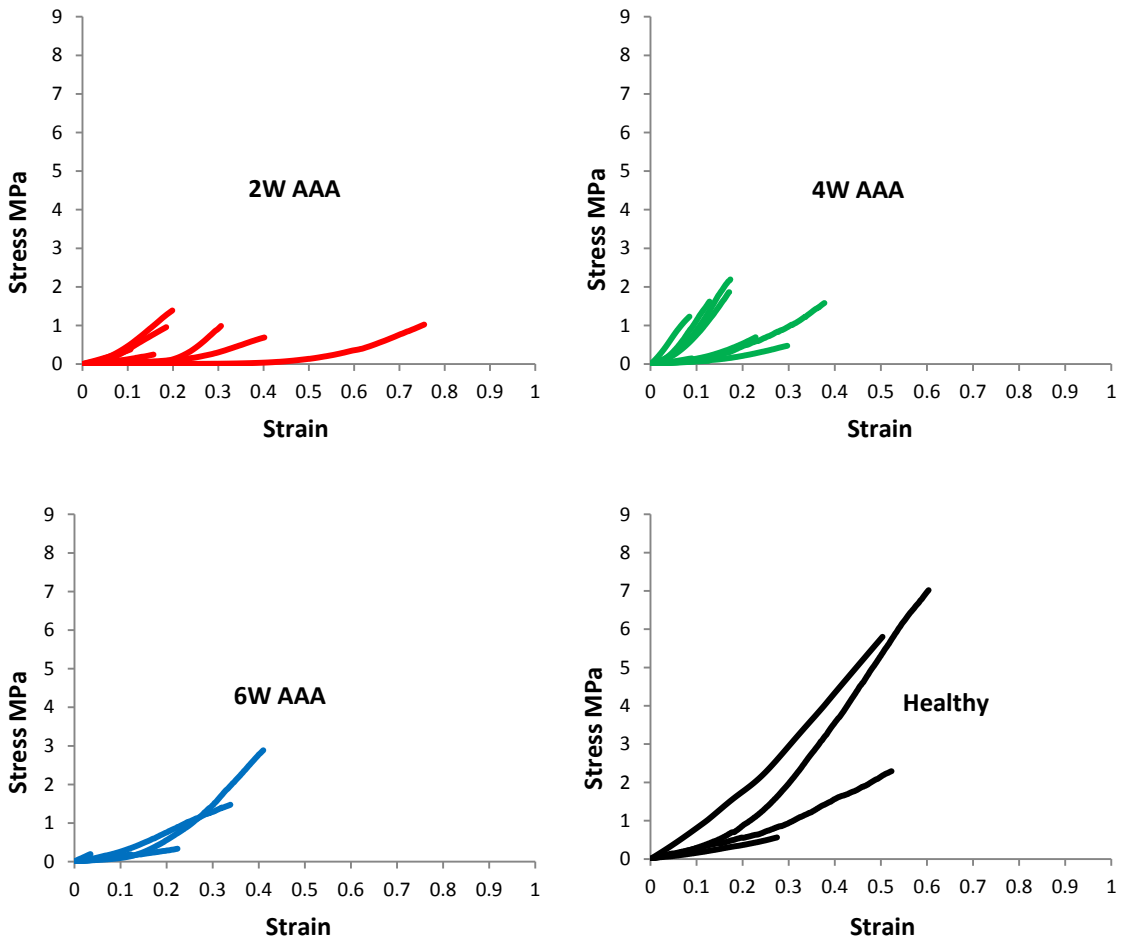

Figure 21: Uniaxial test data in the axial directions for healthy, two week AAA, four week AAA, and six week AAA.

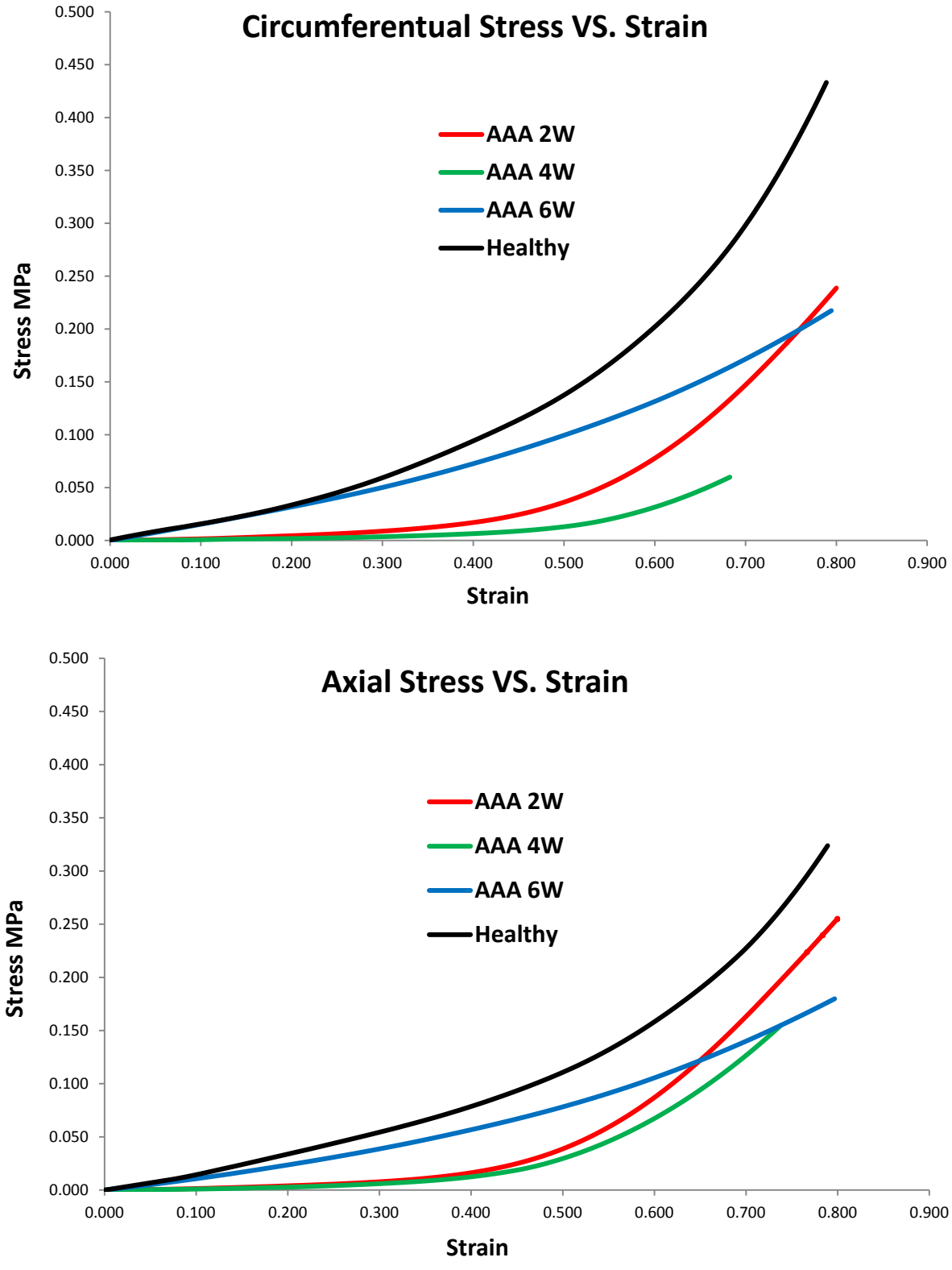

Figure 22: Averaged biaxial data in circumferential and axial directions.

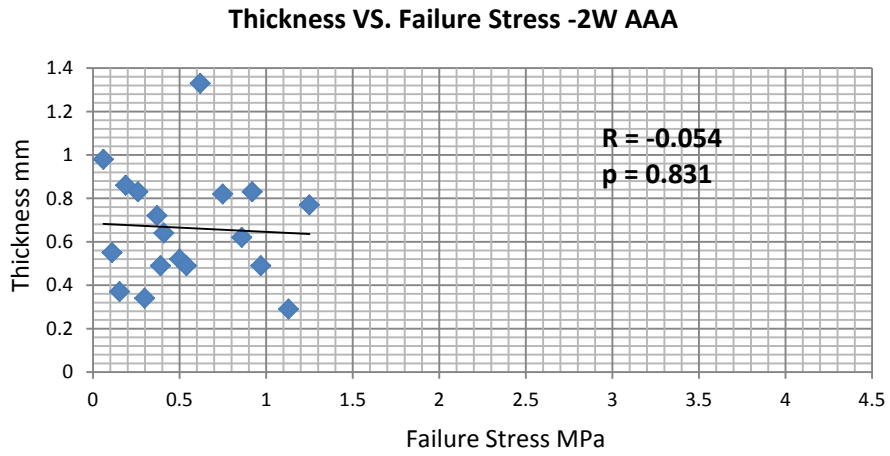

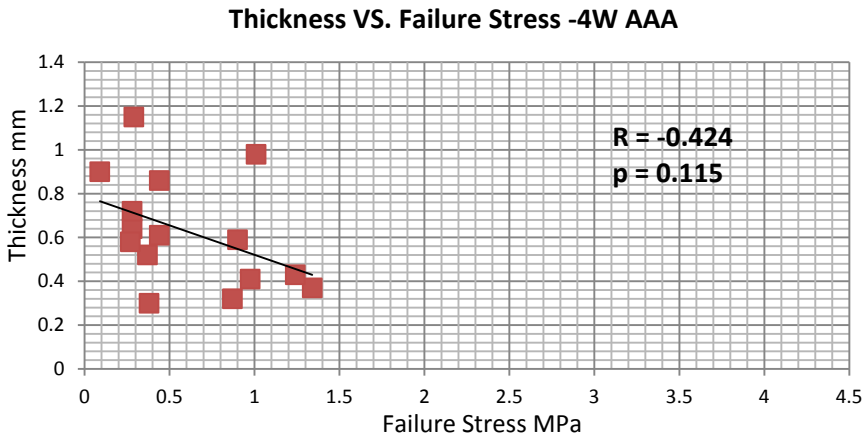

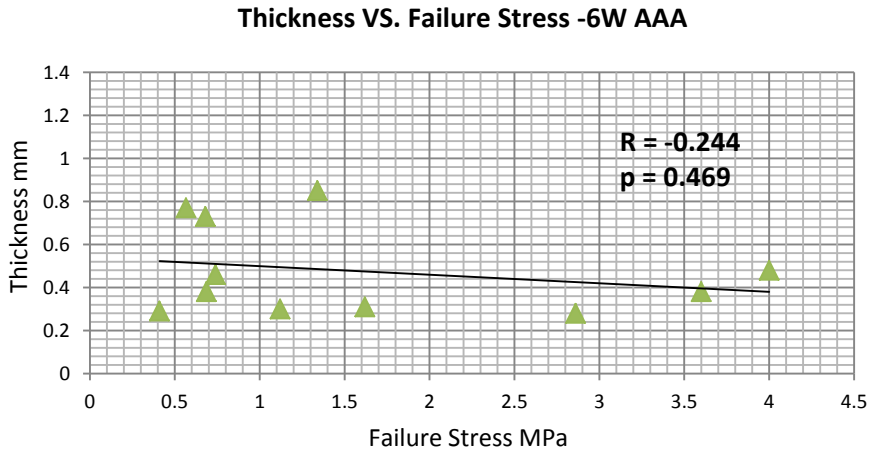

Figure 23: Correlation between thickness and failure stress at two weeks, four weeks, and six weeks. A negative correlation between thickness and failure stress is at peak with four weeks.

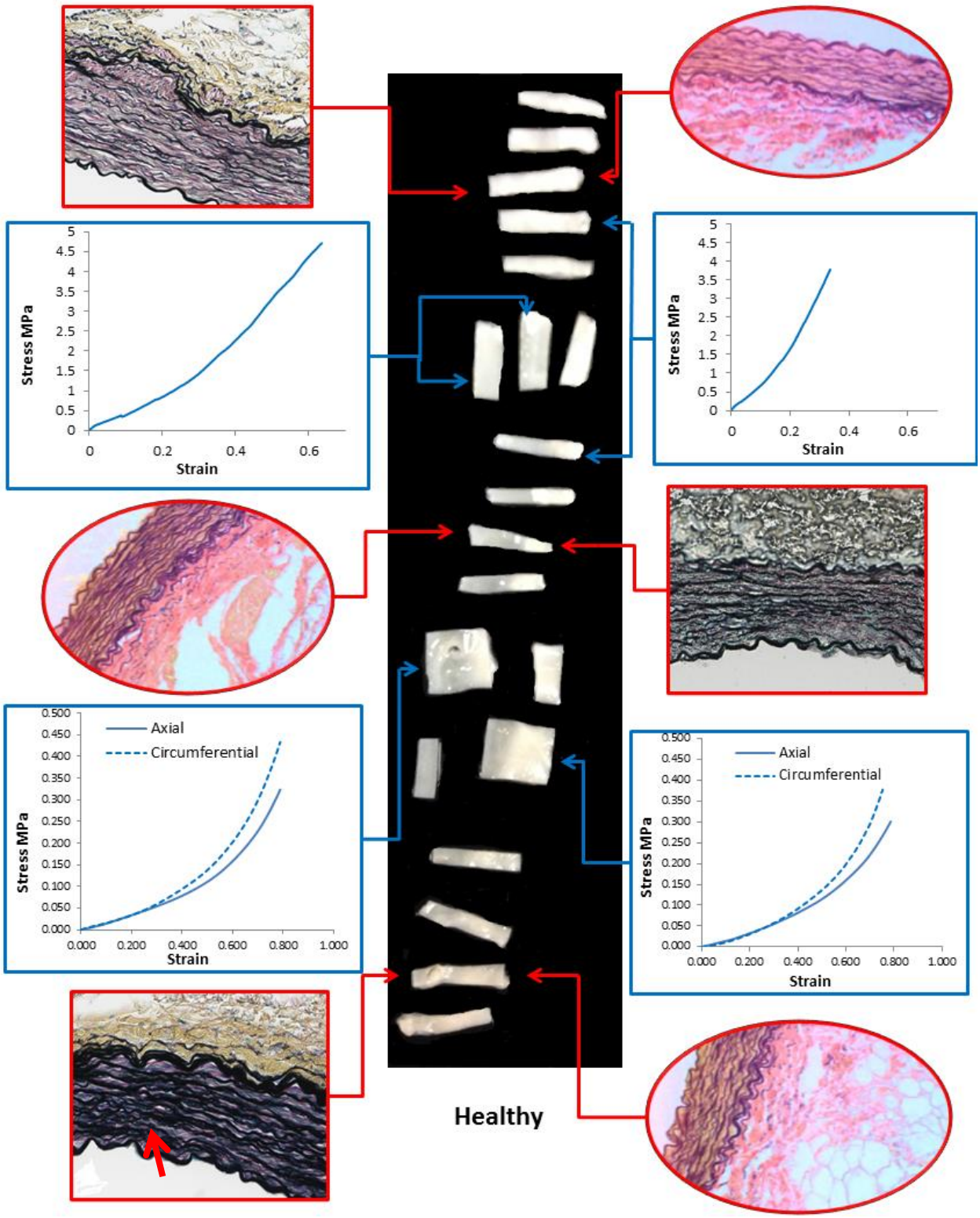

Figure 24: Uniaxial, biaxial, VVG (Circular shape), and Movat (Square shape) histology results in healthy aorta. Red arrow point to elastin (black color).

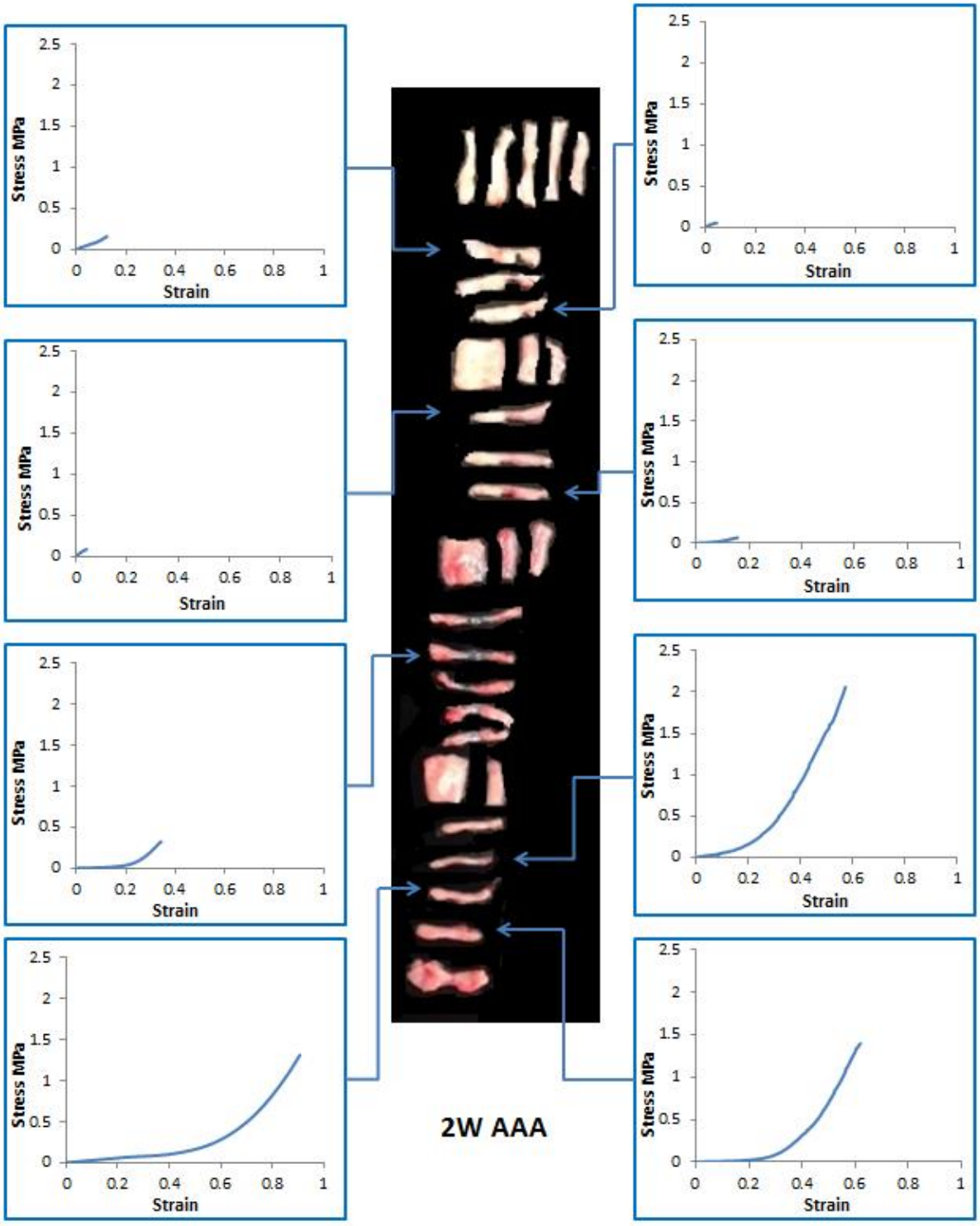

Figure 25: Results of the uniaxial tests for two week AAA in circumferential direction. The mechanical behavior is inconsistent with location.

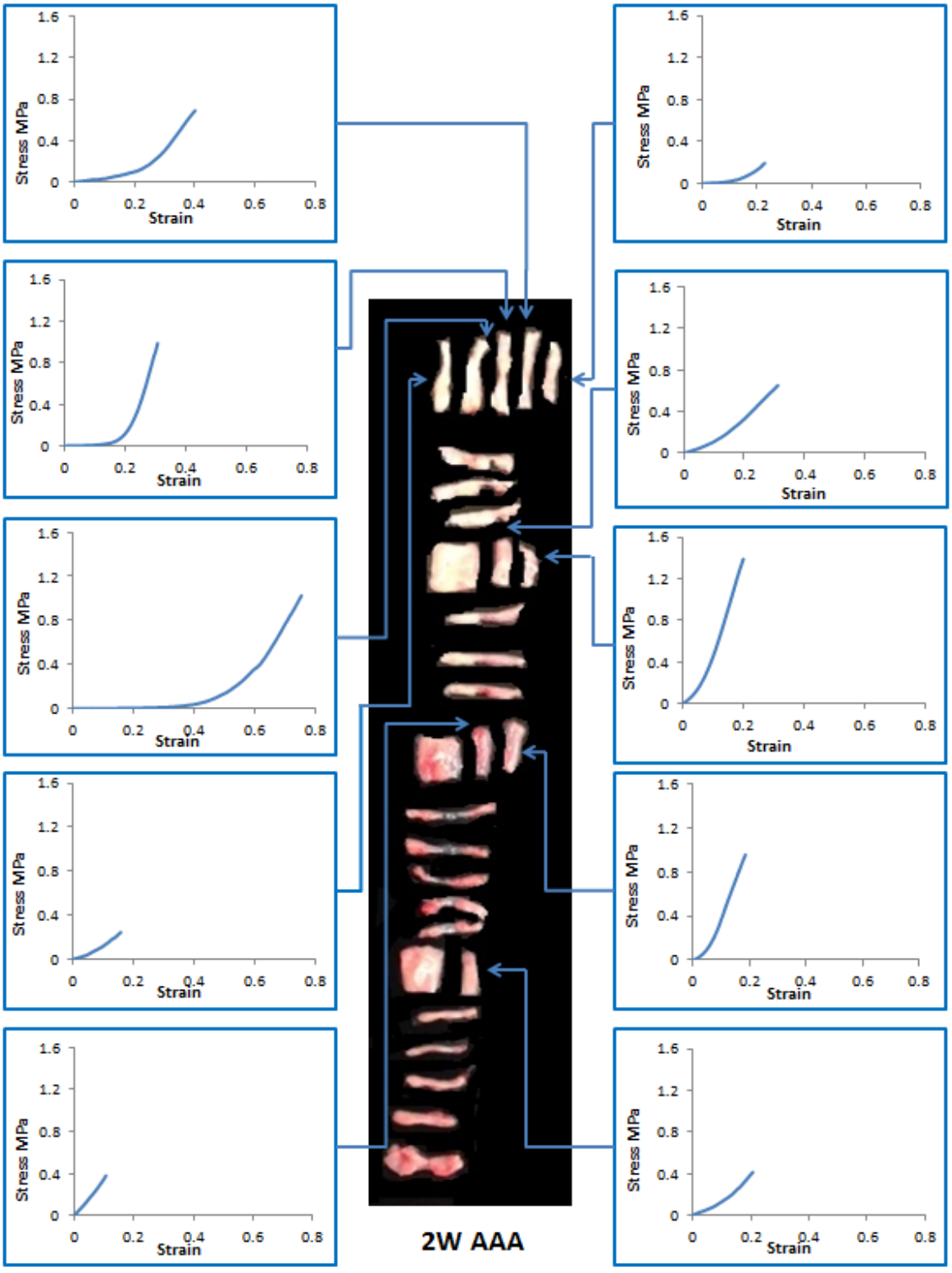

Figure 26: Results of the uniaxial tests for two week AAA in axial direction. The mechanical behavior is inconsistent with location.

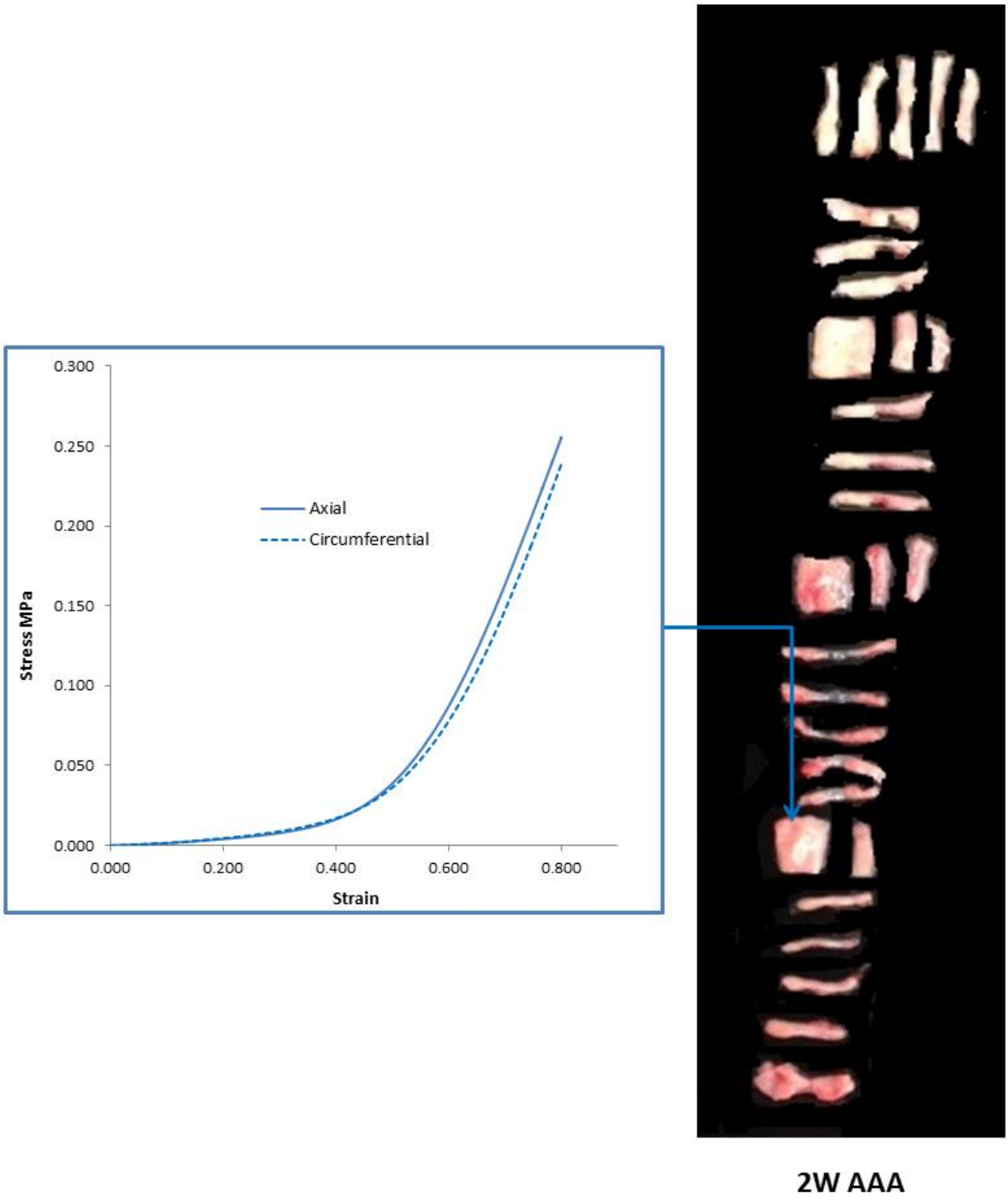

Figure 27: Biaxial data for two week AAA.

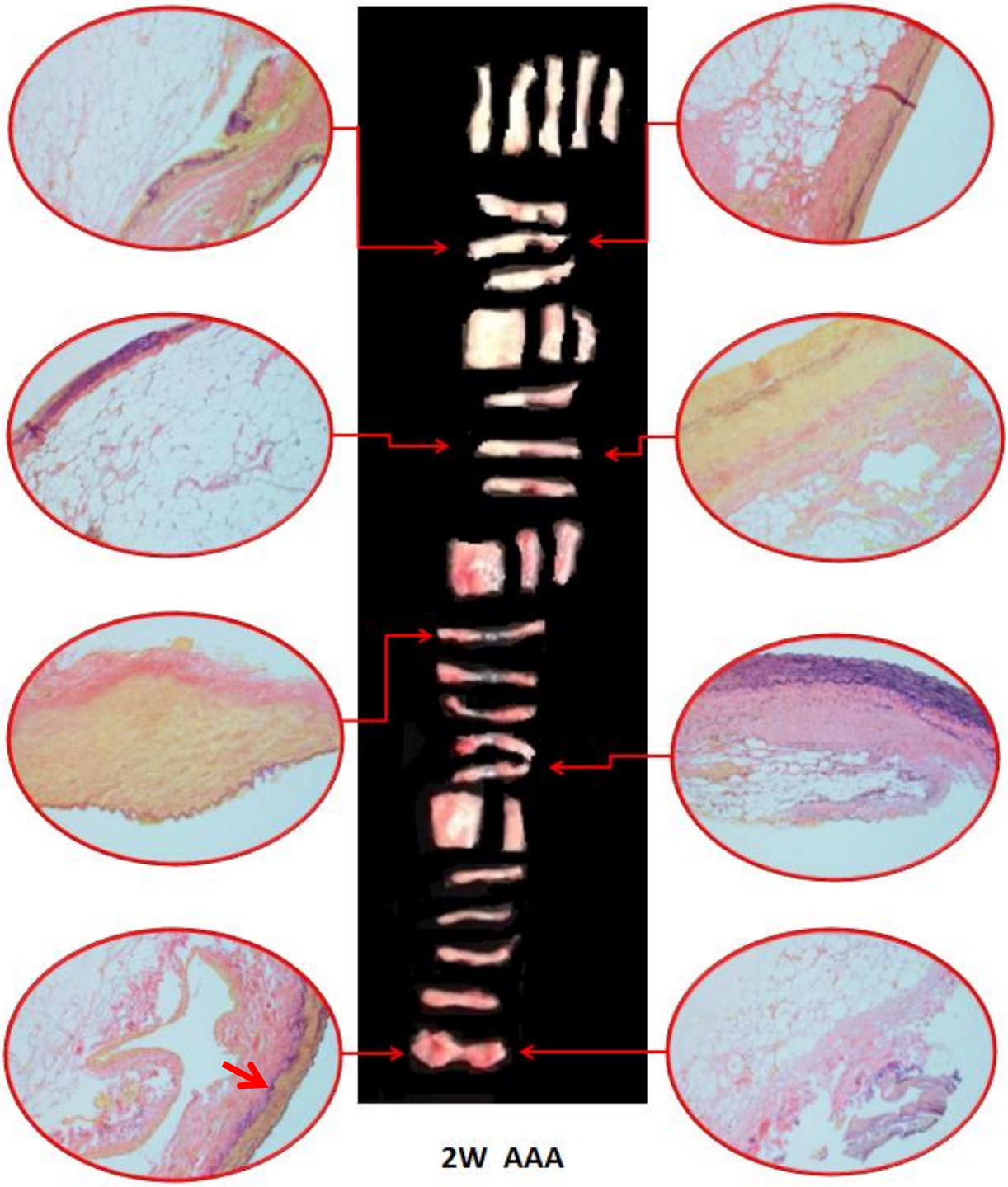

Figure 28: VVG histology stains for specimens from two weeks AAA. Red arrow point to elastin (black color).

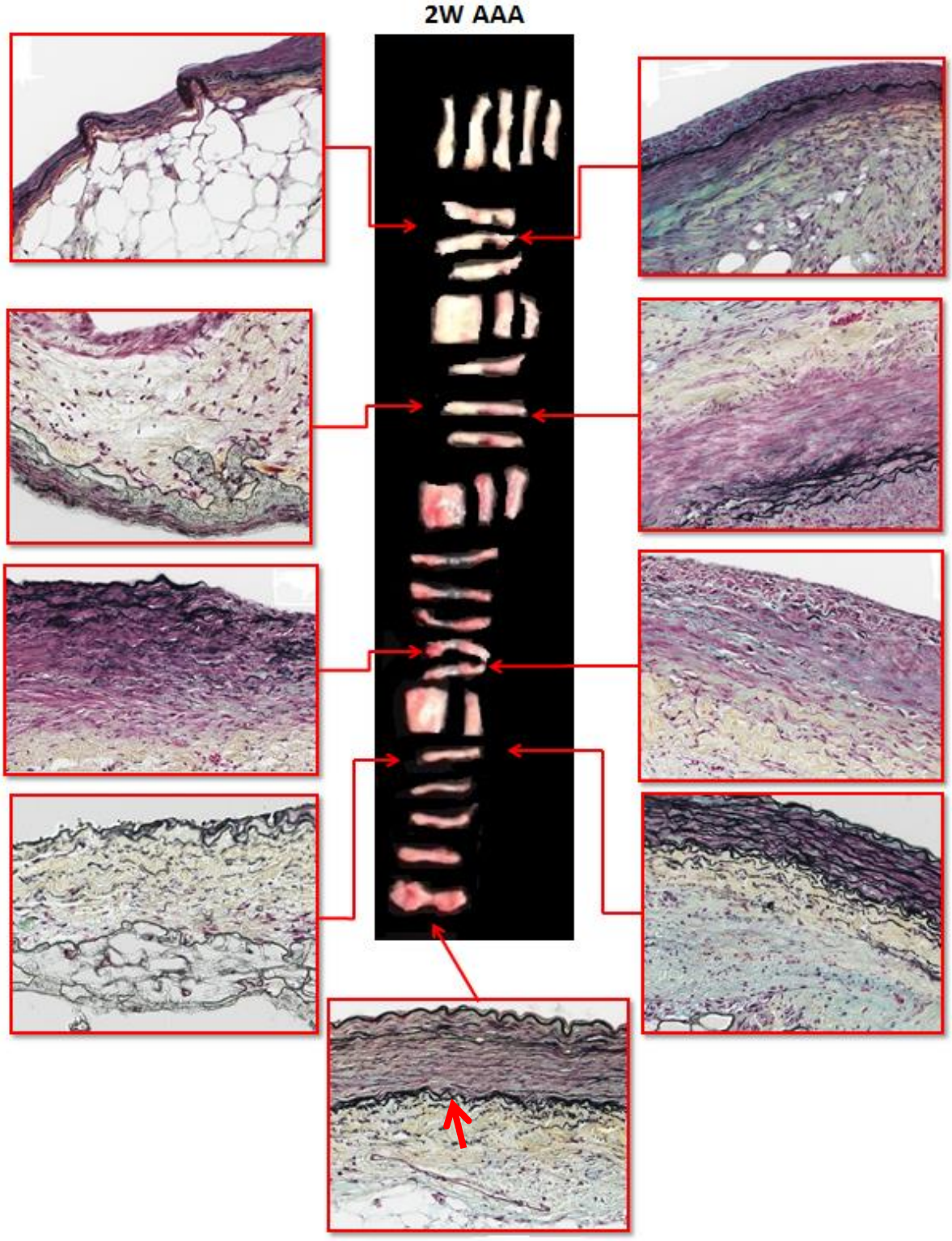

Figure 29: Movat histology stains for specimens from two week AAA. Red arrow point to elastin (black color).

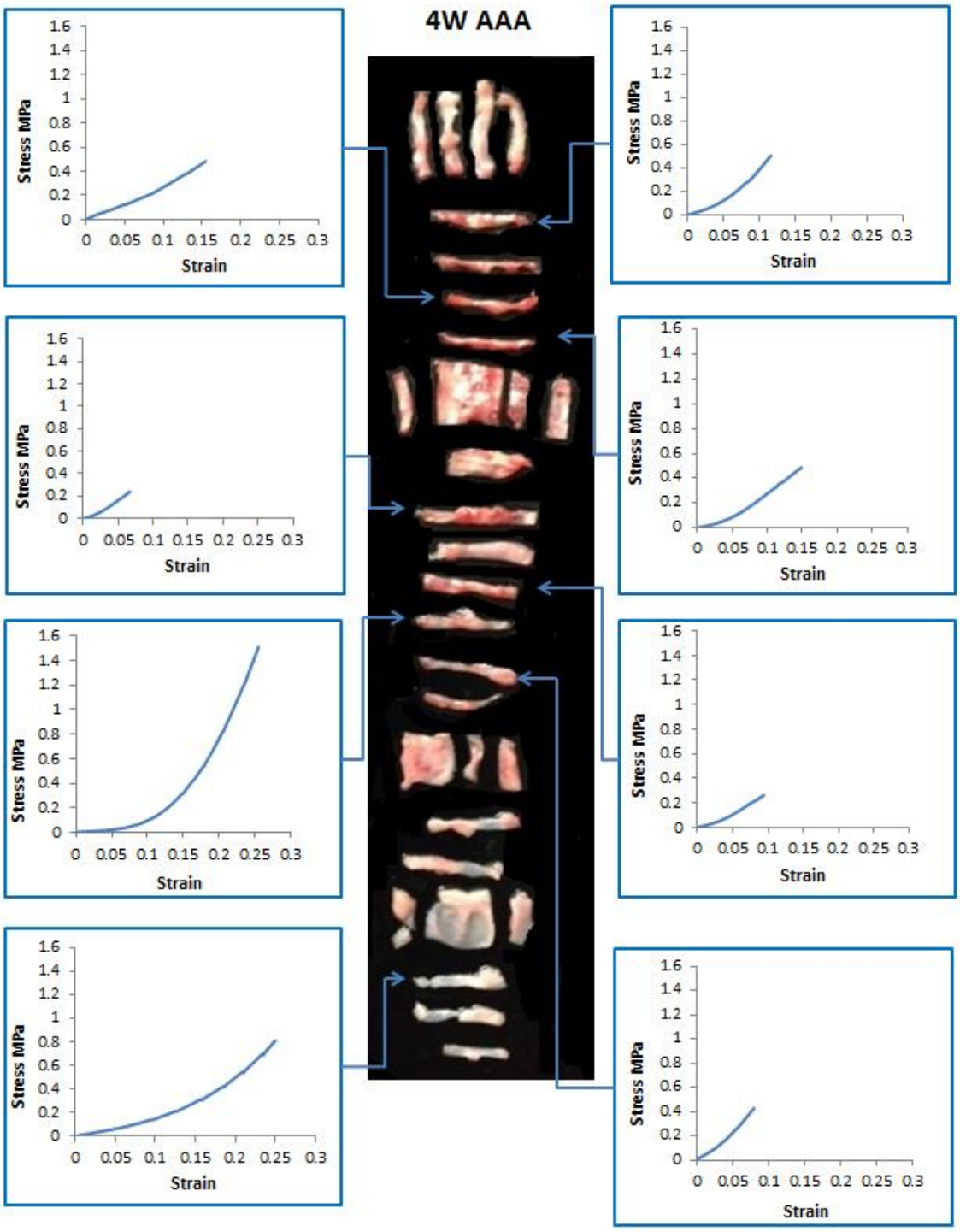

Figure 30: Results of uniaxial tests for four week AAA in circumferential direction. The mechanical behavior is inconsistent with location.

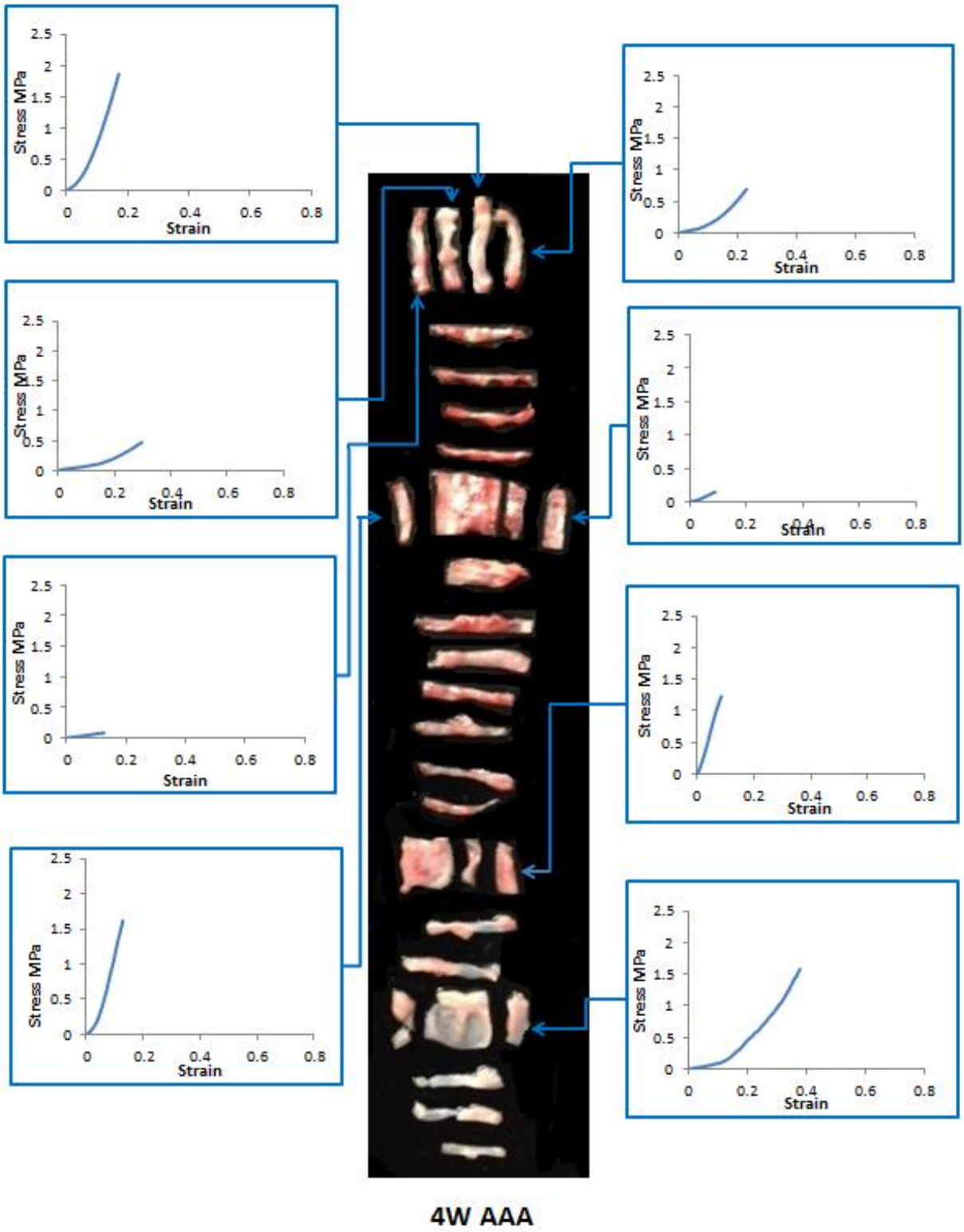

Figure 31: Results of uniaxial tests for four week AAA in axial direction. The mechanical behavior is inconsistent with location.

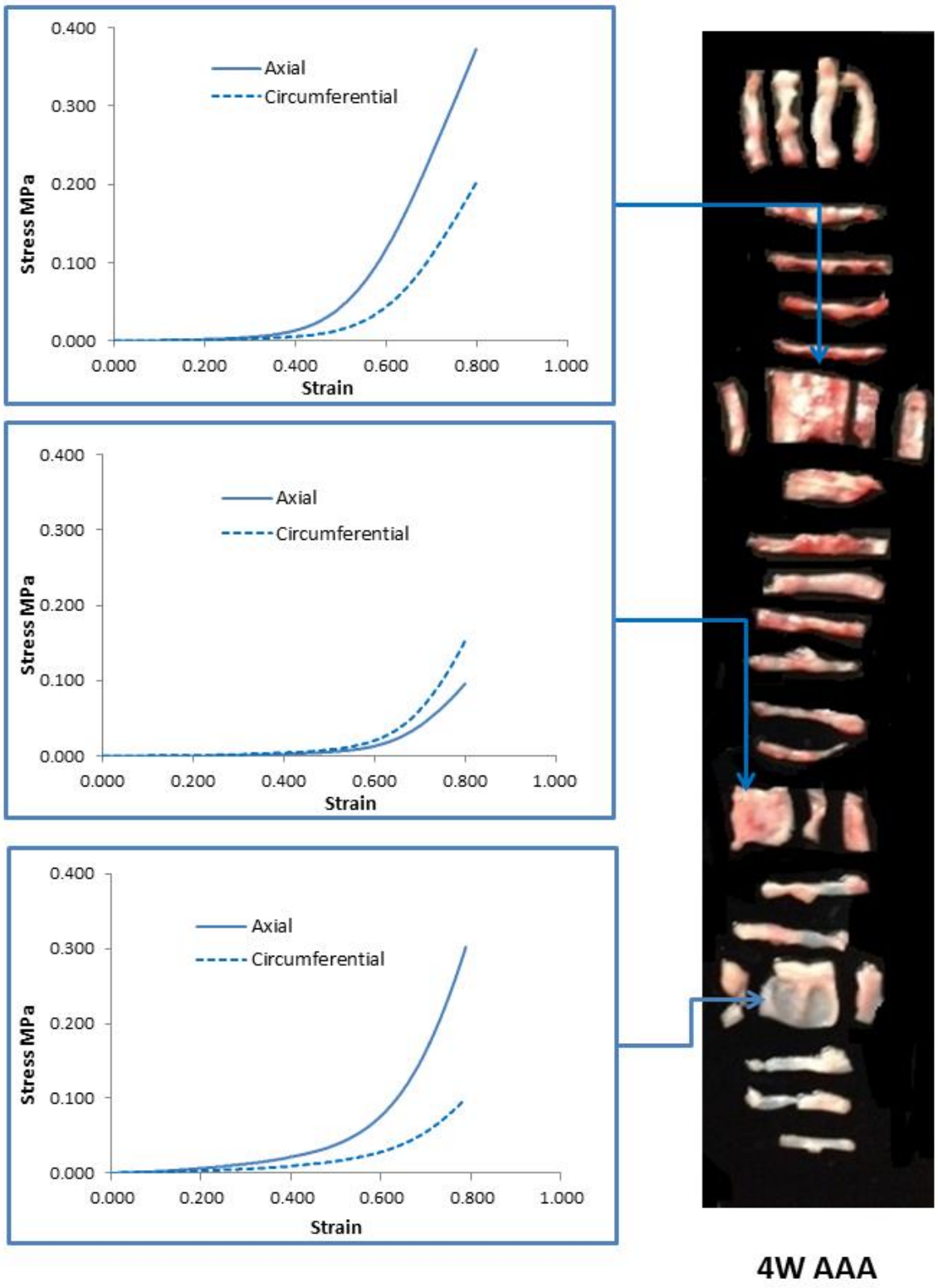

Figure 32: Biaxial data for three specimens of four week AAA.

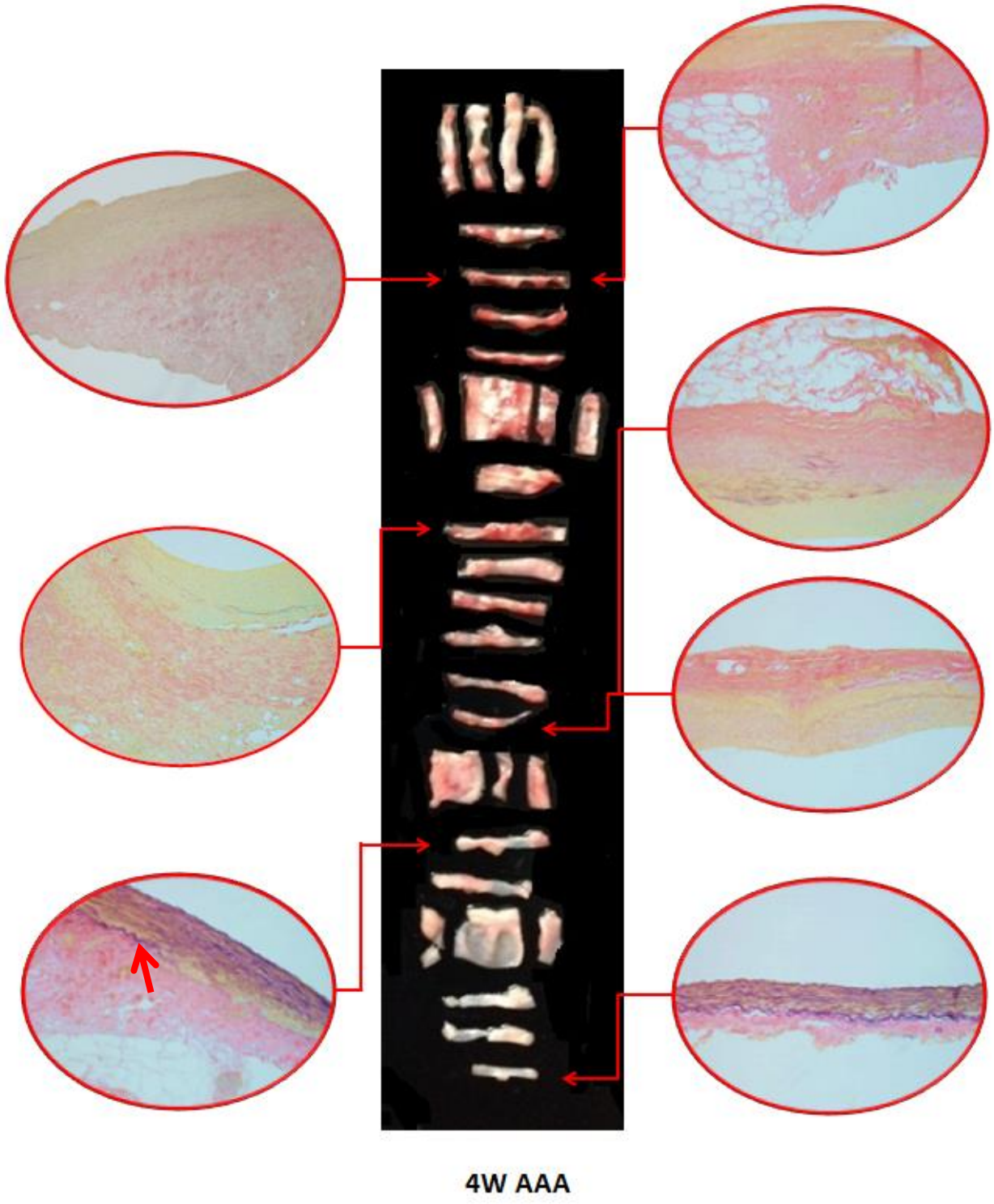

Figure 33: VVG histology stains for four week AAA. Red arrow pint to elastin (black color).

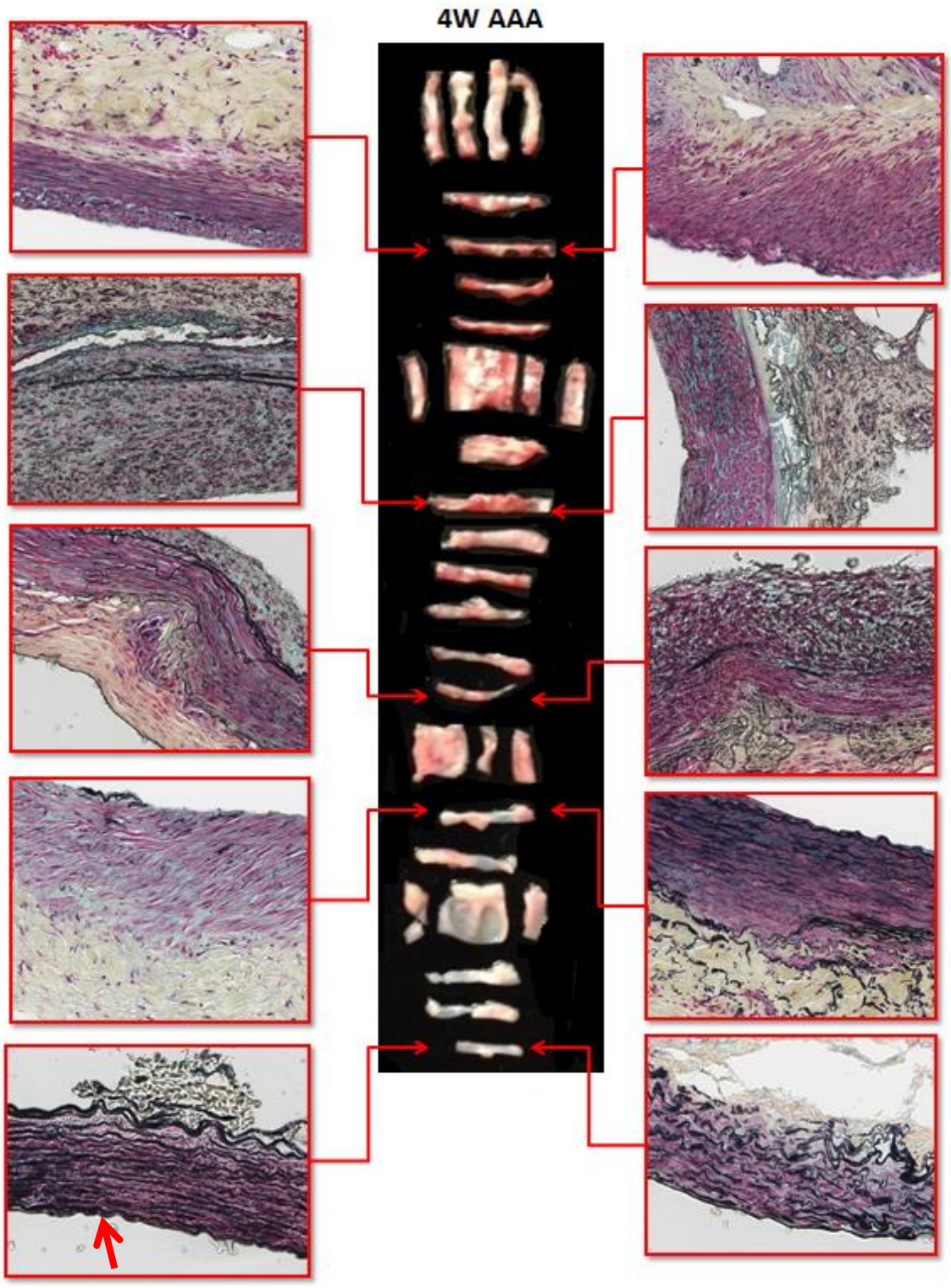

Figure 34: Movat histology stains for four week AAA. Red arrow point to elastin (black color).

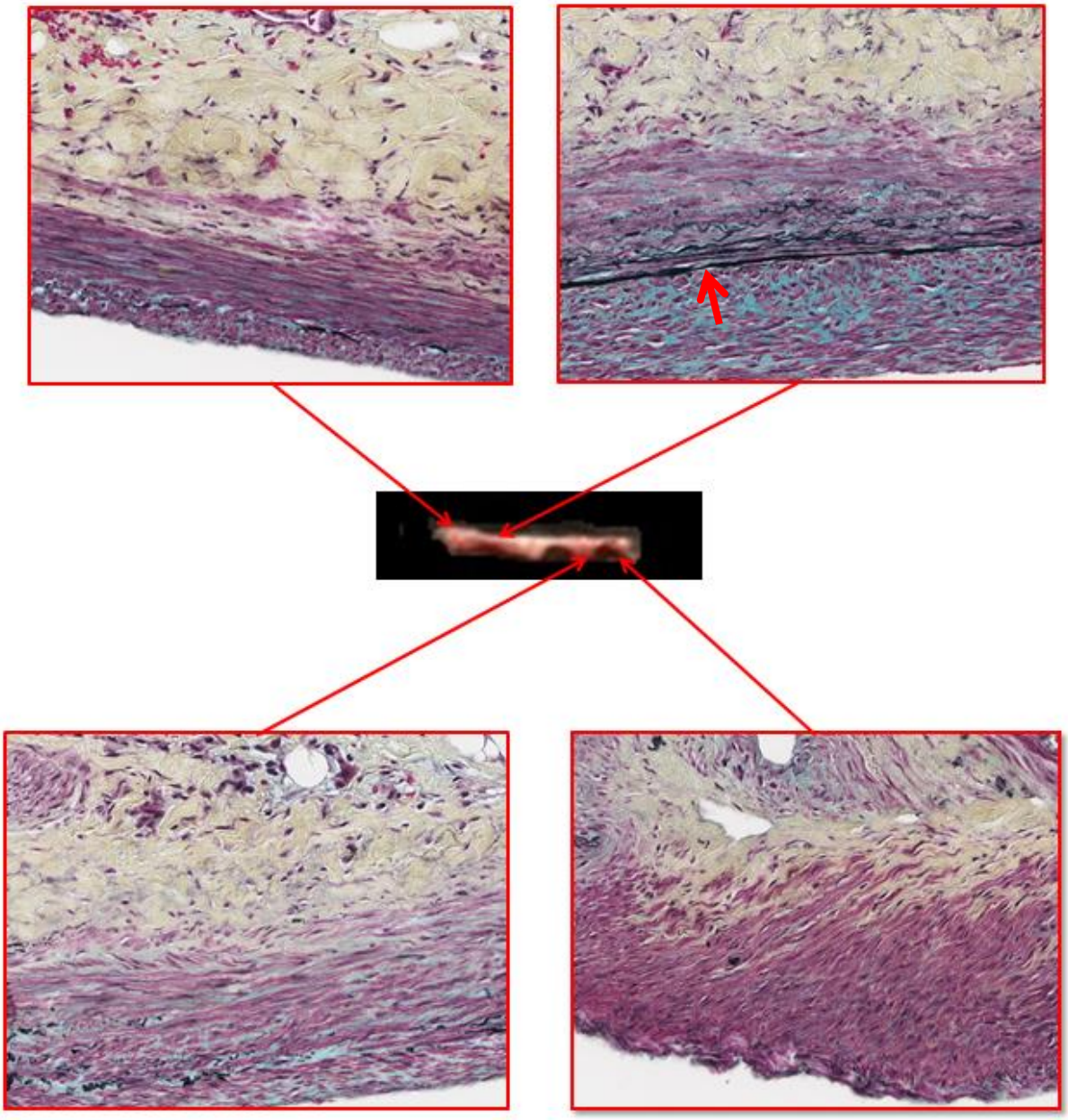

Figure 35: Movat histology stains for one segment of four week AAA. The four different regions show a wide variation of elastin content. Red arrow point to elastin (black color).

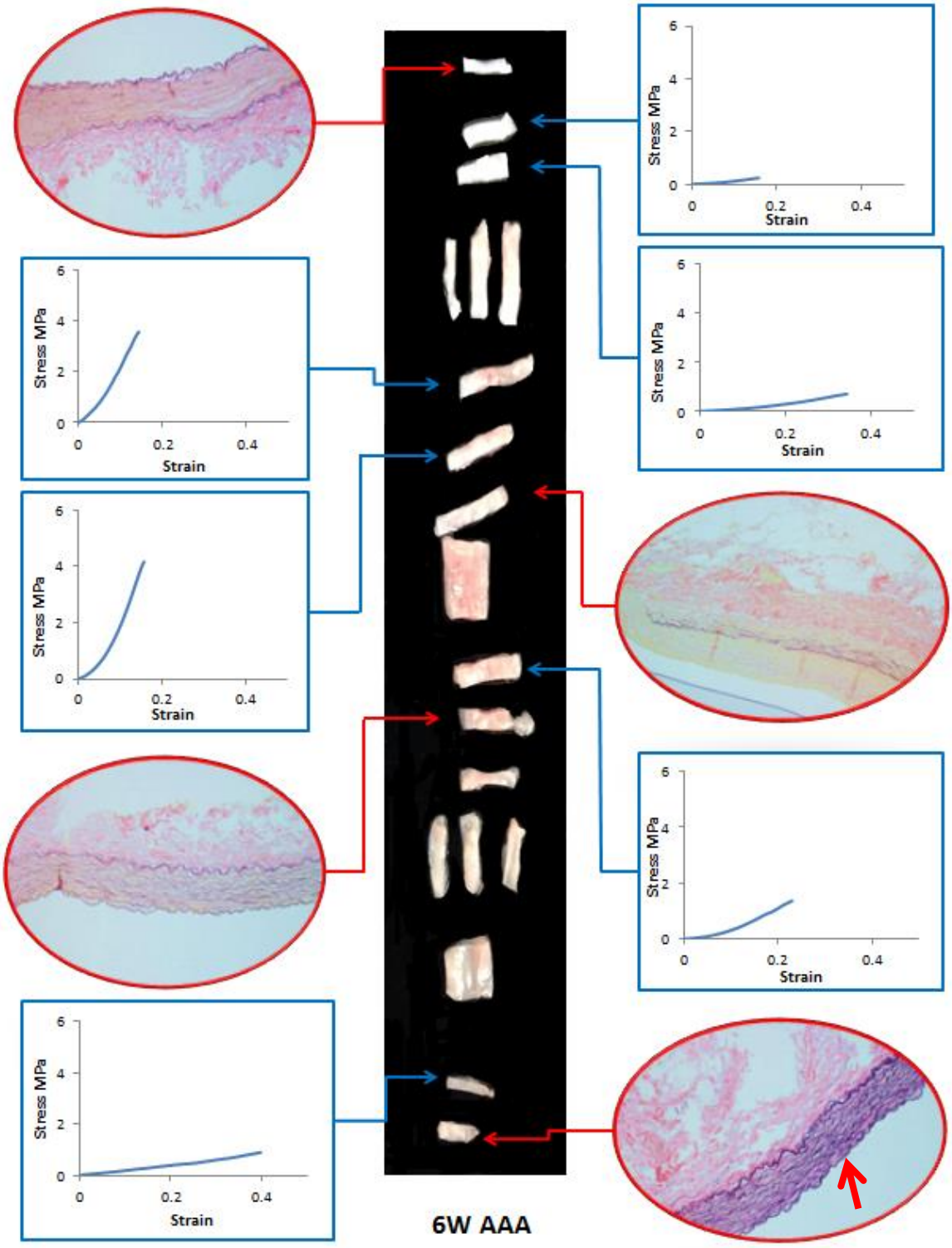

Figure 36: Uniaxial properties in circumferential direction and VVG histology stains for four week AAA. Red arrow point to elastin (black color).

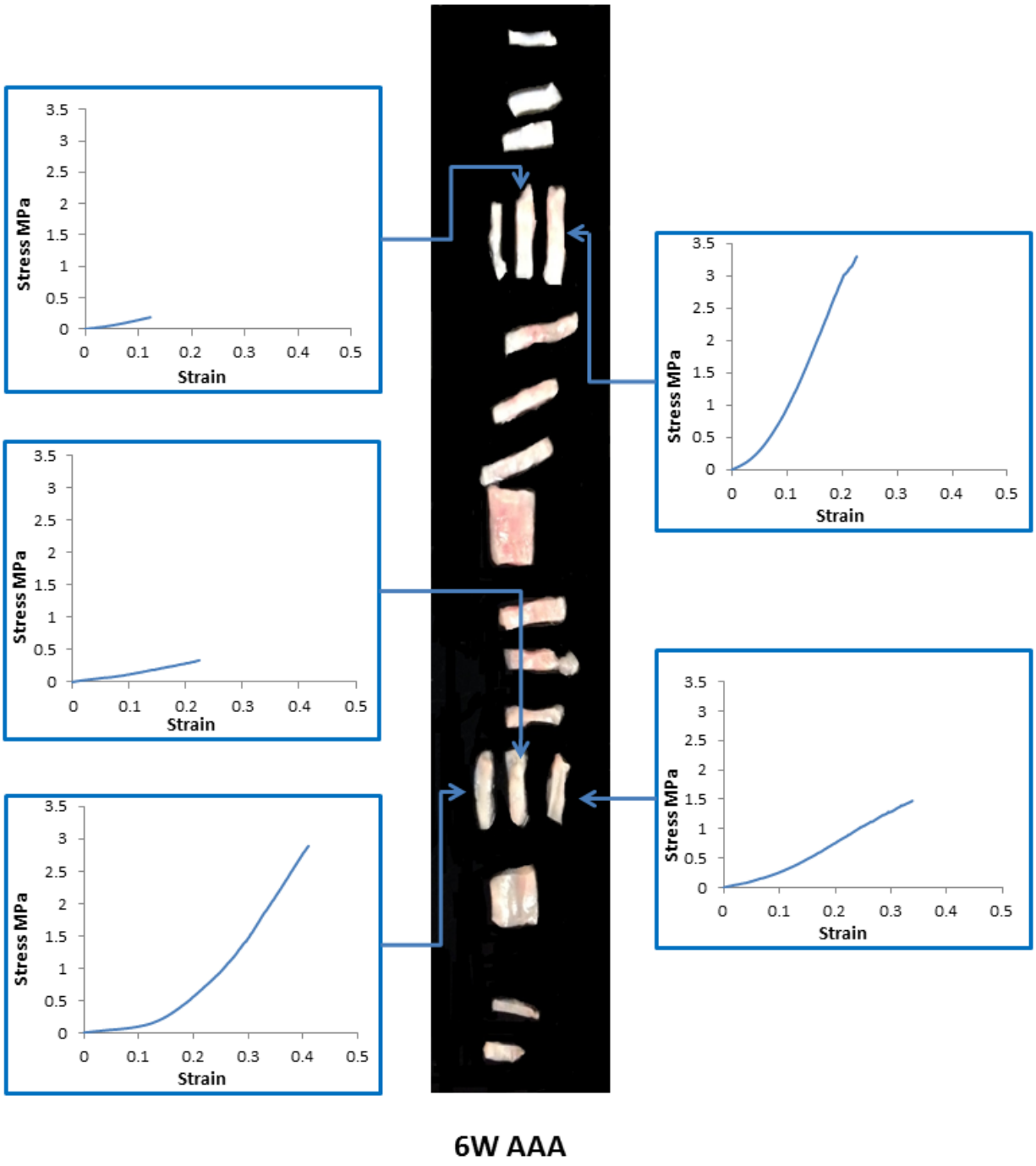

Figure 37: Results of uniaxial tests for six week AAA in axial direction. The mechanical behavior is inconsistent with location.

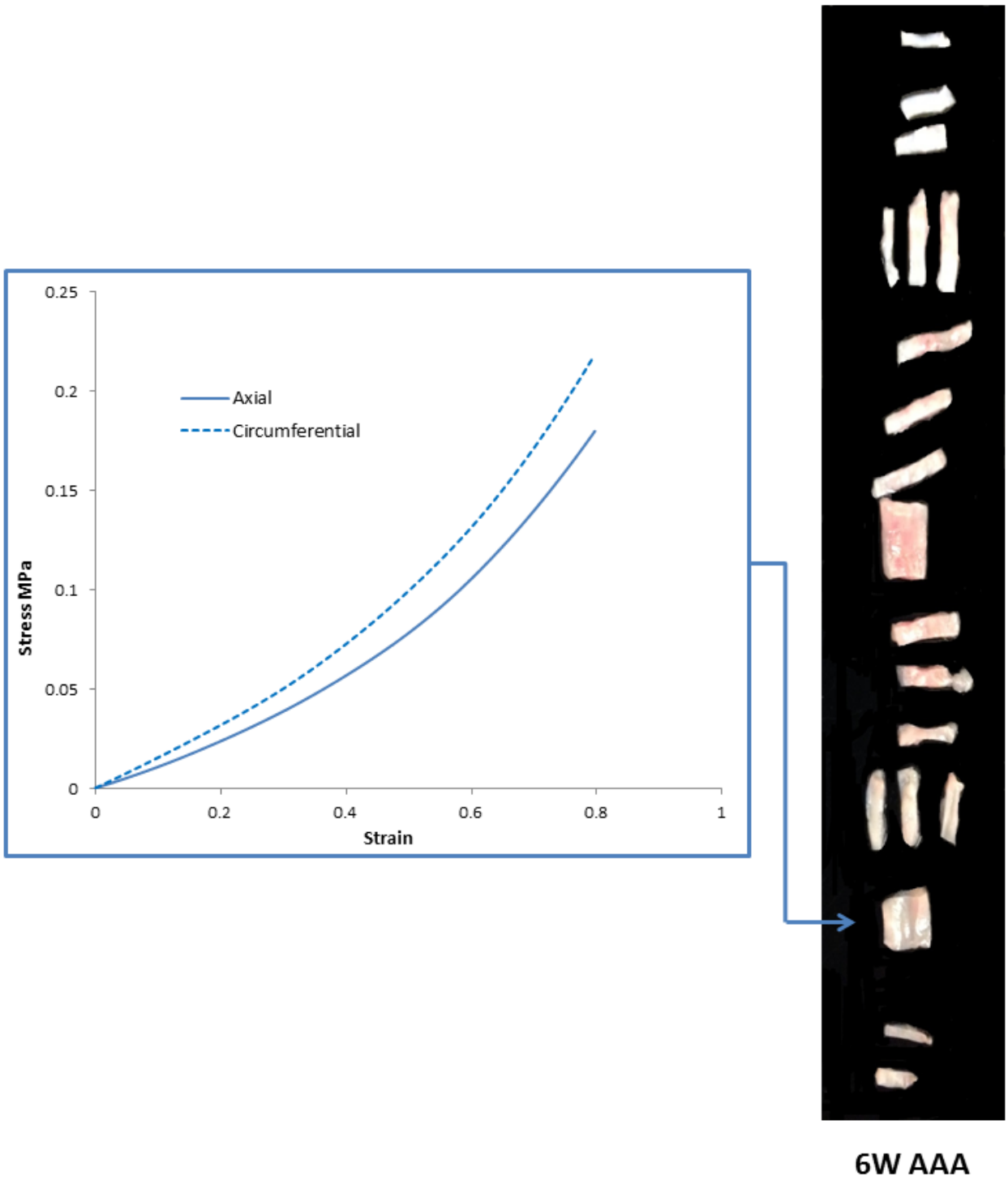

Figure 38: Biaxial properties for one specimen of six week AAA.

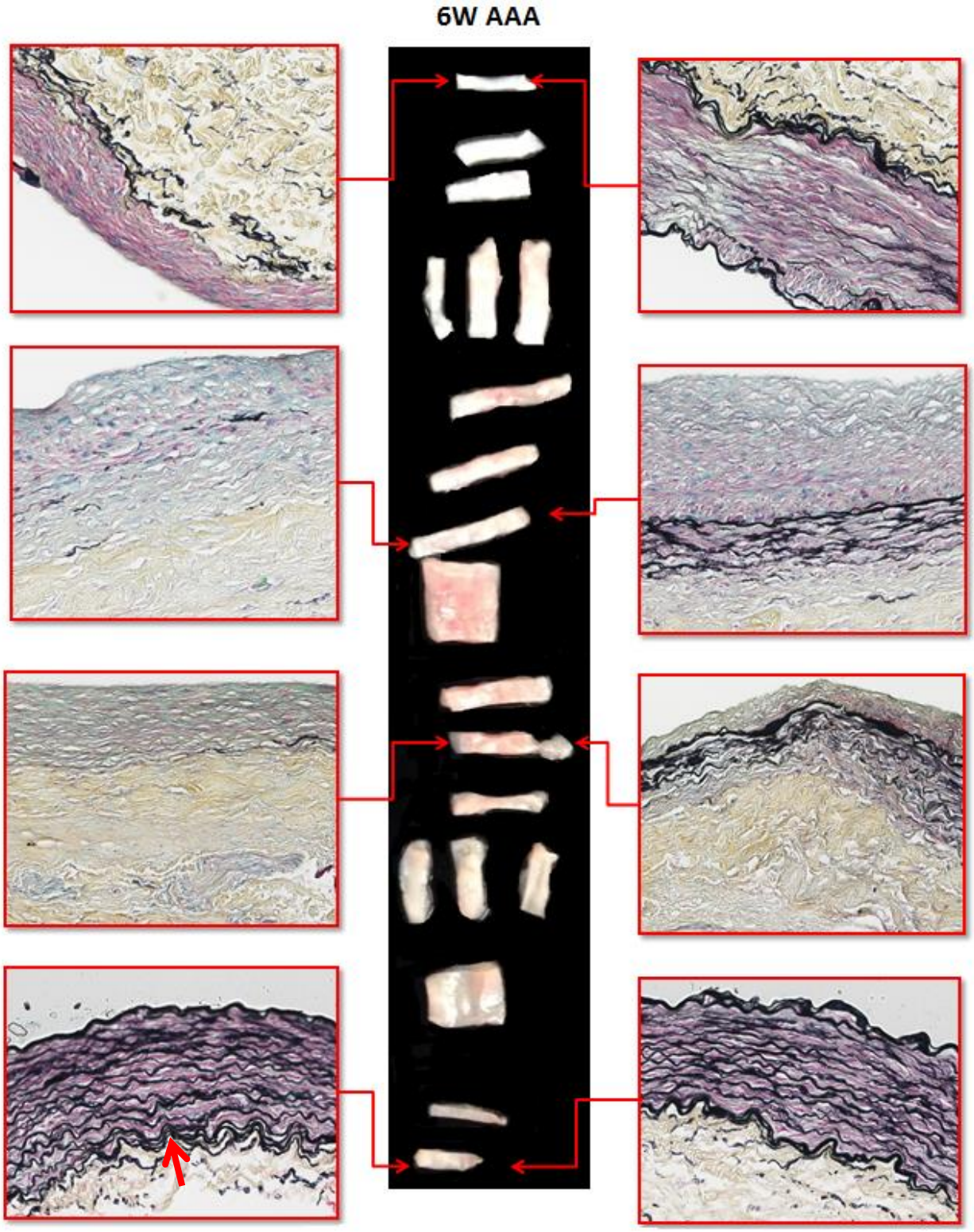

Figure 39: Movat histology stains for six week AAA. Red arrow point to elastin (black color).

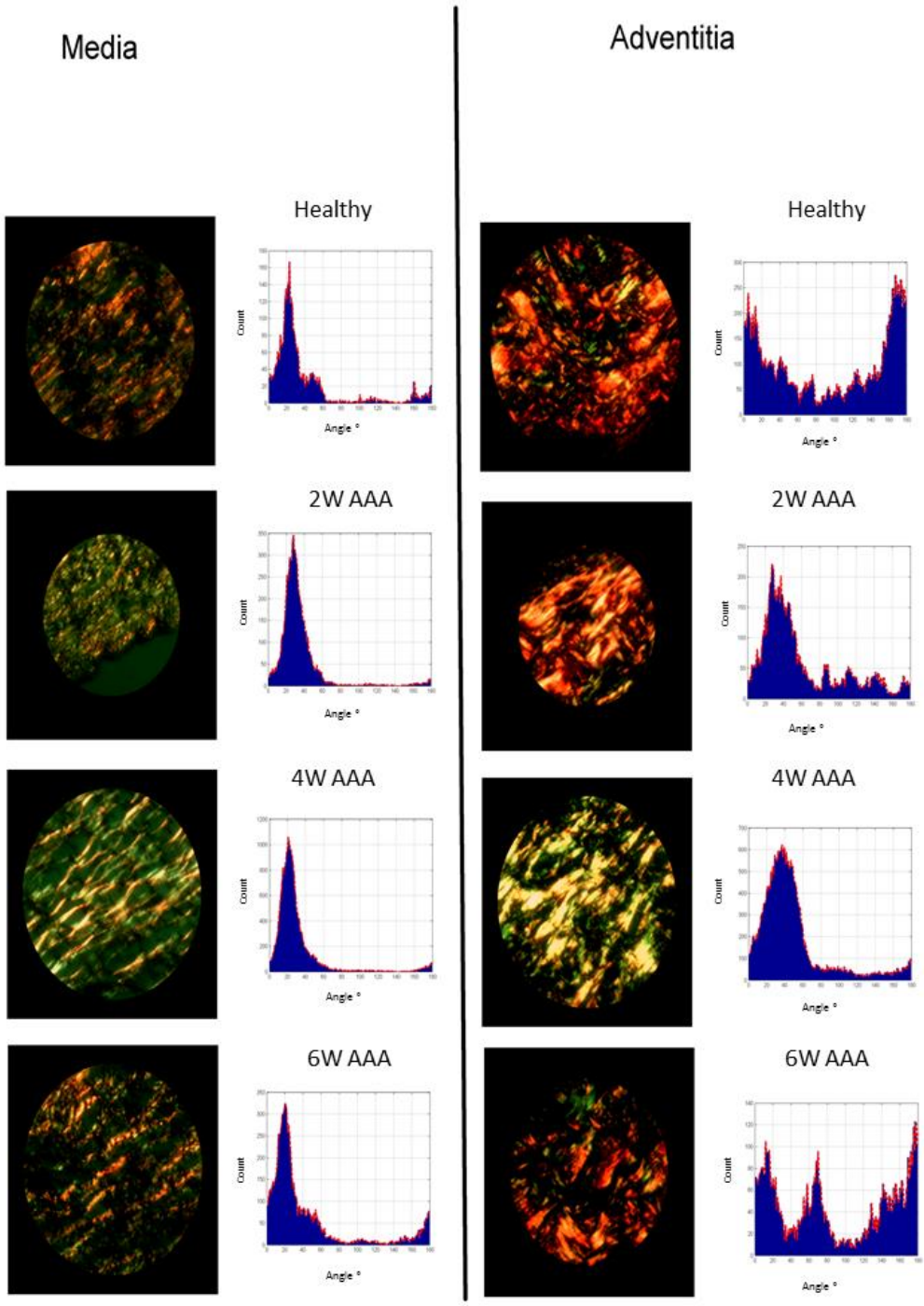

Figure 40: PSR histology analysis under polarized microscope. The media appears to have a predominant direction for the collagen fibers, while the adventitia seems to have two main directions for the healthy tissue, one at the two week and four week aneurysm progression stage, and more than two at the six week stage.

CHAPTER 5 DISCUSSION

An AAA is a local dilation of the aorta until it ruptures with catastrophic consequences that may end up with the patient's death. (LeFevre, 2014, Smolock and Lyden, 2014) It is usually asymptomatic and its detection prior to rupture is very challenging. In general, an AAA is often diagnosed accidentally when a patient undergoes imaging for a different purpose. (Smolock and Lyden, 2014, Shimazaki and Ueda, 2014) When detected, the clinical approach to avoid AAA rupture is endovascular or open repair surgery (Shimazaki and Ueda, 2014). The clinical decision for surgical intervention relies on weighting the risk of rupture against the risk of surgery (Epstein et al., 2014). The risk of rupture is assessed based on the maximum diameter and growth, both of which have been proven to be poor predictor of rupture for all patients. The main issue facing the advancement of AAA risk assessment and treatment is the lack of initial stage information, specifically the remodeling of the aorta wall and changes in its mechanical properties. Therefore, the main aim of this work was to develop a pilot study of controlled AAA in a rabbit model to understand AAA evolution, aortic tissue degeneration, and determine whether similar characteristics exist between this model and human AAAs. The success of this pilot study will push for a systematic larger sample of controlled AAAs in rabbits and continue to improve our understanding of AAA evolution in human.

Factors contributing to the development of AAAs in humans have not been completely clarified, but according to the limited data collected, they are commonly divided to two related processes: extracellular matrix (EM) degeneration and inflammation (figure 6) (LeFevre, 2014, Smolock and Lyden, 2014). Degradation of extracellular matrix is believed to be initiated by apoptosis of

VSMCs or due to genetic disease, whereas inflammation is believed to be introduced by increased extracellular proteinase activity, neovascularisation, and atherosclerosis (figure 6) (Choke et al., 2005, Rensen et al., 2007, Lopez-Candales et al., 1997, Wilson et al., 2006, Martufi and Gasser, 2013). All these factors contribute to AAA formation, but the process is still unclear due to the lack of human AAA data collected at initial stages. Since AAA is usually asymptomatic, collecting any data from the initial stage is almost impossible, especially because all collected data are from advanced aneurysms that have reached a threshold diameter of 5 – 5.5 cm (Smolock and Lyden, 2014, Shimazaki and Ueda, 2014).

The lifespan of an aneurysm can be described by four phases: formation, remodeling, pre-rupture, and rupture (figure 9). The characteristics of human AAA in the literature can also be divided according to the lifespan phases with continuous increase in diameter, degradation of elastin at the formation stage, increases in collagen synthesis during the repair stage (collagen I, III), degradation of collagen during the pre-rupture stage, and finally local failure of collagen that leads to rupture (Henderson et al., 1999, Martinez-Pinna et al., 2013, Rensen et al., 2007, Thompson et al., 1997, Raghavan et al., 1996, Wilson et al., 2003, Di Martino et al., 2006, Kadoglou and Liapis, 2004, Vorp and Geest, 2005, Martufi and Gasser, 2013). Also, other characteristics of AAA include increase in wall thickness, significant reduction of tissue strength compared to healthy, and the presence of thrombus (Vorp et al., 2001, Di Martino et al., 1998, Bluestein et al., 2009, Vorp and Geest, 2005, Di Martino et al., 2006, Monteiro et al., 2014, Teng et al., 2015). AAA could also be a consequence of other conditions such as atherosclerotic and Marfan's syndrome (Palazzuoli et al., 2008, Golledge and Norman, 2010, Robinson and Booms, 2001, Lindeman et al., 2010). It is generally accepted that the rupture occurs when collagen

degradation exceeds its synthesis (Wadgaonkar et al., 2015, Vorp, 2007, Tsamis et al., 2013, Vorp et al., 1998, Martufi and Gasser, 2013). Researchers have investigated the mechanical properties of healthy abdominal aorta and AAAs using uniaxial and biaxial testing. Most collected tissues are from ruptured or elective repair (more than 5 - 5.5 cm diameter) patients and the mechanical behaviors reported in the literature about advanced and ruptured AAAs are not consistent (table 2). Raghavan et al, (Raghavan et al., 2006) demonstrated that the mechanical behavior varied regionally and the failure tension of the specimen strip closer to the rupture site was low compared to its neighbor in the same aneurysm. This could explain the variation between these studies, in addition to the fact that no information is known at the time of surgical repair on the exact time frame and stage of aneurysm development. For example, we cannot speculate whether a patient with a maximum diameter of 5.5 cm had an aneurysm for 1, 5, or 10 years (figure 9). Other factors could also contribute to these inconsistent results such as age, gender, genetic disease, and health condition of patients. Further research is essential to better understand the mechanical behavior of AAA tissue. In particular, we aimed to understand the effect of elastin reduction and extracellular matrix disruption (which are demonstrated in human aneurysms) on the remodeling of the aortic wall and the changes in the mechanical properties of the tissue. The only resource to understand these characteristics of aortic remodeling and AAA progression is using animal models.

When generating aneurysms in animals, the method employed has significant impact on the results. Two main methods are commonly used to induce AAAs in animals, which are chemical (calcium chloride and elastase) or physical (patch and graft) (Gertz et al., 1988, Gertz et al., 2013, Chiou et al., 2001, Parodi et al., 1991, Criado et al., 1995). Since the physical models do

not replicate the pathology of aneurysms in humans, we used chemical models. We chose this model because we have extensive expertise at the University of Calgary working with rabbit model, the rabbit has acceptable abdominal aorta size for mechanical testing, and rabbits are relatively inexpensive to house and maintain. In addition to the information provided by Bi et al, (Bi et al., 2013b) about this model, our study provided additional information regarding growth, mechanical properties, and histological analysis starting from healthy and over a period of six weeks of aneurysm development. We did not include sham experiments, which are rabbits incubated with saline solution for 20 min, because Bi et al, (Bi et al., 2013b) reported no significant (number of rabbits =12) changes in this group. Therefore, we assumed that the dilation of the aorta is due to the elastase and $CaCl_2$ solution and not due to surgical trauma. Instead of comparing aneurysmal data to sham, we compared it to healthy rabbit aorta.

We successfully generated AAAs in the three rabbits using a $CaCl_2$ and elastase solution for with a 20 min induction time as the pilot study. Continuous growth of the aorta was observed over 30 days but we observed that the aortic size appeared to have diminished at the six week stage. We compared the biomechanical properties of tissues sampled from a healthy rabbit aorta, two week AAA, four week AAA, and six week AAA. We found that the healthy tissue exhibited a higher tensile strength than aneurysmal tissue at all stages and also had thinner walls when compared to the AAA tissue. We observed that the six week AAA became stiffer compared to the behavior of both the healthy aorta and the other aneurysm stages. Also, the histological analysis demonstrated remarkable elastin degradation in aneurysmal walls compared to healthy tissues. A substantial increase in collagen content was observed as the aneurysm progressed showing a peak in the six week AAA. Our results align with Bi et al. experiments as they reported

continuous dilation of abdominal aorta over 4 weeks, continued elastin degradation, and continued synthesis of collagen. These results are also compatible with our mechanical testing where we observed weaker behavior for the aneurysmal tissue, especially at the four week AAA. This is due to the process of elastin degradation and separation between wall layers that was confirmed by our histological analysis. However, in our study we observed a reverse in the dilatation and the aneurysm size appeared reduced at the six week mark. While some literature would indicate that VSMC production and elastin regeneration could accounted for this self-healing tendency in induced aneurysm models, our histological analysis did not support this conclusion. No elastin regeneration was observed in the central regions of the six week aneurysm (figure 39). Although specimens that were closer to the iliac bifurcation (specimens at the bottom) did have a high content of elastin. We cannot assume this resulted from a healing process because the areas in the centre of the aneurysm did not recover elastin content, which suggests that the specimens at the edges might not have come in contact fully with the $CaCl_2$ and elastase solution. During surgery all precautions were taken to target the same position in all rabbits but we acknowledge that there are variations in aorta length between rabbits and human error is possible during the surgical procedure. Therefore, we cannot assume that the healing process is location specific where some areas recover while others do not. On the other hand, the mechanical testing of the six week AAA tissues demonstrated them to be stiffer and weaker than the healthy AAA which suggests that the tissue had not healed. Interestingly, the six week AAA tissues were stronger and stiffer than those at two and four weeks AAA suggesting that the body is attempting to repair the aneurysm. This process appears to be a fibrotic process of repair where more collagen is laid down to replace the lost elastin. The shift towards a higher collagen ratio is consistent with the observed changes in mechanical properties, and the observed differences

between healthy and six week AAA tissues. Further histological analysis comparing all areas of six week AAA specimens to healthy tissue, namely specific elastin content, VSMCs number, and collagen content, is essential to determine with more detail the remodeling process and to conclude whether the observed reduction in diameter in the six week aneurysm was a healing process or a remodeling process of the aneurysmal tissue. It is interesting to note that a similar shift in the ratio between collagen and elastin (with higher collagen content) was observed in human AAA histologies (Schlatmann and Becker, 1977, Di Martino et al., 2006, Jones, 2011, Rodella et al., 2016, Raaz et al., 2015).

The combination of elastase and $CaCl_2$ solution generated non-symmetric fusiform aneurysms. This is expected because of the surgical techniques used by wrapping sterilize gauze around the aorta. This suggests that the gauze had direct contact with some areas which ultimately had more exposure to the solution than other areas. Even though all efforts have been taken to wrap the gauze tightly around the aorta, it becomes slightly loose when wetted with the solution. The 3D model reconstruction of the aneurysms demonstrated complex (fusiform) geometry especially at two and four weeks AAA with maximum diameter of 5.11 mm and 6.92 mm respectively (figure 13). One of the limitations of the present study, due to number of subjects, is that no comparison can be made between the size of the aneurysm at different stages (2 weeks, 4 weeks, etc) because the growth was measured on different rabbits and in only one rabbit per group. Multiple imaging on the same rabbit could help better understand the progression, however in our case this was difficult due to 1) resource constraints for the technical staff and equipment required for the procedures, and 2) the necessity of having to sacrifice/ligation the femoral artery after accessing it for an angiographic procedure, which limited the angiographic procedures to one per animal.

We acknowledge that rabbits have different abdominal aorta size and this should be controlled in future experiments. The uniaxial results of the mechanical tests suggested that an increase in maximum diameter is associated with a weakening of the aortic wall by affecting its structural integrity. In fact, the failure stress of the two and four week AAA was lower than both the healthy and the six week AAA. For the six week aneurysmal tissue, the failure stress was higher than any other aneurysmal tissue, and it was associated with a smaller diameter, suggesting a remodeling mechanism as an attempt to repair the lesion.

The mechanical properties of AAA walls are not homogenous but vary with location in the same rabbit. Large variability is also observed in human aneurysms as well; however, due to the surgical techniques used to develop the aneurysm by wrapping the gauze around the aorta, we cannot guarantee that the regional differences are not in any way affected by the experimental technique. The healthy rabbit shows consistent mechanical properties throughout the whole abdominal aorta, similar to what is expected in healthy human aortas specimens from the same subject. Our findings point out that weaker tissue samples exhibit a thicker wall. This local variation in AAA tissue is even clearer when we examine at the histological analysis data, which shows additional elastin degradation in weaker aortic segments and deposition of other tissue components, fibrin, and mucin. For the two weeks and four week AAAs, a relationship was found between uniaxial strength and the amount of elastin, integrity of wall layers, and thickness of the wall. A thickening of the wall, less elastin content, and a delamination of the wall layers seem to be indicative of a weaker tissue segment. Also, we observed an increase in fibrin content which reached a peak in the four week AAA, which suggests increased inflammation in the aortic wall. Subsequently, fibrin content appears to decrease in the six week AAA, which

suggests decreased inflammation. The collagen content in the tunica media is often higher for the six week AAA. This observation could explain the uniaxial properties of the six week tissue which appears to be stiffer and stronger when compared to the two and four week samples. Also, the tissue collected form the six week AAA exhibited higher stiffness in the circumferential direction than longitudinal direction, which suggests that the collagen deposition is mostly along the circumference of the aorta, where the stresses are expected to be higher. To better understand collagen orientation, we investigated the dispersion of local collagen fiber orientation according to their mean direction using PSR histology analysis. We observed the dispersion in both the media and adventitia layers for healthy and aneurysmal wall tissue. The mean dispersion in the media layer increased from healthy to two week AAA and reached the peak at four week stage. This observation supports the hypothesis that the fiber deposition is in the direction of the dominant stress component. For the six week AAA, the dispersion value in the tunica media decreases to values approaching the healthy dispersion value. This suggests that the six week AAA tissue had less inflammation and perhaps more functioning, load bearing fibers than did the tissue collected at other stages of aneurysm induction. Therefore, collagen fibers were deposited assuming a structure similar to the healthy tissue but leading to different and non-physiological mechanical properties. We provided evidence from both the histology and mechanical testing that the healthy aortic tissue is stronger and more elastic than the six weeks aneurysmal tissue. We observed that the dispersion was higher in the media than adventitia layer finding which support the idea that collagen turnover is more intense in the middle layer of the wall.

Rabbit model of AAA vs. AAA formation in humans

One of the clearest features of human AAAs is the increase in aorta size that accompanies AAA pathology and this is associated with the degradation of elastin and apoptosis of vascular smooth muscle cells (VSMCs) (Choke et al., 2005, Henderson et al., 1999, Fukui et al., 2003, Rensen et al., 2007, Vorp and Geest, 2005, Martufi and Gasser, 2013). Also, an increase in extracellular proteinases activity appears to contribute to the degeneration process, leading to AAA formation. The exact mechanisms of proteinases activation are still unknown, but it is commonly believed that increased MMPs activity contributes to vessel expansion by degrading elastin. In general, it is believed that MMP-2 plays a role during early aneurysm formation, whereas MMP-9 is related to the continued expansion of moderate-sized aneurysms (Sakalihasan et al., 1996, McMillan et al., 1997, Choke et al., 2005, Wilson et al., 2006, Jones, 2011). On the other hand, the neovascularisation process disrupts the structure of the media layer by introducing inflammatory cells which leads to continues matrix degradation (Choke et al., 2006, Holmes et al., 1995, Ailawadi et al., 2003). The body's response to elastin degradation is by increasing collagen synthesis during the early stages of aneurysm formation. Rodella et al, (Rodella et al., 2016) demonstrated that fibroblasts and SMCs in aneurysmal tissue increase local production of type I collagen, which is more resistant and less elastic compared to type III collagen. Bode et al, (Bode et al., 2000) demonstrated that collagen type III was highly present in the media layer of AAA tissue. It is still unclear what type of collagen is synthesized during early or advanced stages of aneurysm formation. To better understand how the human AAA relates to this model, we need to observe the characteristics of AAAs in the rabbit model. Bi et al, (Bi et al., 2013b) reported significant decreases in elastin content and SMCs by day 5, significant increases in collagen type I by day 30 compared to day 5, significant decreases in collagen type III by day 30, significant

increases in MMP-2 and MMP-9 expression after 5 days, and significant increases in capillary density after 30 days. Our histological analysis confirmed the decreases in elastin and increases in collagen by four weeks. There are some similar characteristics, therefore, between this model and human AAA, such as continuous increases in diameter, decreases in elastin content, decreases in VSMCs, increases in MMP-9 activity, increases in collagen content, and increases in capillary density. To better understand the AAA developed in rabbits, we need to understand how $CaCl_2$ and elastase is degrading the elastin. Gertz et al, (Gertz et al., 2013) investigated how the $CaCl_2$ affects aorta wall using Von Kossa-stained tissue sections with correlative transmission electron microscopy. He demonstrated that the peri-adventitially applied $CaCl_2$ diffused into the aortic wall and bounded to the internal elastic lamina and the elastic lamellae in the media layer. This calcium–elastic complex altered the antigenicity of the elastic tissue and attracted inflammatory cells (monocytes and macrophages) that appeared to degrade the calcium–elastic tissue complex and disrupt the normal lamellar unit of the arterial media, resulting in progressive luminal dilatation. On the other hand, using elastase as to generate AAA degraded elastic lamellae, increased inflammatory cells, and increased MMPs activity (Anidjar et al., 1990). The detailed mechanism of elastin degradation using both $CaCl_2$ and elastase is still not known and more research is needed. However, this rabbit model seems to be closer to inflammatory AAAs in humans. More histological research is needed to understand both human AAAs and AAAs developed in this model.

Mechanical properties of rabbit AAA model vs. human AAA.

Mechanical properties of healthy abdominal aorta and AAA in humans have been quantified using uniaxial testing. The value of failure stress is not consistent, but there is an overall trend of

weaker aneurysmal tissue compared to healthy (Raghavan et al., 1996, J. Thubrikar, 2001, Vande Geest et al., 2006a, Xiong et al., 2008, Teng et al., 2015). We are observing the same with our rabbit model where aneurysmal tissues are weaker than healthy (Table 3,4). To be specific, we compared failure stress of the averaged rabbit model with Raghavan et al, (Raghavan et al., 1996) results as he tested both healthy and AAA tissue from human. Since AAA with a diameter of 5- 5.5 cm is double the original aorta size in human, we estimated that four weeks is relatively compatible with the human condition, since at that point the maximum diameter in the rabbit aorta has doubled compared with a healthy rabbit aorta. Raghavan et al, (Raghavan et al., 1996) reported that the failure stress of healthy tissue was 2.01 MPa and aneurysmal tissue (Maximum diameter > 5 cm) was 0.86 MPa on average, which is more than half the stress. In our experiments, we saw a greater difference between healthy to four week AAA in rabbits with 3.28 MPa to 0.62 MPa, respectively. This suggests that the rabbit tissue was highly damaged and weaker compared to humans. A reasonable explanation for this difference is the fact that this animal model is an acute model whereas the human AAA is chronic. The time taken to reach AAA with double the aorta size in human is still unknown but it is likely to be more than four weeks. Moreover the strength of aortic tissue decreases with age, so the lower healthy value found by Raghavan et al, (Raghavan et al., 1996) could also depend in part on the age of the subjects. On the other hand, biaxial testing of human AAA demonstrated that the tissues are stiffer than healthy and exhibit more anisotropic behavior, with preferential stiffening in the circumferential direction (Geest et al., 2006, O'Leary et al., 2014). In the rabbit model, we observed more isotropic behavior with two and four week AAA, which could suggest a degradation of fibers, that is not yet replaced by directional collagen deposition. In humans specimens are collected at an unknown time in the development of the aneurysm, so we cannot

make speculations regarding the stage of remodeling and of deposition of collagen. Vande Geest et al, (Geest et al., 2006) showed increased anisotropy in aneurysm tissue, which could be due to an effective directional collagen deposition in the direction of the maximum stress. It is also interesting to note that the stiffer direction in four week AAA was not constant and changed from axial to circumferential depending on the location of the specimen, which suggests that the disruption of elastin and the remodeling process of collagen varied with location. In conclusion, it is difficult to compare directly the mechanical properties of the rabbit AAA model with human AAAs, but many features appear to concur and to help in explaining the remodeling process in the aorta following elastin disruption, and the effect that the lack of elastin and collagen deposition has on mechanical properties.

Other characteristics of human AAAs and the rabbit model of AAAs.

Atherosclerosis is a chronic condition that could lead to AAA formation in humans (Jones, 2011). We did not observe this characteristic in our animal model. Ideally, we need a specific atherosclerotic model of AAAs to investigate the relationship between atherosclerosis and AAA. On the other hand, intraluminal thrombus is found in about 75% of all AAAs, which contribute to lowering the wall stress (Choke et al., 2005, Jones, 2011). We did not observe any thrombus in the animal model; it is unclear if the reason is the lack of sufficient time or the absence of hemodynamic conditions. The differences in fibrinogen formation between rabbits and humans could also help explain such findings. Studying thrombus formation is important to understand the mechanical properties of AAAs in humans, and developing an animal model with evidence of thrombus may require further efforts.

Comparing rabbit models with other animal models.

Animal models provide an *in vivo* understanding of AAA enlargement and rupture, and continue to play an essential role in advancing medical treatment of AAAs. The methodology to develop AAAs in animals could be divided in two approaches: chemical and physical. The physical method does not replicate the pathology of aneurysms in humans therefore it is not discussed in here. Chemically induced animal models are conducted on both small and large animals. Small animals such as mice, rat, and rabbit are easier to handle and a cheaper option in order to understand AAA formation and the remodeling process. They are frequently induced by $CaCl_2$, elastase, angiotensin II, or involve genetically modified models (Gertz et al., 2013, Tsui, 2010, Lysgaard Poulsen et al., 2016). The elastase models in small animals provide pathological findings similar to this rabbit model, including dilation of the aorta, degradation of elastin, and inflammation. However, these rodent models produce an inflammatory response that develops over a short period of time and the size of the aorta reaches a stable size or shrinks with time, which is similar to the rabbit model. However, Cho et al, (Cho et al., 2009) reported aneurysm rupture and presence of thrombus in male rats that were induced by infusion of elastase and treated with exogenous testosterone. The $CaCl_2$ model has been used with different concentrations and with the combination of other chemical substances such as phosphate that resulted in enhanced calcification of the aorta (Schlatmann and Becker, 1977). The pathological results of the $CaCl_2$ model are similar to the elastase model and to our rabbit model except that more calcification is observed depending on the concentration of $CaCl_2$ and whether phosphate was also used. The angiotensin II model is used in an apolipoprotein E deficient (ApoE- /-) mouse. It promotes the enlargement of the suprarenal aorta accompanied by atherosclerosis, medial hypertrophy, accumulation of macrophages in the external elastic lamina, and thrombosis

(Cho et al., 2009). This model reproduces AAA with atherosclerosis and thrombus, which is lacking in the rabbit model. However, the angiotension II model is mainly used in mice which makes mechanical testing challenging due to their small aortas. The genetically modified animals are mainly used to understand how the absence of some genes could increase or decrease the chance of forming AAA and they are also mainly used for testing drugs (Cho et al., 2009). AAA models in larger animals, which have a closer anatomical size to human, are mainly used to test surgical techniques and new devices before incorporation into the clinic. Large animals experiments are more complex in term of surgeries and expensive compared to small animals (Gertz et al., 2013, Tsui, 2010, Lysgaard Poulsen et al., 2016). Since our goal for this work was to improve our understanding of remodeling aneurysmal tissue in a pilot study, the small animal model was more appropriate and affordable.

CHAPTER 6 CONCLUSION, LIMITATIONS, FUTURE WORK

Conclusion

In vivo animal models increase our understanding of the pathophysiology of AAAs. We presented a pilot controlled rabbit experimental study that included AAA development using periaortic incubation of $CaCl_2$ and elastase. The maximum diameter of the aorta rapidly increased to reach a peak at four week, and then reduced at six weeks. The healthy aorta was stronger than all aneurysmal tissue. The six week AAA had the stiffest and strongest properties compared to the other aneurysmal tissues. The histological analysis illustrated a general medial thickening in the aortic wall with aneurysmal dilatation as well as substantial elastin degradation and separation between the wall layers. Wall remodeling was observed with aneurysmal tissue, where the six week AAA had the highest collagen content. In general, we observed a negative correlation between wall thickness and tissue strength.

To date, no animal model of AAAs has been developed that accurately mirrors the pathology of human disease but some share similar biochemical and cellular mechanisms to those involved in human AAAs. Our *in vivo* rabbit model represents an acute model of AAAs (as opposed to a chronic model in humans) that has similar characteristics to human AAAs including:

1. Maximum diameter increases to double the normal diameters.
2. Similar aneurysm shape between rabbits and humans, specifically fusiform aneurysm.
3. Elastin degradation with aneurysmal growth.
4. Wall structure is altered in term of wall thickness, collagen remodeling, and degree of inflammation.

5. Aneurysmal tissue is weaker than healthy tissue.

The main difference between the rabbit model and human AAA is the acute nature of the former; whereas dilatation in animal models occurs within days or weeks, aneurysm formation in humans is believed to take years. We observed the stabilization of the aortic size in the six week AAA. The novelty of this study was the concurrent analysis of the histology and of the mechanical properties of several segments of aneurysmal tissue at each stage. To our knowledge this is the first study that evaluated the mechanical behaviors of AAA tissue in the rabbit. In conclusion, remodeling of the aortic tissue and changes in micro-constituents (collagen, elastin) appear to have an important role in the progression of an aneurysm.

Limitations and Future Work

There are several limitations to the present study. These include the small sample size, since the study was designed as a pilot investigation. An appropriate sample size should be more than one rabbit per each stage; a larger systematic study of controlled AAA in rabbits could substantiate the results of this study and offer the opportunity to determine the statistical significance. In addition, future experiments should include the histological analysis of a rabbit AAA model at time zero (animal sacrificed immediately after the application of $CaCl_2$ and elastase) in order to understand the immediate effects of $CaCl_2$ and elastase on healthy tissue. This would provide a clearer understanding of how fast elastin is degrading after 20 min of $CaCl_2$ and elastase incubation. Even though the Bi et al, (Bi et al., 2013b) study demonstrated that a sham group did not develop any vessel dilation, it is very important to repeat this control group to ensure that rabbits develop aneurysms due to $CaCl_2$ and elastase incubation, and not due to the trauma of surgical manipulation.

Another limitation is the variation in aorta size between rabbits. We do not know the initial size of the aorta and this can introduce inaccuracy in the data. One possible option is to scan the rabbit before incubating the vessel. However, this will increase the labor time and expenses. Also, it is important to have the same rabbits scanned initially, and at two, four, and six week stages to validate that the aorta size is changing with time and to observe any reduction in the size. As previously mentioned, this will increase the cost of the study and cannot be done with 3D digital subtraction angiography since numerous cannulations of the same access vessel is not possible in rabbits. Instead, this will require a method such as CT or MRI, with intravenous contrast administration in order to less invasively image the rabbits.

Another issue with this study is the observed reduction of the diameter at the six week stage, which may suggest that the degeneration of the aorta is reversed. Although we cannot reliably correlate this finding with the naturally occurring human condition, an attempt to create an alternate model may involve repeating the incubation of $CaCl_2$ and elastase by week four or to develop a method to continuously infuse $CaCl_2$ and elastase with time. Also, introducing a high fat diet or nicotine exposure to the rabbit after induction may alter the progression of aneurysm formation. Finding a technique to develop a chronic model, rather than an acute model, that mirrors human AAAs more closely may improve the relevance of using an animal model to study the human condition. Achieving such a model, however, is challenging since the exact mechanism of AAA formation in humans is still unknown. Most of the data collected from humans are at very advanced stages of aneurysm formation or rupture, which limits our understanding of how they form. A promising but technically challenging solution is to develop a noninvasive method to identify mechanical and histological changes from imaging features.

Another limitation of this study is the preparation and analysis of histology. Even though the histology preparation stages such as fixation of the tissue, its dehydration, clearing, sectioning, and staining were conducted by the same technician, there is no record of time taken to finish all samples. Moreover, there is no report of the orientation in which the tissue sections were sliced. These factors could alter the observed results and introduce an error. In addition, neither a validated scoring system nor a blind viewing methodology was used to analyze the histological results. This could introduce a human error as only the principal investigator analyzed the slides. Also, no specific methodology was used to select the location of interest on each slide but only through observation. It is essential to include all of these procedures in future experiments.

In addition to the information about rabbit AAA models, this study reports the mechanical properties of rabbit AAAs at different stages. Further analyses, however, are important to understand the formation and development of AAA in this model. For example, histological and biochemical analysis are important to quantify elastin, collagen, collagen type, VSMCs, MMPs, and all other cells in the AAA tissue. Understanding the contribution of hemodynamic stress is also important especially because we created infrarenal AAAs, which are very close to the iliac bifurcation and likely subject to significant hemodynamic stresses that influences their development. Using computational fluid dynamics on the 3D model reconstructed for the rabbits at each stage will provide essential information about the effects of blood flow. Finally, the results of this pilot study could be useful to validate biomechanical models of AAA tissue remodeling as an initial step. Specifically, micro-structurally motivated growth biomechanical

models could be tested using the combined results from the mechanical and the histological analysis.

REFERENCES

ABE, T., HIROHATA, M., TANAKA, N., UCHIYAMA, Y., KOJIMA, K., FUJIMOTO, K., NORBASH, A. M. & HAYABUCHI, N. 2002. Clinical benefits of rotational 3D angiography in endovascular treatment of ruptured cerebral aneurysm. *American journal of neuroradiology,* 23**,** 686-688.

AILAWADI, G., ELIASON, J. L. & UPCHURCH, G. R. 2003. Current concepts in the pathogenesis of abdominal aortic aneurysm. *Journal of vascular surgery,* 38**,** 584-588.

AMALINEI, C. & CĂRUNTU, I.-D. 2013. *Etiology and Pathogenesis of Aortic Aneurysm*.

ANIDJAR, S., SALZMANN, J.-L., GENTRIC, D., LAGNEAU, P., CAMILLERI, J.-P. & MICHEL, J.-B. 1990. Elastase-induced experimental aneurysms in rats. *Circulation,* 82**,** 973-981.

ANXIONNAT, R., BRACARD, S., MACHO, J., DA COSTA, E., VAILLANT, R., LAUNAY, L., TROUSSET, Y., ROMEAS, R. & PICARD, L. 1998. 3D angiography. *J Neuroradiol,* 25**,** 251-262.

BARBARA YOUNG, J. W. H. 2000. *wheater's functional histology* Sydney, Australia, Churchill Livingstone.

BI, Y., ZHONG, H., XU, K., NI, Y., QI, X., ZHANG, Z. & LI, W. 2013a. Performance of a modified rabbit model of abdominal aortic aneurysm induced by topical application of porcine elastase: 5-month follow-up study. *European Journal of Vascular and Endovascular Surgery,* 45**,** 145-152.

BI, Y., ZHONG, H., XU, K., ZHANG, Z., QI, X., XIA, Y. & REN, L. 2013b. Development of a novel rabbit model of abdominal aortic aneurysm via a combination of periaortic calcium chloride and elastase incubation. *PloS one,* 8**,** e68476.

BLUESTEIN, D., DUMONT, K., DE BEULE, M., RICOTTA, J., IMPELLIZZERI, P., VERHEGGHE, B. & VERDONCK, P. 2009. Intraluminal thrombus and risk of rupture in patient specific abdominal aortic aneurysm–FSI modelling. *Computer methods in biomechanics and biomedical engineering,* 12**,** 73-81.

BODE, M. K., SOINI, Y., MELKKO, J., SATTA, J., RISTELI, L. & RISTELI, J. 2000. Increased amount of type III pN-collagen in human abdominal aortic aneurysms: evidence for impaired type III collagen fibrillogenesis. *Journal of vascular surgery,* 32**,** 1201-1207.

BORON, W. F. & BOULPAEP, E. L. 2016. *Medical physiology*, Elsevier Health Sciences.

CANCHI, T., KUMAR, S., NG, E. & NARAYANAN, S. 2015. A review of computational methods to predict the risk of rupture of abdominal aortic aneurysms. *BioMed research international,* 2015.

CHIOU, A. C., CHIU, B. & PEARCE, W. H. 2001. Murine aortic aneurysm produced by periarterial application of calcium chloride. *Journal of Surgical Research,* 99**,** 371-376.

CHO, B. S., WOODRUM, D. T., ROELOFS, K. J., STANLEY, J. C., HENKE, P. K. & UPCHURCH, G. R. 2009. Differential regulation of aortic growth in male and female rodents is associated with AAA development. *Journal of Surgical Research,* 155**,** 330-338.

CHOKE, E., COCKERILL, G., WILSON, W., SAYED, S., DAWSON, J., LOFTUS, I. & THOMPSON, M. 2005. A review of biological factors implicated in abdominal aortic

aneurysm rupture. *European Journal of Vascular and Endovascular Surgery,* 30**,** 227-244.
CHOKE, E., THOMPSON, M. M., DAWSON, J., WILSON, W. R. W., SAYED, S., LOFTUS, I. M. & COCKERILL, G. W. 2006. Abdominal aortic aneurysm rupture is associated with increased medial neovascularization and overexpression of proangiogenic cytokines. *Arteriosclerosis, thrombosis, and vascular biology,* 26**,** 2077-2082.
COLLIN. 2016. *Iws.collin.edu* [Online]. Available: http://iws.collin.edu/cdoumen/HistoCCCCD/LabSlides/Connective.html.
CRIADO, E., MARSTON, W. A., WOOSLEY, J. T., LIGUSH, J., CHUTER, T. A., BAIRD, C., SUGGS, C. A., MAURO, M. A. & KEAGY, B. A. 1995. An aortic aneurysm model for the evaluation of endovascular exclusion prostheses. *Journal of vascular surgery,* 22**,** 306-315.
DI MARTINO, E., MANTERO, S., INZOLI, F., MELISSANO, G., ASTORE, D., CHIESA, R. & FUMERO, R. 1998. Biomechanics of abdominal aortic aneurysm in the presence of endoluminal thrombus: experimental characterisation and structural static computational analysis. *European Journal of Vascular and Endovascular Surgery,* 15**,** 290-299.
DI MARTINO, E. S., BOHRA, A., GEEST, J. P. V., GUPTA, N., MAKAROUN, M. S. & VORP, D. A. 2006. Biomechanical properties of ruptured versus electively repaired abdominal aortic aneurysm wall tissue. *Journal of Vascular Surgery,* 43**,** 570-576.
DOELLO, K. 2014. A New Pentachrome Method for the Simultaneous Staining of Collagen and Sulfated Mucopolysaccharides. *The Yale journal of biology and medicine,* 87**,** 341.
EDELMAN, R. R. 1993. MR angiography: present and future. *AJR. American journal of roentgenology,* 161**,** 1-11.
EMEDICINE. 2016. *Abdominal Aortic Aneurysm Workup: Approach Considerations, Laboratory Studies, Ultrasonography* [Online]. Available: http://emedicine.medscape.com/article/1979501-workup#c10.
EPSTEIN, D., SCULPHER, M., POWELL, J., THOMPSON, S., BROWN, L. & GREENHALGH, R. 2014. Long-term cost-effectiveness analysis of endovascular versus open repair for abdominal aortic aneurysm based on four randomized clinical trials. *British Journal of Surgery,* 101**,** 623-631.
FREESTONE, T., TURNER, R., HIGMAN, D., LEVER, M. & POWELL, J. 1997. Influence of hypercholesterolemia and adventitial inflammation on the development of aortic aneurysm in rabbits. *Arteriosclerosis, thrombosis, and vascular biology,* 17**,** 10-17.
FREESTONE, T., TURNER, R. J., COADY, A., HIGMAN, D. J., GREENHALGH, R. M. & POWELL, J. T. 1995. Inflammation and matrix metalloproteinases in the enlarging abdominal aortic aneurysm. *Arteriosclerosis, thrombosis, and vascular biology,* 15**,** 1145-1151.
FUKUI, D., MIYAGAWA, S., SOEDA, J., TANAKA, K., URAYAMA, H. & KAWASAKI, S. 2003. Overexpression of transforming growth factor β1 in smooth muscle cells of human abdominal aortic aneurysm. *European journal of vascular and endovascular surgery,* 25**,** 540-545.
GASSER, T. C., OGDEN, R. W. & HOLZAPFEL, G. A. 2006. Hyperelastic modelling of arterial layers with distributed collagen fibre orientations. *Journal of the royal society interface,* 3**,** 15-35.

GEEST, J. P. V., SACKS, M. S. & VORP, D. A. 2004. Age dependency of the biaxial biomechanical behavior of human abdominal aorta. *Journal of biomechanical engineering,* 126**,** 815-822.
GEEST, J. P. V., SACKS, M. S. & VORP, D. A. 2006. The effects of aneurysm on the biaxial mechanical behavior of human abdominal aorta. *Journal of biomechanics,* 39**,** 1324-1334.
GERTZ, S. D., KURGAN, A. & EISENBERG, D. 1988. Aneurysm of the rabbit common carotid artery induced by periarterial application of calcium chloride in vivo. *Journal of Clinical Investigation,* 81**,** 649.
GERTZ, S. D., MINTZ, Y., BEERI, R., RUBINSTEIN, C., GILON, D., GAVISH, L., BERLATZKY, Y., APPELBAUM, L. & GAVISH, L. 2013. Lessons from Animal Models of Arterial Aneurysm. *Aorta,* 1**,** 244.
GOLESTANI, R., RAZAVIAN, M., NIE, L., ZHANG, J., JUNG, J.-J., YE, Y., DE ROO, M., HILGERINK, K., LIU, C. & ROBINSON, S. P. 2015. Imaging vessel wall biology to predict outcome in abdominal aortic aneurysm. *Circulation: Cardiovascular Imaging,* 8**,** e002471.
GOLLEDGE, J., IYER, V., JENKINS, J., BRADSHAW, B., CRONIN, O. & WALKER, P. J. 2014. Thrombus volume is similar in patients with ruptured and intact abdominal aortic aneurysms. *Journal of vascular surgery,* 59**,** 315-320.
GOLLEDGE, J. & NORMAN, P. E. 2010. Atherosclerosis and Abdominal Aortic Aneurysm Cause, Response, or Common Risk Factors? *Arteriosclerosis, thrombosis, and vascular biology,* 30**,** 1075-1077.
HENDERSON, E. L., GENG, Y.-J., SUKHOVA, G. K., WHITTEMORE, A. D., KNOX, J. & LIBBY, P. 1999. Death of smooth muscle cells and expression of mediators of apoptosis by T lymphocytes in human abdominal aortic aneurysms. *Circulation,* 99**,** 96-104.
HIGASHIKATA, T., YAMAGISHI, M., SASAKI, H., MINATOYA, K., OGINO, H., ISHIBASHI-UEDA, H., HAO, H., NAGAYA, N., TOMOIKE, H. & SAKAMOTO, A. 2004. Application of real-time RT-PCR to quantifying gene expression of matrix metalloproteinases and tissue inhibitors of metalloproteinases in human abdominal aortic aneurysm. *Atherosclerosis,* 177**,** 353-360.
HILL, M. A. 2016. *Blood Vessel Wall Cartoon* [Online]. Available: https://embryology.med.unsw.edu.au/embryology/index.php/File:Blood_vessel_wall_cartoon.jpg.
HOLMES, D. R., LIAO, S., PARKS, W. C. & HOMPSON, R. W. 1995. Medial neovascularization in abdominal aortic aneurysms: a histopathologic marker of aneurysmal degeneration with pathophysiologic implications. *Journal of vascular surgery,* 21**,** 761-772.
HOPKINS 2016. Aneurysm | Johns Hopkins Medicine Health Library.
IAIZZO, P. A. 2009. *Handbook of cardiac anatomy, physiology, and devices*, Springer Science & Business Media.
J. THUBRIKAR, M. L., F. ROBICSEK, J. AL-SOUDI, B. FOWLER, M 2001. Mechanical properties of abdominal aortic aneurysm wall. *Journal of medical engineering & technology,* 25**,** 133-142.
JAHANGIR, E., LIPWORTH, L., EDWARDS, T. L., KABAGAMBE, E. K., MUMMA, M. T., MENSAH, G. A., FAZIO, S., BLOT, W. J. & SAMPSON, U. K. 2015. Smoking, sex,

risk factors and abdominal aortic aneurysms: a prospective study of 18 782 persons aged above 65 years in the Southern Community Cohort Study. *Journal of epidemiology and community health,* 69**,** 481-488.
JOHN VARELLAS, C. Y. 2016. *Connective Tissues* [Online]. Available: http://www.seewhyanatomy.com/connective-tissues/es2eyayqapdnwviuppl39wpu3jhw1w.
JONES, G. T. 2011. *The Pathohistology of Abdominal Aortic Aneurysm*.
KADOGLOU, N. P. & LIAPIS, C. D. 2004. Matrix metalloproteinases: contribution to pathogenesis, diagnosis, surveillance and treatment of abdominal aortic aneurysms. *Current medical research and opinion,* 20**,** 419-432.
KHAN, S., VERMA, V., VERMA, S., POLZER, S. & JHA, S. 2015. Assessing the potential risk of rupture of abdominal aortic aneurysms. *Clinical radiology,* 70**,** 11-20.
LEFEVRE, M. L. 2014. Screening for abdominal aortic aneurysm: US Preventive Services Task Force recommendation statement. *Annals of internal medicine,* 161**,** 281-290.
LEFEVRE, M. L. & ON BEHALF OF THE, U. S. P. S. T. F. 2014. Screening for abdominal aortic aneurysm: U.s. preventive services task force recommendation statement. *Annals of Internal Medicine,* 161**,** 281-290.
LINDEMAN, J. H. 2015. The pathophysiologic basis of abdominal aortic aneurysm progression: a critical appraisal. *Expert review of cardiovascular therapy,* 13**,** 839-851.
LINDEMAN, J. H., ASHCROFT, B. A., BEENAKKER, J.-W. M., VAN ES, M., KOEKKOEK, N. B., PRINS, F. A., TIELEMANS, J. F., ABDUL-HUSSIEN, H., BANK, R. A. & OOSTERKAMP, T. H. 2010. Distinct defects in collagen microarchitecture underlie vessel-wall failure in advanced abdominal aneurysms and aneurysms in Marfan syndrome. *Proceedings of the National Academy of Sciences,* 107**,** 862-865.
LOPEZ-CANDALES, A., HOLMES, D. R., LIAO, S., SCOTT, M. J., WICKLINE, S. A. & THOMPSON, R. W. 1997. Decreased vascular smooth muscle cell density in medial degeneration of human abdominal aortic aneurysms. *The American journal of pathology,* 150**,** 993.
LYSGAARD POULSEN, J., STUBBE, J. & LINDHOLT, J. S. 2016. Animal Models Used to Explore Abdominal Aortic Aneurysms: A Systematic Review. *European Journal of Vascular and Endovascular Surgery*.
MARTINEZ-PINNA, R., MADRIGAL-MATUTE, J., TARIN, C., BURILLO, E., ESTEBAN-SALAN, M., PASTOR-VARGAS, C., LINDHOLT, J. S., LOPEZ, J. A., CALVO, E. & DE CENIGA, M. V. 2013. Proteomic analysis of intraluminal thrombus highlights complement activation in human abdominal aortic aneurysms. *Arteriosclerosis, thrombosis, and vascular biology,* 33.
MARTUFI, G. & GASSER, T. C. 2011. A constitutive model for vascular tissue that integrates fibril, fiber and continuum levels with application to the isotropic and passive properties of the infrarenal aorta. *Journal of biomechanics,* 44**,** 2544-2550.
MARTUFI, G. & GASSER, T. C. 2013. Review: the role of biomechanical modeling in the rupture risk assessment for abdominal aortic aneurysms. *Journal of biomechanical engineering,* 135**,** 021010.
MARTUFI, G., SATRIANO, A., MOORE, R. D., VORP, D. A. & DI MARTINO, E. S. 2015. Local Quantification of Wall Thickness and Intraluminal Thrombus Offer Insight into the

Mechanical Properties of the Aneurysmal Aorta. *Annals of Biomedical Engineering,* 43**,** 1759-1771.
MCMILLAN, W. D. & PEARCE, W. H. 1999. Increased plasma levels of metalloproteinase-9 are associated with abdominal aortic aneurysms. *Journal of vascular surgery,* 29**,** 122-129.
MCMILLAN, W. D., TAMARINA, N. A., CIPOLLONE, M., JOHNSON, D. A., PARKER, M. A. & PEARCE, W. H. 1997. Size matters the relationship between MMP-9 expression and aortic diameter. *Circulation,* 96**,** 2228-2232.
MEDLINEPLUS. 2016. *Abdominal aortic aneurysm: MedlinePlus Medical Encyclopedia* [Online]. Available: https://medlineplus.gov/ency/article/000162.htm.
MENASHI, S., CAMPA, J. S., GREENHALGH, R. M. & POWELL, J. T. 1987. Collagen in abdominal aortic aneurysm: typing, content, and degradation. *Journal of vascular surgery,* 6**,** 578-582.
MICHEL, J.-B., MARTIN-VENTURA, J.-L., EGIDO, J., SAKALIHASAN, N., TRESKA, V., LINDHOLT, J., ALLAIRE, E., THORSTEINSDOTTIR, U., COCKERILL, G. & SWEDENBORG, J. 2010. Novel aspects of the pathogenesis of aneurysms of the abdominal aorta in humans. *Cardiovascular research***,** cvq337.
MIRAUX, S., SERRES, S., THIAUDIÈRE, E., CANIONI, P., MERLE, M. & FRANCONI, J.-M. 2004. Gadolinium-enhanced small-animal TOF magnetic resonance angiography. *Magnetic Resonance Materials in Physics, Biology and Medicine,* 17**,** 348-352.
MITCHELL, G. R. & TOJEIRA, A. 2013. Role of anisotropy in tissue engineering. *Procedia Engineering,* 59**,** 117-125.
MONTEIRO, J. A. T., DA SILVA, E. S., RAGHAVAN, M. L., PUECH-LEÃO, P., DE LOURDES HIGUCHI, M. & OTOCH, J. P. 2014. Histologic, histochemical, and biomechanical properties of fragments isolated from the anterior wall of abdominal aortic aneurysms. *Journal of vascular surgery,* 59**,** 1393-1401. e2.
NEVITT, M. P., BALLARD, D. J. & HALLETT JR, J. W. 1989. Prognosis of abdominal aortic aneurysms. *New England Journal of Medicine,* 321**,** 1009-1014.
NORMAN, P. & POWELL, J. 2007. Abdominal aortic aneurysm the prognosis in women is worse than in men. *Circulation,* 115**,** 2865-2869.
NORTHWELL. 2016. *Center for Aortic Disease | Northwell Health, formerly North Shore-LIJ Health System* [Online]. Available: https://www.northwell.edu/find-care/locations/center-aortic-disease.
NOVAK, K., POLZER, S., TICHY, M. & BURSA, J. 2015. Automatic evaluation of collagen fiber directions from polarized light microscopy images. *Microscopy and Microanalysis,* 21**,** 863-875.
NOWICKI, W., BRUDNICKI, W., IWAŃCZYK, M., JABŁOŃSKI, R. & SKOCZYLAS, B. 2010. VARIATION IN BRANCHES OF THE ABDOMINAL AORTA IN EUROPEAN RABBIT.
O'LEARY, S. A., HEALEY, D. A., KAVANAGH, E. G., WALSH, M. T., MCGLOUGHLIN, T. M. & DOYLE, B. J. 2014. The biaxial biomechanical behavior of abdominal aortic aneurysm tissue. *Annals of biomedical engineering,* 42**,** 2440-2450.
PALAZZUOLI, A., GALLOTTA, M., GUERRIERI, G., QUATRINI, I., FRANCI, B., CAMPAGNA, M. S., NERI, E., BENVENUTI, A., SASSI, C. & NUTI, R. 2008. Prevalence of risk factors, coronary and systemic atherosclerosis in abdominal aortic

aneurysm: comparison with high cardiovascular risk population. *Vasc Health Risk Manag,* 4**,** 877-883.
PANCHERI, F. Q., PEATTIE, R. A., REDDY, N. D., AHAMED, T., LIN, W., OUELLETTE, T. D., IAFRATI, M. D. & DORFMANN, A. L. 2016. Histology and Biaxial Mechanical Behavior of Abdominal Aortic Aneurysm Tissue Samples. *Journal of Biomechanical Engineering*.
PARODI, J. C., PALMAZ, J. & BARONE, H. 1991. Transfemoral intraluminal graft implantation for abdominal aortic aneurysms. *Annals of vascular surgery,* 5**,** 491-499.
POLZER, S., GASSER, T. C., BURSA, J., STAFFA, R., VLACHOVSKY, R., MAN, V. & SKACEL, P. 2013a. Importance of material model in wall stress prediction in abdominal aortic aneurysms. *Medical engineering & physics,* 35**,** 1282-1289.
POLZER, S., GASSER, T. C., FORSELL, C., DRUCKMÜLLEROVA, H., TICHY, M., STAFFA, R., VLACHOVSKY, R. & BURSA, J. 2013b. Automatic identification and validation of planar collagen organization in the aorta wall with application to abdominal aortic aneurysm. *Microscopy and Microanalysis,* 19**,** 1395-1404.
RAAZ, U., ZÖLLNER, A. M., SCHELLINGER, I. N., TOH, R., NAKAGAMI, F., BRANDT, M., EMRICH, F. C., KAYAMA, Y., EKEN, S. & ADAM, M. 2015. Segmental aortic stiffening contributes to experimental abdominal aortic aneurysm development. *Circulation***,** CIRCULATIONAHA. 114.012377.
RAGHAVAN, M. & VORP, D. A. 2000. Toward a biomechanical tool to evaluate rupture potential of abdominal aortic aneurysm: identification of a finite strain constitutive model and evaluation of its applicability. *Journal of biomechanics,* 33**,** 475-482.
RAGHAVAN, M. L., HANAOKA, M. M., KRATZBERG, J. A., DE LOURDES HIGUCHI, M. & DA SILVA, E. S. 2011. Biomechanical failure properties and microstructural content of ruptured and unruptured abdominal aortic aneurysms. *Journal of biomechanics,* 44**,** 2501-2507.
RAGHAVAN, M. L., KRATZBERG, J., DE TOLOSA, E. M. C., HANAOKA, M. M., WALKER, P. & DA SILVA, E. S. 2006. Regional distribution of wall thickness and failure properties of human abdominal aortic aneurysm. *Journal of biomechanics,* 39**,** 3010-3016.
RAGHAVAN, M. L., WEBSTER, M. W. & VORP, D. A. 1996. Ex vivo biomechanical behavior of abdominal aortic aneurysm: Assessment using a new mathematical model. *Annals of Biomedical Engineering,* 24**,** 573-582.
REEPS, C., GEE, M., MAIER, A., GURDAN, M., ECKSTEIN, H.-H. & WALL, W. A. 2010. The impact of model assumptions on results of computational mechanics in abdominal aortic aneurysm. *Journal of Vascular Surgery,* 51**,** 679-688.
REEPS, C., MAIER, A., PELISEK, J., HÄRTL, F., GRABHER-MEIER, V., WALL, W., ESSLER, M., ECKSTEIN, H.-H. & GEE, M. 2013. Measuring and modeling patient-specific distributions of material properties in abdominal aortic aneurysm wall. *Biomechanics and modeling in mechanobiology,* 12**,** 717-733.
RENSEN, S., DOEVENDANS, P. & VAN EYS, G. 2007. Regulation and characteristics of vascular smooth muscle cell phenotypic diversity. *Netherlands Heart Journal,* 15**,** 100-108.

ROBINSON, P. & BOOMS, P. 2001. Human Genome and Diseases:¶ The molecular pathogenesis of the Marfan syndrome. *Cellular and Molecular Life Sciences CMLS,* 58**,** 1698-1707.

RODELLA, L. F., REZZANI, R., BONOMINI, F., PERONI, M., COCCHI, M. A., HIRTLER, L. & BONARDELLI, S. 2016. Abdominal aortic aneurysm and histological, clinical, radiological correlation. *Acta histochemica,* 118**,** 256-262.

ROSIN, N. L., AGABALYAN, N., OLSEN, K., MARTUFI, G., GABRIEL, V., BIERNASKIE, J. & DI MARTINO, E. S. 2016. Collagen structural alterations contribute to stiffening of tissue after split-thickness skin grafting. *Wound Repair and Regeneration*.

ROWE, V. L., STEVENS, S. L., REDDICK, T. T., FREEMAN, M. B., DONNELL, R., CARROLL, R. C. & GOLDMAN, M. H. 2000. Vascular smooth muscle cell apoptosis in aneurysmal, occlusive, and normal human aortas. *Journal of vascular surgery,* 31**,** 567-576.

S RAUT, S., CHANDRA, S., SHUM, J., B WASHINGTON, C., C MULUK, S., A FINOL, E. & F RODRIGUEZ, J. 2013. Biological, Geometric and Biomechanical Factors Influencing Abdominal Aortic Aneurysm Rupture Risk: A Comprehensive Review. *Recent Patents on Medical Imaging,* 3**,** 44-59.

SAKALIHASAN, N., DELVENNE, P., NUSGENS, B. V., LIMET, R. & LAPIÈRE, C. M. 1996. Activated forms of MMP 2 and MMP 9 in abdominal aortic aneurysms. *Journal of vascular surgery,* 24**,** 127-133.

SCHLATMANN, T. J. & BECKER, A. E. 1977. Histologic changes in the normal aging aorta: implications for dissecting aortic aneurysm. *The American journal of cardiology,* 39**,** 13-20.

SHANG, E. K., NATHAN, D. P., BOONN, W. W., LYS-DOBRADIN, I. A., FAIRMAN, R. M., WOO, E. Y., WANG, G. J. & JACKSON, B. M. 2013. A modern experience with saccular aortic aneurysms. *Journal of vascular surgery,* 57**,** 84-88.

SHERIF, C., MARBACHER, S. & FANDINO, J. 2009. High-resolution three-dimensional 3 T magnetic resonance angiography for the evaluation of experimental aneurysm in the rabbit. *Neurological research,* 31**,** 869-872.

SHIMAZAKI, Y. & UEDA, H. 2014. Abdominal Aortic Aneurysm. *Interdisciplinary Concepts in Cardiovascular Health.* Springer.

SMOLOCK, C. J. & LYDEN, S. P. 2014. Abdominal Aortic Aneurysm. *Cleveland Clinic Manual of Vascular Surgery.* Springer.

STANFORD. 2016. *Abdominal Aortic Aneurysm* [Online]. Available: https://stanfordhealthcare.org/medical-conditions/blood-heart-circulation/abdominal-aortic-aneurysm.html.

TENG, Z., FENG, J., ZHANG, Y., HUANG, Y., SUTCLIFFE, M. P., BROWN, A. J., JING, Z., GILLARD, J. H. & LU, Q. 2015. Layer-and direction-specific material properties, extreme extensibility and ultimate material strength of human abdominal aorta and aneurysm: a uniaxial extension study. *Annals of biomedical engineering,* 43**,** 2745-2759.

THOMPSON, R. W., LIAO, S. & CURCI, J. A. 1997. Vascular smooth muscle cell apoptosis in abdominal aortic aneurysms. *Coronary artery disease,* 8**,** 623-632.

TSAMIS, A., KRAWIEC, J. T. & VORP, D. A. 2013. Elastin and collagen fibre microstructure of the human aorta in ageing and disease: a review. *Journal of the Royal Society Interface,* 10**,** 20121004.

TSUI, J. C. 2010. Experimental models of abdominal aortic aneurysms. *The open cardiovascular medicine journal,* 4.

VANDE GEEST, J. P., DILLAVOU, E. D., DI MARTINO, E. S., OBERDIER, M., BOHRA, A., MAKAROUN, M. S. & VORP, D. A. 2006a. Gender-Related Differences in the Tensile Strength of Abdominal Aortic Aneurysm. *Annals of the New York Academy of Sciences,* 1085**,** 400-402.

VANDE GEEST, J. P., WANG, D. H. J., WISNIEWSKI, S. R., MAKAROUN, M. S. & VORP, D. A. 2006b. Towards A Noninvasive Method for Determination of Patient-Specific Wall Strength Distribution in Abdominal Aortic Aneurysms. *Annals of Biomedical Engineering,* 34**,** 1098-1106.

VOGEL, B., SIEBERT, H., HOFMANN, U. & FRANTZ, S. 2015. Determination of collagen content within picrosirius red stained paraffin-embedded tissue sections using fluorescence microscopy. *MethodsX,* 2**,** 124-134.

VOLOKH, K. & VORP, D. 2008. A model of growth and rupture of abdominal aortic aneurysm. *Journal of biomechanics,* 41**,** 1015-1021.

VORP, D. A. 2007. Biomechanics of abdominal aortic aneurysm. *Journal of biomechanics,* 40**,** 1887-1902.

VORP, D. A. & GEEST, J. P. V. 2005. Biomechanical determinants of abdominal aortic aneurysm rupture. *Arteriosclerosis, thrombosis, and vascular biology,* 25**,** 1558-1566.

VORP, D. A., LEE, P. C., WANG, D. H., MAKAROUN, M. S., NEMOTO, E. M., OGAWA, S. & WEBSTER, M. W. 2001. Association of intraluminal thrombus in abdominal aortic aneurysm with local hypoxia and wall weakening. *Journal of Vascular Surgery,* 34**,** 291-299.

VORP, D. A., RAGHAVAN, M. & WEBSTER, M. W. 1998. Mechanical wall stress in abdominal aortic aneurysm: influence of diameter and asymmetry. *Journal of Vascular Surgery,* 27**,** 632-639.

WADGAONKAR, A. D., III, J. H. B., WEIHE, E. K., ZIMMERMAN, S. L., FISHMAN, E. K. & JOHNSON, P. T. 2015. Abdominal Aortic Aneurysms Revisited: MDCT with Multiplanar Reconstructions for Identifying Indicators of Instability in the Pre- and Postoperative Patient. *RadioGraphics,* 35**,** 254-268.

WHITBREAD, F., PETERSON, R. L. & MCGONIGLE, T. P. 1996. Vesicular-arbuscular mycorrhizal associations of American ginseng (Panax quinquefolius) in commercial production. *Canadian Journal of Botany,* 74**,** 1104-1112.

WILSON, K. A., LEE, A. J., HOSKINS, P. R., FOWKES, F. G. R., RUCKLEY, C. V. & BRADBURY, A. W. 2003. The relationship between aortic wall distensibility and rupture of infrarenal abdominal aortic aneurysm. *Journal of vascular surgery,* 37**,** 112-117.

WILSON, W. R. W., ANDERTON, M., SCHWALBE, E. C., JONES, J. L., FURNESS, P. N., BELL, P. R. & THOMPSON, M. M. 2006. Matrix metalloproteinase-8 and-9 are increased at the site of abdominal aortic aneurysm rupture. *Circulation,* 113**,** 438-445.

XIONG, J., WANG, S. M., ZHOU, W. & WU, J. G. 2008. Measurement and analysis of ultimate mechanical properties, stress-strain curve fit, and elastic modulus formula of human abdominal aortic aneurysm and nonaneurysmal abdominal aorta. *Journal of vascular surgery,* 48**,** 189-195.

ZENDEHBUDI, G. R. & KAZEMI, A. 2007. The accuracy of thin-shell theory in estimation of aneurysm rupture. *Journal of biomechanics,* 40**,** 3230-3235.

COPY RIGHT PERMISSION

The image taking from Colin website is under FAIR DEALING is an exception in the Copyright Act that allows you to use a work in the context of research or private study, criticism, review, education and news reporting as long as you cite the source properly. The website has no contact email and it state that it is used to help student.

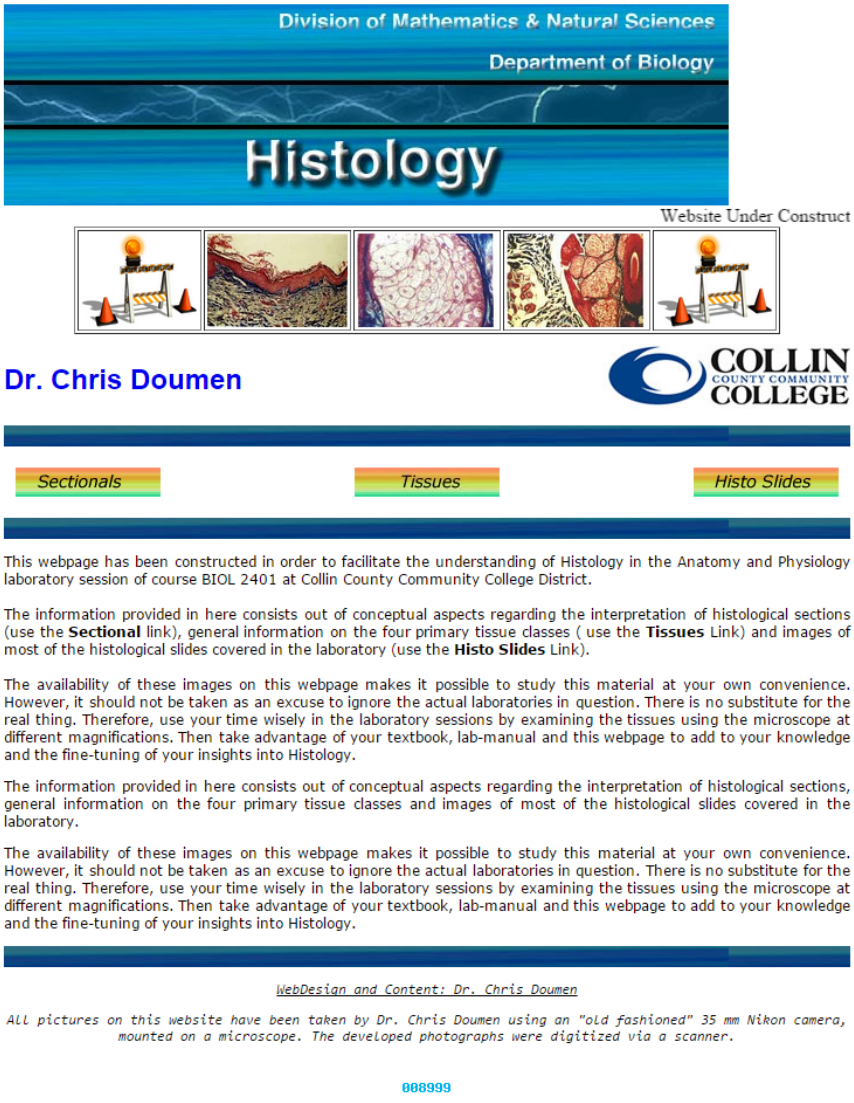

The image taking from Northwell.com website is under FAIR DEALING is an exception in the Copyright Act that allows you to use a work in the context of research or private study, criticism, review, education and news reporting as long as you cite the source properly. I emailed the website and I have not received any response.

The image taking from (Nowicki et al., 2010) website is under FAIR DEALING is an exception in the Copyright Act that allows you to use a work in the context of research or private study, criticism, review, education and news reporting as long as you cite the source properly. I emailed the author and I have not received any response.

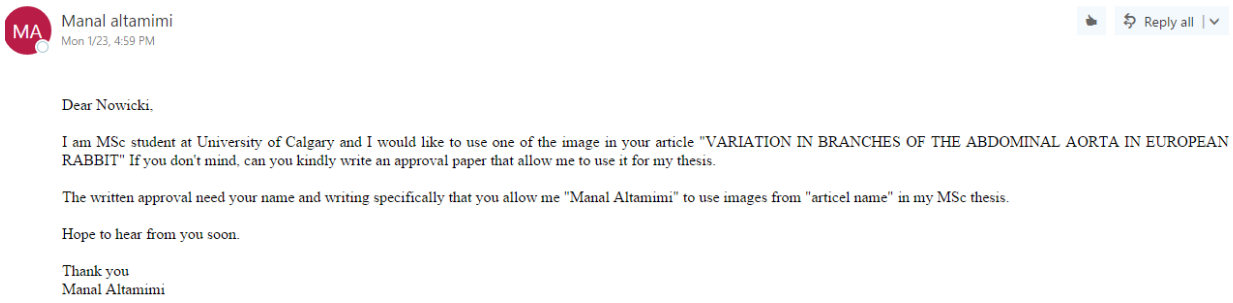

Manal altamimi
Mon 1/23, 4:59 PM

Reply all

Dear Nowicki,

I am MSc student at University of Calgary and I would like to use one of the image in your article "VARIATION IN BRANCHES OF THE ABDOMINAL AORTA IN EUROPEAN RABBIT" If you don't mind, can you kindly write an approval paper that allow me to use it for my thesis.

The written approval need your name and writing specifically that you allow me "Manal Altamimi" to use images from "articel name" in my MSc thesis.

Hope to hear from you soon.

Thank you
Manal Altamimi

consist mainly of connective tissue fibres.
blends with the connective tissue surrounding the vessel.
definition of the outer limit of the tunica adventitia is arbitrary.

Links: Medicine Prac | Science Prac | Blood Vessel Development | Cardiovascular System Development

Cite this page: Hill, M.A. 2017 **Embryology** *Blood vessel wall cartoon.jpg*. Retrieved January 23, 2017, from https://embryology.med.unsw.edu.au/embryology/index.php/File:Blood_vessel_wall_cartoon.jpg

What Links Here?

File history

Click on a date/time to view the file as it appeared at that time.

	Date/Time	Thumbnail	Dimensions	User	Comment
current	**18:21, 7 July 2012**	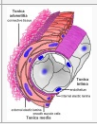	450 × 600 (71 KB)	Z8600021 (Talk | contribs)	{{Blue Histology}}

You cannot overwrite this file.

File usage

The following 3 pages link to this file:

ANAT2241 Cardiovascular System
ANAT2511 Circulatory System
HM Practical - Blood Vessel Histology

Categories: Indexed pages | Blue Histology | Histology | Cardiovascular | Cartoon

This page was last modified on 9 May 2013, at 12:34.

About Us: Legal Disclaimer

Legal Notices and Disclaimers

Terms and Conditions of Use

Welcome to the Stanford Health Care's Web Site (the "Site"). Please read the following Terms and Conditions of Use ("Terms") carefully before using the Site. It governs your relationship with Stanford Health Care regarding your use of the Site.

You should not substitute information on the Stanford Health Care Web site for professional advice.

This Web site provides general educational information. This information is not provided in the course of a professional relationship between a health care provider and a patient. It is not intended to be, and should not be used as, a substitute for medical treatment by a health care professional.

Stanford Health Care is not making a diagnosis of your condition or a recommendation about the course of treatment for your particular circumstances through the use of this Web site. You should not assume that information on a particular topic on the site is complete or up-to-date. You should never disregard or delay seeking medical advice because of what you have read on this Web site.

Your Permission to use the Stanford Health Care Web site.

Stanford Health Care give you limited personal permission to use the Web site. Your permission to use the Web site is limited in a number of ways. For example, the only use for which you may use, download, or print material contained on this Site is for internal non-profit research purposes. Any commercial use, such as selling content, creating course packs, or posting information on another Web site, is prohibited. You also may not:

- frame all or part of the Web site.
- change or delete any proprietary notices from materials downloaded or printed out from the Web site.
- systemically download or print materials from the Web site.
- transmit or provide any data from the Web site to a third party.
- use the Web site in a manner contrary to any applicable law.

Your permission terminates immediately, without any further action by Stanford Health Care, if you breach these Terms. You may not transfer or assign your permission to any other party.

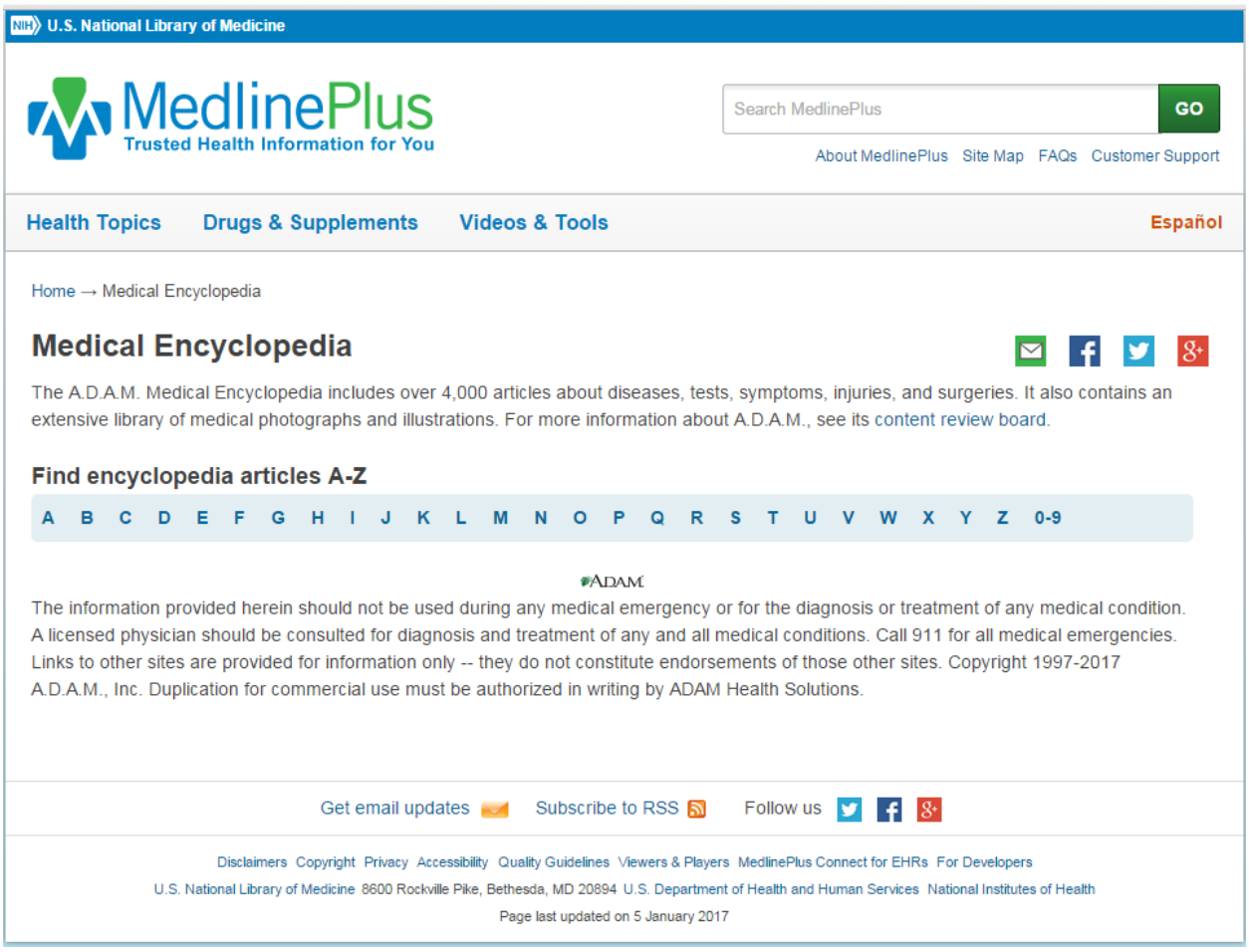
U.S. National Library of Medicine
MedlinePlus
Trusted Health Information for You
Search MedlinePlus
GO
About MedlinePlus Site Map FAQs Customer Support
Health Topics Drugs & Supplements Videos & Tools Español
Home → Medical Encyclopedia
Medical Encyclopedia
The A.D.A.M. Medical Encyclopedia includes over 4,000 articles about diseases, tests, symptoms, injuries, and surgeries. It also contains an extensive library of medical photographs and illustrations. For more information about A.D.A.M., see its content review board.
Find encyclopedia articles A-Z
A B C D E F G H I J K L M N O P Q R S T U V W X Y Z 0-9
ADAM
The information provided herein should not be used during any medical emergency or for the diagnosis or treatment of any medical condition. A licensed physician should be consulted for diagnosis and treatment of any and all medical conditions. Call 911 for all medical emergencies. Links to other sites are provided for information only -- they do not constitute endorsements of those other sites. Copyright 1997-2017 A.D.A.M., Inc. Duplication for commercial use must be authorized in writing by ADAM Health Solutions.
Get email updates Subscribe to RSS Follow us
Disclaimers Copyright Privacy Accessibility Quality Guidelines Viewers & Players MedlinePlus Connect for EHRs For Developers
U.S. National Library of Medicine 8600 Rockville Pike, Bethesda, MD 20894 U.S. Department of Health and Human Services National Institutes of Health
Page last updated on 5 January 2017

To Whom It May Concern:

I, John Varellas, creator and content manager of seewhyanatomy.com. Give permission to Manal Altamimi to use any or all histology images found on the above mentioned website (seewhyanatomy.com) for use in his MSc thesis.

For any further inquiries or concerns please feel free to contact me directly at the information provided below.

The image taking from Emedicine website is under FAIR DEALING is an exception in the Copyright Act that allows you to use a work in the context of research or private study, criticism, review, education and news reporting as long as you cite the source properly.

Medscape Terms of Use

The Medscape Network, described below, provides users with a wide array of services including, without limitation, news, reference resources, sponsored programming, personalized content, continuing medical education and communication platforms (collectively, the "Services"). The Services are provided to users of the Medscape Network subject to the following Terms of Use (the "Terms"). You will always be able to view the most current version of these Terms by clicking on the Terms of Use link at the bottom of any page of a Medscape Network website or without our mobile applications. **By using the Services, you agree to these Terms, whether or not you are a registered member of the Medscape Network. These Terms govern your use of the Services and create a binding legal agreement that we may enforce against you in the event of a violation. If you do not agree to all of these Terms of Use, do not use the Services!**

Scope of these Terms of Use

The Medscape Network includes the websites medscape.com and medscape.org (the "Medscape Sites") and the Medscape mobile device applications, which include Medscape Mobile, MedPulse and Medscape CME & Education (the "Medscape Apps"). WebMD LLC owns and operates medscape.com and Medscape Mobile and MedPulse and its affiliated company, Medscape, LLC, owns and operates medscape.org and Medscape CME & Education. References to "WebMD" in these Terms of Use mean WebMD LLC and references to "Medscape" mean Medscape, LLC. References to "we" or "our" mean WebMD and Medscape.

WebMD may offer other services to physicians and healthcare professionals outside of the Medscape Network, such as WebMD Connect which is offered through WebMD's consumer website, www.webmd.com. These other services are not governed by these Terms but by the terms of use applicable to the property through which these services are offered.

Account Registration

You must register an account with the Medscape Network to access all of the Services. Registration requires you to provide us with your name, email address, profession, specialty and other information specified in the registration form ("Registration Information"), and to select a username and password that will be associated with your account. You agree that your Registration Information is true, accurate, current, and complete, and you will promptly update your Registration Information as necessary so that it continues to be true, accurate, current and complete. We may attempt to verify the accuracy of the Registration Information that you have provided and update it as necessary. You are solely responsible for maintaining the confidentiality and security of your Medscape account username and password and you may not permit another person to use your username and password to access the Services. You are responsible for all activity that occurs under your account. If you believe that the security of your account information has been compromised, you should immediately change your username and password through the account settings feature or notify us and we will assist you. We shall have no liability for any unauthorized access to or use of your account information.

Use of the Services

The Services are intended for physicians and other healthcare professionals. By using the Services, you represent and warrant that you have the right, authority, and capacity to agree to and abide by these Terms and that you are not prohibited from using the Services or any portion thereof.

The information and tools that we make available through the Services are provided for educational and informational purposes only. While we hope you find the Services useful to you as a healthcare professional, they are in no way intended to serve as a diagnostic service or platform, to provide certainty with respect to a diagnosis, to recommend a particular product or therapy or to otherwise substitute for the clinical judgment of a qualified healthcare professional. You agree that you will not use the Services with the intention of creating any kind of physician/patient relationship, e.g., to diagnose or treat users. You are solely responsible for evaluating the information obtained from the Services and for your use or misuse of such information in connection with your treatment decisions or otherwise. You agree that you shall be solely responsible for your compliance with all laws and standards of professional practice applicable to you and the practice of medicine or other relevant health profession.

If you are a consumer who chooses to access the professional-level information made available through the Services, you should not rely on that information as professional medical advice or use the Services as a replacement for any relationship with your physician or other qualified healthcare professional. For medical concerns, including decisions about medications and other treatments, consumers should always consult their physician or, in serious cases, seek immediate assistance from emergency medical personnel.

Subject to your compliance with these Terms, you are granted a limited, non-exclusive, non-transferable and non-sublicensable license to use the Services and to view the information and materials made available through the Services, including User Content, as defined below, ("Medscape Content") solely for your personal and professional use. You shall not

use, copy, adapt, modify, prepare derivative works based upon, distribute, license, sell, transfer, publicly display, publicly perform, transmit, stream, broadcast or otherwise exploit the Services, Medscape Content, the Medscape Sites or the Medscape Apps, except as expressly permitted in these Terms. All rights not expressly granted herein are reserved to WebMD, Medscape and their respective licensors, as applicable.

The Medscape Network may contain links to third-party websites or resources which are not part of the Medscape Network. You agree that we are not responsible or liable for these websites and resources including, without limitation, their availability or the content and information that they provide. The inclusion in the Medscape Network of third party resources, including links to third party websites, does not imply our endorsement of these resources.

You agree that you will not engage in any of the following activities in connection with your use of the Services:

1. Forge headers or otherwise manipulate identifiers in order to disguise the origin of any content transmitted through the Services;
2. Use, display, mirror or frame a Medscape Site or Medscape App, or any component thereof, or WebMD or Medscape's trademark, logo or other proprietary information, without the written consent of WebMD or Medscape, as applicable;
3. Remove any copyright, trademark or other proprietary rights notices contained within the Medscape Network, including those of WebMD or Medscape and any of their respective licensors;
4. Infringe or use the WebMD or Medscape brand, logos and/or trademarks in any business name, email, URL or other context unless expressly approved in writing by WebMD or Medscape, as applicable;
5. Attempt to circumvent any protective technological measure associated with the Services;
6. Attempt to access or search a Medscape Site, Medscape App or any content contained therein through the use of any engine, software, tool, agent, device or mechanism (including scripts, bots, spiders, scraper, crawlers, data mining tools or the like) other than through software generally available through web browsers;
7. Post, upload, transmit or otherwise distribute chain letters, pyramid schemes, advertising or spam;
8. Impersonate or misrepresent your affiliation with another person or entity;
9. Harvest or otherwise collect information about others, including email addresses;
10. Interfere with or disrupt any of the Services or the associated computer or technical delivery systems;
11. Interfere with, or attempt to interfere with, the access of any user, host or network, including, without limitation, sending a virus, overloading, flooding, spamming, or mail-bombing a Medscape Site or a Medscape App;
12. Fail to respect another user's privacy. This includes revealing another user's password, phone number, address, instant messenger I.D. or address or any other personally identifiable information; or
13. Use a Medscape Site, Medscape App, the Services or any Medscape Content in any manner not permitted by these Terms.

We may (but are not obligated to) do any or all of the following without notice:

1. Record or pre-screen User Content submissions to public areas within the Medscape Network;
2. Investigate your use of the Services as we deem appropriate to comply with any applicable law, regulation, government request or legal process;
3. Remove User Content which we believe does not comply with these Terms of Use;
4. Terminate your access to the Medscape Network upon our determination that you have violated these Terms of Use; and
5. Edit Medscape Content.

Information that you Make Available through the Services

Certain Services enable users to submit content which may include, without limitation, text, images, photographs, figures, charts, graphics, reports, data and sound ("User Content"). User Content does not include Registration Information. When you submit User Content through the Services you automatically grant to us a perpetual, non-exclusive, worldwide, royalty-free, fully paid up, transferable, sub-licensable (through multiple tiers) license to distribute, transmit, copy, host, publicly display and perform, excerpt, index, tag, modify, adapt, sell, create derivative works from, and otherwise use and exploit such User Content in any media, form or format now known or hereafter developed, both within and outside of the Medscape Network for any purpose that is consistent with the Medscape Privacy Policy. You agree that you are solely responsible for all User Content that you submit through the Services. You represent and warrant that you either are the sole and exclusive owner of all User Content or you have all rights, licenses, consents and releases that are necessary to grant to us the rights in such User Content as specified in these Terms.

You are solely responsible for ensuring that the User Content that you make available through the Services complies with applicable laws including, without limitation, those relating to privacy, and also best clinical and ethical practices. Prior to submitting any User Content to the Services, you must remove any information that identifies an individual or could reasonably enable the identification of an individual, e.g., name, e-mail address, social security number, insurance number or other unique identification number, biometric identifiers, facial photographs, photographs of identifying marks such as tattoos or scars. You shall be solely responsible for any claims arising from your failure to de-identify User Content that you submit through the Services.

You agree that you will not use the Services to make available User Content that:

1. you do not have the right to make available under any contractual or fiduciary agreement or law;
2. infringes, misappropriates or violates a third party's patent, copyright, trademark, trade secret, moral rights or other intellectual property rights, or rights of publicity or privacy;
3. results in the violation of any applicable law or regulation, including, but not limited to, the Health Insurance Portability and Accountability Act (HIPAA) or any other applicable privacy laws;
4. is unlawful, harmful, obscene, defamatory, threatening, harassing, abusive, slanderous, offensive, or embarrassing to any other person or entity;
5. promotes discrimination, bigotry, racism, hatred, harassment or harm against any individual or group;
6. promotes illegal activity;
7. is fraudulent, false, misleading or deceptive;
8. constitutes an advertisement or solicitation of business; or
9. contains viruses or other harmful computer code designed to interrupt, destroy or limit the use of any computer software or hardware.

Proprietary Rights

You acknowledge and agree that the Medscape Network and any software used in connection with the Medscape Network ("Software") contain proprietary and confidential information that is protected by applicable intellectual property and other laws. You further acknowledge and agree that the Medscape Content is protected by copyrights, trademarks, service marks, patents or other proprietary rights and laws. Except as expressly permitted by applicable law or as authorized by us or the applicable licensor, you agree not to modify, rent, lease, loan, sell, distribute, transmit, broadcast, publicly perform, create derivative works from, or "scrape" for commercial or any other purpose, the Medscape Network, the Medscape Content or the Software, in whole or in part. Any use of the Medscape Network or the Services not expressly permitted by these Terms is a breach of these Terms and may violate our and third parties' intellectual property rights.

You may view information provided through the Services online, download individual articles to your computer or mobile device for later reading or print a copy of an article for yourself. You may not remove any copyright notices from our materials. You agree not to access the Services by any means other than through the interface that is provided by us for use in accessing the Services.

Privacy Policy

The Medscape Privacy Policy, located at http://www.medscape.com/public/privacy, provides information about our collection, use and disclosure of information about users of the Services. By accessing and using the Services, you agree to the terms of the Privacy Policy and acknowledge and agree that the Privacy Policy forms an integral part of these Terms.

Dealing with Third Parties

Your correspondence or business dealings with, or participation in promotions of, advertisers or other third parties found on or through the Services, including requests for and delivery of goods or services, and any other terms, conditions, warranties or representations associated with such dealings, are solely between you and such third party. You agree that we shall not be responsible or liable for any loss or damage of any sort incurred as the result of any such dealings or as the result of the introduction of such third parties through the Services.

Laws that Govern this Agreement

We control those components of the Services made available through our respective websites from our offices within the state of New York in the United States of America. By accessing the Services, you agree that the statutes and laws of the state of New York, without regard to choice of laws principles, will apply to all matters relating to use of the Services.

Notwithstanding the foregoing, you may be subject to certain obligations and responsibilities associated with the jurisdiction in which you practice medicine or another health profession. We make no representation as to the legal compliance of the Services or the Medscape Content and you are solely responsible for compliance with the laws of your jurisdiction, with respect to your use and misuse of the Services and the Medscape Content.

Termination and Modification

You agree that we may, under certain circumstances and without prior notice, discontinue, temporarily or permanently, the Services (or any part thereof) or eliminate your account and remove any User Content that you have made available through the Services, with or without notice, for any of the following reasons (which are not intended to be exclusive): (a) breaches or violations of these Terms or other incorporated agreements or guidelines, (b) requests by law enforcement or other government agencies, (c) a request by you, (d) discontinuance or material modification to the Services (or any part thereof),

(e) technical or security issues or problems, (f) extended periods of inactivity, and/or (g) your engagement in fraudulent or illegal activities. You agree that all terminations for cause shall be made at our sole discretion, and we shall not be liable to you or any third party for any termination of your account or access to the Services.

Disclaimer

THE MEDSCAPE NETWORK, SERVICES, MEDSCAPE SITES, MEDSCAPE APPS AND MEDSCAPE CONTENT ARE PROVIDED "AS IS", WITHOUT WARRANTY OF ANY KIND, EITHER EXPRESS OR IMPLIED. WITHOUT LIMITING THE FOREGOING, WE EXPRESSLY DISCLAIM ANY WARRANTIES, EXPRESS IMPLIED, INCLUDING WARRANTIES OF MERCHANTABILITY, FITNESS FOR A PARTICULAR PURPOSE, QUIET ENJOYMENT OR NON-INFRINGEMENT, AND ANY WARRANTIES ARISING OUT OF COURSE OF DEALING OR USAGE OF TRADE. WE MAKE NO WARRANTY THAT THE MEDSCAPE NETWORK, SERVICES, MEDSCAPE SITES, MEDSCAPE APPS AND MEDSCAPE CONTENT WILL MEET YOUR REQUIREMENTS OR BE AVAILABLE ON AN UNINTERRUPTED, SECURE, OR ERROR-FREE BASIS. WE MAKE NO WARRANTY AS TO THE ACCURACY, TIMELINESS, COMPLETENESS OR RELIABILITY OF ANY CONTENT OBTAINED THROUGH THE SERVICES. NO INFORMATION PROVIDED THROUGH THE SERVICES OR BY US IN ORAL OR WRITTEN FORM WILL CREATE ANY WARRANTY NOT EXPRESSLY MADE HEREIN YOUR RELIANCE UPON THE CONTENT OBTAINED OR USED BY YOU THROUGH THE SERVICES IS SOLELY AT YOUR OWN RISK. YOU ARE SOLELY RESPONSIBLE FOR ALL OF YOUR COMMUNICATIONS AND INTERACTIONS WITH OTHER USERS OF THE MEDSCAPE NETWORK. YOU UNDERSTAND THAT WE DO NOT ASSUME RESPONSIBILITY FOR SCREENING ANY USER OF THE MEDSCAPE NETWORK NOR DO WE VERIFY OR TAKE RESPONSIBILITY FOR USER CONTENT. WE DO NOT PROVIDE MEDICAL ADVICE AND WE DO NOT RECOMMEND OR ENDORSE ANY SPECIFIC PRODUCTS, PRODUCT USERS, THERAPIES, TESTS, PHYSICIANS, HEALTHCARE PROFESSIONS OR OPINIONS.

Liability

In no event will WebMD, Medscape or any other person or entity involved in creating, developing or delivering the Medscape Network, the Medscape Sites, the Medscape Apps, the Services or the Content be liable for any damages (including, without limitation, incidental and consequential damages, personal injury/wrongful death, lost profits, or damages resulting from lost data or business interruption) arising out of or in connection with these Terms or from the use of or inability to access or use the Medscape Network, the Medscape Sites, the Medscape Apps, the Services or the Medscape Content, or from any communications or interactions with other persons with whom you communicate or interact as a result of your use of the Services, whether based on warranty, contract, tort, or any other legal theory, and whether or not we, our licensors, ours suppliers, or any third parties mentioned with the Services are advised of the possibility of such damages. We, our licensors, our suppliers, or any third parties mentioned within the Services are not liable for any personal injury, including death, caused by your use or misuse of the Services or any information provided through the Services. Any claims arising in connection with your use of the Services must be brought within one (1) year of the date of the event giving rise to such action occurred. Remedies under these Terms are exclusive and are limited to those expressly provided for in these Terms. The limitations of damages set forth above are fundamental elements of the basis of the bargain between us and you.

Indemnity

You agree to defend, indemnify, and hold each of us and our respective officers, directors, employees, agents, licensors, and suppliers, harmless from and against any claims, actions or demands, liabilities and settlements including without limitation, reasonable legal and accounting fees, resulting from, or alleged to result from, your access to or use of the Medscape Network, the Medscape Sites, the Medscape Apps, the Services and the Medscape Content or your violation of these Terms.

Notice and Take Down Procedures and Copyright Agent

If you believe any materials within the Medscape Network infringe your copyright, you may request removal of those materials (or access thereto) by contacting Medscape Customer Support at MedscapeCustomerSupport@webmd.net and providing the following information:

1. Identification of the copyrighted work that you believe to be infringed. Please describe the work, and where possible include a copy or the location (e.g., URL) of an authorized version of the work.
2. Identification of the material that you believe to be infringing and its location. Please describe the material, and provide us with its URL or any other pertinent information that will allow us to locate the material.
3. Your name, address, telephone number and (if available) e-mail address.
4. A statement that you have a good faith belief that the complained of use of the materials is not authorized by the copyright owner, its agent, or the law.
5. A statement that the information that you have supplied is accurate, and indicating that "under penalty of perjury," you are the copyright owner or are authorized to act on the copyright owner's behalf.
6. A signature or the electronic equivalent from the copyright holder or authorized representative.

We may terminate the account of any user who we determine is a repeat infringers.

Modifications

We reserve the right, at our sole discretion, to modify, discontinue or terminate any of the Services, the Medscape Content or these Terms, at any time and without prior notice. If we modify these Terms in a material way, we will provide notice of such modification within the Medscape Network. By continuing to access or use the Services after we have modified these Terms, you agree to be bound by the modified Terms. If the modified Terms are not acceptable to you, you agree to immediately stop using the Medscape Network and the Services.

Complete Agreement

Except as expressly provided in a particular "legal notice" on the website, these Terms constitute the entire agreement between you, WebMD and Medscape with respect to your use (and prior use) of the Medscape Network and the associated Services and Medscape Content.

These Terms constitute the entire and exclusive understanding and agreement between WebMD, Medscape and you regarding Medscape Network and the Services and these Terms supersede and replace any and all prior oral or written understandings or agreements between WebMD, Medscape and you regarding the Medscape Network and the Services.

Assignment

You may not assign or transfer these Terms, by operation of law or otherwise, without WebMD and Medscape's prior written consent. Any attempt by you to assign or transfer these Terms, without such consent, will be null and of no effect. WebMD or Medscape may assign or transfer these Terms, at its sole discretion, without restriction. Subject to the foregoing, these Terms will bind and inure to the benefit of the parties, their successors and permitted assigns

Notices

Any notices or other communications permitted or required hereunder, including those regarding material modifications to these Terms, will be in a written form and given: (i) by us via email (in each case to the email address included in your Registration Information); or (ii) by posting within the Medscape Network. For notices made by e-mail, the date of receipt will be deemed the date on which such notice is transmitted.

No Waiver

Our failure to enforce any right or provision of these Terms will not constitute a waiver of future enforcement of that right or provision. Except as expressly set forth in these Terms, the exercise by either party of any of its remedies under these Terms will be without prejudice to its other remedies under these Terms or otherwise.

Survival

All provisions of these Terms shall survive termination of your Medscape Network account except for your license to access and use the Services and the Medscape Content.

Contact Us

If you have questions about the Services or these Terms, or you wish to provide feedback, please contact us at MedscapeCustomerSupport@webmd.net. By submitting feedback and suggestions, you grant a non-exclusive, perpetual, irrevocable, and royalty-free license to any intellectual property rights you may have in your feedback and suggestions to us to use to improve the Services.

Last updated: November 10, 2015.
